Coal Liquefaction Liquid Quality:
Influence of Temperature and Heating Approach on Solvent Extraction of Coal

by

Ioan-Tudor Apan

A thesis submitted in partial fulfillment of the requirements for the degree of

Master of Science

in

Chemical Engineering

Department of Chemical and Materials Engineering
University of Alberta

ABSTRACT

This project evaluated the impact of reaction temperature and of additional heating steps on the quality of the liquids obtained from solvent extraction of a lignite coal with tetralin. The points of focus were the coal liquid yield, physical properties, aromatic content and iron pyrite conversion. All experiments were carried out in micro-batch reactors, nitrogen atmosphere and autogenous pressure, with a coal to solvent ratio of 1:3. First, the influence of extraction temperature was investigated by performing extraction at different temperatures in the range 340 to 415 ^{0}C, for 1 h. The second part of the project involved 9 different heating scenarios combining a low temperature step in the range 100 to 200 ^{0}C followed by a high temperature step in the range 350 to 415 ^{0}C. It was found that performing liquefaction at lower temperatures is beneficial in terms of coal liquid density, aromatic content and iron pyrite conversion, while higher temperatures favor a better yield, lower coal liquid boiling points and the formation of aromatics with higher aliphatic hydrogen content. Adding an additional low temperature step led to higher liquid yields, lower coal liquid boiling points and higher aliphatic hydrogen content of the aromatics contained in the coal liquids, while the coal liquid density remained predominantly unchanged.

ACKNOWLEDGEMENT

First of all, I would like to thank my supervisor, Dr. Arno De Klerk, for all the support and guidance provided during the development of this work, but also for his kind, patient and easygoing spirit that made my research activity a more pleasant experience.

Secondly, I would like to thank Ghazaleh Haghighat for her indispensable help during the initial stages of my experimental work.

I would also like to express my tremendous gratitude towards Glaucia and Ivor for all their support during difficult times, and for their friendship. Special thanks to Natalia and Jose, Ashley, Hasin, Xue, Navjot, Vanessa, Sepideh and Nuvaid for their moral support, and for being my friends.

Additionally, I would also like to thank Dr. Shaofeng Yang, Dr. Moshfiqur Rahman, Samuel and Nitya for their immediate response when I needed urgent help with essential laboratory analyses.

Finally, I would like acknowledge the Canadian Centre for Clean Coal/Carbon and Mineral Processing Technologies (C^5MPT) for funding this work.

TABLE OF CONTENTS

LIST OF TABLES

LIST OF FIGURES

CHAPTER 1 – INTRODUCTION TO DIRECT COAL LIQUEFACTION

1.1 Background

The abundance and availability of coal has led to its use as an energy resource in a variety of ways and to variable extents, depending on the historical, technological and economical context of each epoch and geographical region. The earliest records describe the coal simply being burned as a heating fuel in late twelfth-century England, this activity being banned a century later as an offence punishable by death due to the generated emissions [1]. During the following centuries, despite the less drastic attitudes towards it, coal combustion was still a restricted activity, until the eighteenth century, when the industrial revolution enabled the extensive use of coal combustion through the development of more or less successful methods that decreased the environmental impact [1]. If at the beginning of the twentieth century, coal was still the dominant energy source, it soon diminished in importance, as other energy sources such as crude oil started to prevail [2]. However, by 1980 a lot of focus was driven back to alternative energy sources such as coal, after a decade of "energy crises, feedstock shortages and soaring fuel costs" which had become "a fact of economic life in the United States and other industrial nations" dependent on foreign sources of crude oil [3]. Research on coal processing technologies received, therefore, a significant momentum gain around the 1980s. As oil prices and energy consumption continue to rise, the abundant coal resources remain a suitable substitute for the diminishing oil feedstock. The possibility of a global shortfall in oil derived products justifies the necessity of technologies such as coal-to-liquids processes to be proactively developed [4].

The processes converting coal into liquid fuels can be collectively described under the generic term of "coal liquefaction". This can be further divided in two sub-categories: indirect coal liquefaction, and direct coal liquefaction. Indirect coal liquefaction involves coal gasification, which converts the coal into synthesis gas. This gas consisting mainly of CO and H_2 is subsequently converted to hydrocarbons through the Fischer-Tropsch process or to other products such as methanol or dimethyl ether, depending on the catalysts used. Direct coal liquefaction, on the other hand, skips the gasification step by converting the coal directly into

liquids, thus being more energy efficient, although the products contain more aromatics, nitrogen and sulfur. There are three categories of direct coal liquefaction: pyrolysis, catalytic liquefaction and solvent extraction. Although all of these methods involve heating the coal to a point in which fragments of its structure are being torn away as free radicals, each method involves a different stabilization alternative of these radicals, to form lighter, stable hydrocarbons. During coal pyrolysis, which involves heating the coal in the absence of air or oxygen, the carbon is removed as char, while the resulted liquids and gases contain more hydrogen. Variations of the process involve different temperature ranges, as well as the possibility to use a hydrogen rich atmosphere, in which case the process is called hydrocarbonization. Catalytic liquefaction uses molecular hydrogen in combination with a solvent in order to stabilize the free radicals in the presence of a suitable catalyst, the process taking place at high temperatures and pressures. Similarly, solvent extraction involves hydrogen stabilization of the coal derived free radicals, but instead of using molecular hydrogen, a hydrogen donor solvent is being used [3].

Among the challenges faced by the solvent extraction process, the preheating of coal-oil slurries has been highlighted as an important issue related to its commercial success [3, 5]. Different strategies, such as comparing the outcome of constant heating rates with the one of lower and higher mean temperature rates, have proven to influence the product yield by balancing the rate of thermal decomposition with the rate of free radical hydrogen stabilization, thereby influencing the proportion of retrogressive reactions [6]. The focus of this project is directed towards the solvent extraction process, specifically on the effect of reaction temperature and other heating approaches on the product yield and quality.

1.2 Objectives and scope of work

The objective of the current project was to determine the effect of reaction temperature and the effect of a two-step heating approach on the quality and yield of the solvent extraction products.

In order for the process to be strictly determined by the temperature variation and by the change in heating approach, limiting various parameters (such as coal rank, solvent type, solvent to coal ratio, coal particle size, reaction time and pressure, reactor type and size, etc.) was

necessary. The literature concerning these parameters was reviewed (Chapter 2) with the purpose of understanding the significance of these options, and to what extent they might play a role in the context of the chosen laboratory experiments. The impact of the liquefaction temperature on the products was then investigated by performing a series of micro-batch reactor experiments at different temperatures (Chapter 3). Finally, various two-step heating scenarios have been carried out in order for them to be compared with the one-step process and between each other, in terms of their impact on product quality and yield (Chapter 4). All the conclusions were then summarized in the final chapter of this project (Chapter 5).

References

[1] Berkowitz, N., *An introduction to coal technology.* Academic Press: New York, 1979.

[2] Haghighat, F. Investigation of solvent extraction of coal at low temperatures. MSc. Thesis, University of Alberta, University of Alberta, Fall 2013.

[3] Nowacki, P. *Coal liquefaction processes*; Noyes Data Corp.: Park Ridge, NJ, 1979.

[4] King, D. L.; De Klerk, A. In *Overview of Feed-to-Liquid (XTL) Conversion;* American Chemical Society: 2011; Vol. 1084, pp 1-24.

[5] *Reaction engineering in direct coal liquefaction*; Shah, Y. T. Ed.; Addison-Wesley: Reading, MA, 1981.

[6] Haghighat, F.; De Klerk, A. Direct coal liquefaction: Low temperature dissolution process. *Energy Fuels* **2014**, *28*, 1012-1019.

CHAPTER 2 – LITERATURE REVIEW ON SOLVENT EXTRACTION OF COAL

2.1 Introduction

The purpose of this literature review is to provide a basic understanding of the main elements that determine the process of coal solvent extraction. Because all the other coal liquefaction technologies mentioned in Chapter 1 do not relate to the topic of this project in a relevant manner, they were not further investigated. Therefore, this chapter is focused on the solvent extraction process exclusively.

The elements discussed throughout the literature review are details concerning the feed materials, the coal types and solvents used during the process, then the key variables that influence the coal extraction and finally some indicators of the product quality.

2.2 Coal characteristics

The characteristics of coal are significantly variable, due to the various factors which influence its formation. Coal forms whenever plant debris gets shielded from microbiological degradation by being covered by silts and then buried under layers of sediments providing sufficient pressure and heat for millions of years. Due to the variety of the vegetation taking part in this process, depending on its geographical region and native era, and because of the different conditions of time, pressure and temperature in which this process can take place, the resulting solids are “often more dissimilar than alike”, the word “coal” being “merely a generic term” [1]. There are therefore no representative molecular structures of coal, but merely average models that usually depict polymeric structures of aromatic rings, aliphatic side chains, hydrogen bonds, ether linkages and other functional groups that build macromolecular networks with high molecular weight (Figure 2.2.1). As a result, coal characterization usually involves other types of classifications as described below.

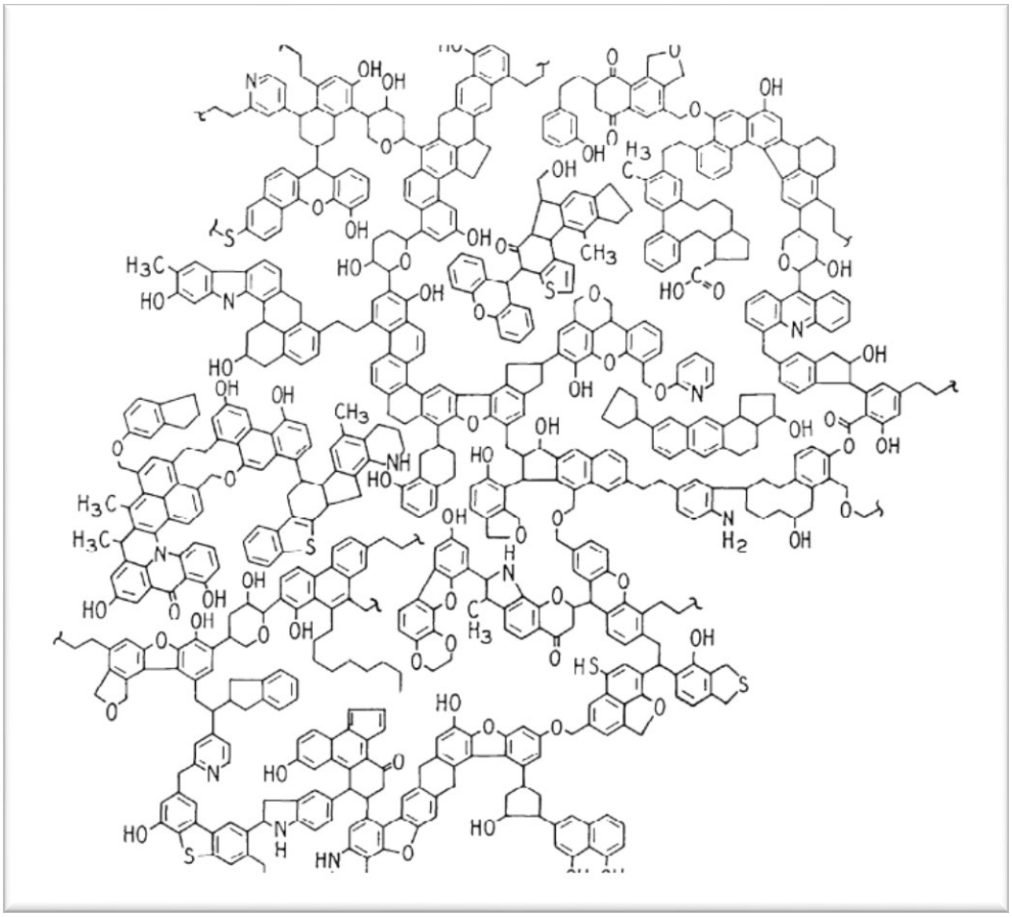

Figure 2.2.1. Model of bituminous coal structure [2]

2.2.1 Physical composition

Coal contains microscopic constituents called macerals. These can be traced to specific components of the plant debris from which the coal originally formed, and are characterized by appearance, chemical composition and optical properties such as refractive index and reflectivity. The 14 different macerals can be categorized in three groups: vitrinite, exinite and inertinite. These can associate in various combinations to form 7 different microlithotype groups: vitrite, liptite, inertite, clarite, durite, vitrinertite and trimacerite [1]. The current project does not further elaborate the role of these coal constituents in the liquefaction process, but literature regarding this topic is very rich in studies on maceral-specific dissolution (for a few examples see [3-7]).

2.2.2 Chemical composition

Despite the difficult characterization of the coal molecular structure, there are two analytical methods which provide information related to the chemical features and behavior of coal: the proximate analysis and the ultimate (elemental) analysis [1].

The proximate analysis describes the coal composition in terms of ash, volatile matter, moisture and, by difference, fixed carbon contents. It can be carried out by following analytical standards [8] which involve thermo-gravimetric experiments. The moisture consists of bulk water present in large cracks and capillaries, and of physically adsorbed water present in the small pores of the coal. The volatile matter includes numerous hydrocarbons, carbon monoxide and chemically combined water, all of which form through the thermal decomposition of the coal. The ash content represents the remaining residue after the coal has been completely incinerated, but it should not be confused with the mineral content of the coal (these minerals are present in the coal in a different form than the minerals remaining in the ash after the incineration) [1].

The ultimate or elemental analysis quantitatively describes the organic coal composition in terms of carbon, hydrogen, nitrogen, sulfur and oxygen [9].

2.2.3 Rank

Classifying coal in ranks based on their carbon contents and burning characteristics led to the following types of coal (in ascending rank order): peat, lignite, subbituminous coal, bituminous coal and anthracite. Counterintuitively, the coal rank is not necessarily equivalent to the quality of the coal. Although low-rank coals are not appropriate for certain applications, they are superior when used in others. An example would be the coal solvent extraction, where low-rank coals, such as lignite, lead to the highest extraction yields, while coals with carbon contents above 90% lead to negligible yields [1].

2.3 Solvents used for coal liquefaction

The hydrogen donor solvents used for coal extraction have different properties that influence the extraction process. Correlations between the extraction yield and solvent properties such as the solubility parameter, the hydrogen donor ability, the electron donor number and the polarity have been made for some commonly used extraction solvents such as tetrahydrofuran, pyridine, quinoline, N-metyl-2 pyrrolidone, 1-naphthol, HT-1006 and tetralin (1,2,3,4 tetrahydronaphthalene) [10]. One particularly popular and predominantly studied solvents used for coal liquefaction is tetralin (Figure 2.3.1). Due to its availability and use in previous work relevant to the current project [11, 12], the properties of this solvent are further described.

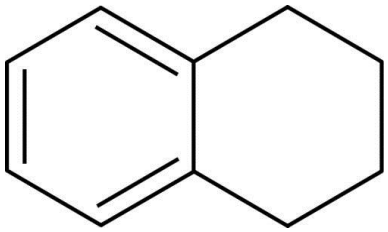

Figure 2.3.1. Molecular structure of tetralin (1,2,3,4 tetrahydronaphthalene)

Tetralin has been described as an "excellent solvent for coal", especially at temperatures between 350 and 450 °C [13]. When donating its four aliphatic hydrogen atoms in order to stabilize the coal derived free radicals, tetralin is converted to naphthalene (Equation 2.3.1) through a free radical mechanism [11, 12].

$$C_{10}H_{12} \rightarrow C_{10}H_8 + 4H^{\bullet} \qquad (2.3.1)$$

Tetralin has a melting point of -35.6 °C and boiling point of 207 °C under atmospheric pressure. Its critical pressure is 36.5 bar, its critical temperature is 447 °C and its critical volume is 0.408 m^3/kmol [14]. The liquid-vapor equilibrium for pure tetralin shown in Figure 2.3.2 [15] is relevant when considering its use as a liquid solvent for coal extraction at temperatures reaching as high as 450 °C.

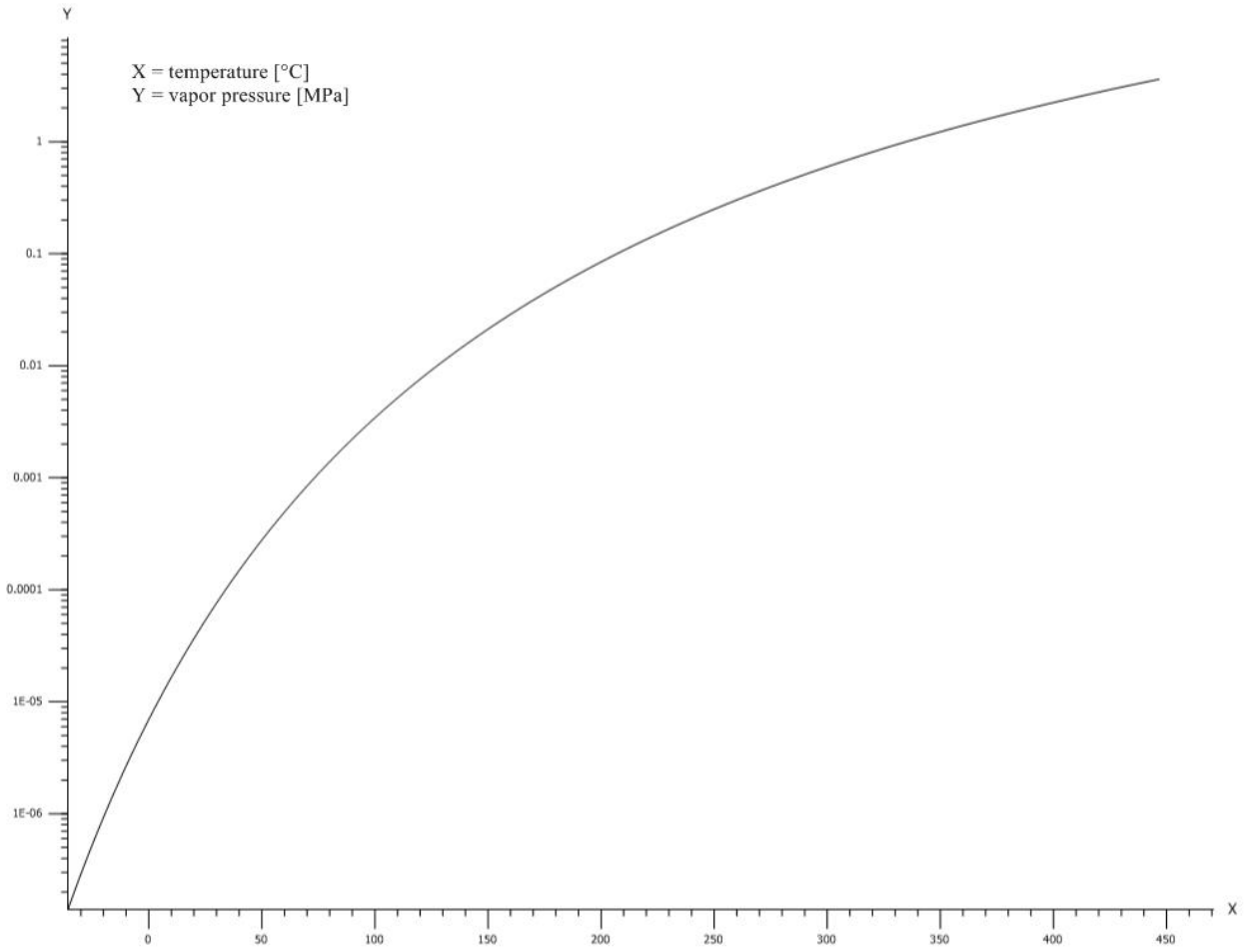

Figure 2.3.2. Liquid-vapor equilibrium curve for pure tetralin [15]

The curve shown in Figure 2.3.2 represents the Antoine equation for pure tetralin, valid for the temperature range from -35.75 to 470.8 °C (Equation 2.3.2) [15].

$$p = 10^{\left(A-\frac{B}{T+C}\right)} \tag{2.3.2}$$

Where A = 7.167

B = 1806.143

C = 213.732

p = vapor pressure expressed in mmHg.

T = temperature expressed in °C.

2.4 Process variables

The extraction process is influenced by different variables which can be related to the feed material (e.g. coal particle size, mechanical treatment, solvent to coal ratio), to the reaction conditions (e.g. reaction temperature, pressure and time), or to different engineering approaches, like using different heating rates and profiles, or performing the extraction in one or more temperature steps.

2.4.1 Influence of feed material on extraction

The coal particle size distribution and porosity can influence the extraction process to a variable extent. Usually, a finer solute would lead to faster reaction rates, due to the higher surface area contacting the solvent [10]. There are, however, factors which limit the maximum grinding degree of the coal. It has been indicated that for certain conditions, there is no more extraction yield benefit when the particle size is smaller than a certain limit (for example particle sizes below 250 μm for extraction of bituminous coal with N-methylpyrrolidone) [11]. Research also showed that the influence of the particle size is only significant in the initial, lower temperature range (~250 °C), while at higher temperatures (above 360 °C) it has no observable effect, due to the rapid disintegration of the coal particles at these temperatures [16]. Other factors which limit the grinding degree are the coal slurry viscosity change and the higher grinding costs [17]. Generally, coal particles less than 0.5 mm in size are considered “fine” particles, but this is just a rough categorization and not a standard one [18].

Mechanical and mechanochemical action has also been reported to influence the macromolecular structure and hence the reactivity of coal, by causing partial destruction of the crosslinking in its organic mass [19]. This is relevant as far as the coal grinding duration and intensity are concerned.

Another factor which can have an effect on the extraction process is the solvent to coal ratio. The extent of this influence is, however, dependent on other factors such as the solvent type. For example, during alkali assisted extraction under the same temperature conditions, increasing the solvent to coal ratio from ~2 to ~10 led to an increase of ~50% extraction yield for

dimethylformamide, but did not change the yield when N-methyl-2-pyrrolidinone was used [20]. Other previous work on lignite coal dissolution in tetralin at low temperatures (100 °C) showed no statistical correlation and no significant variation of the yield obtained for solvent to coal ratios ranging from 2 to 8 [12].

2.4.2 Influence of reaction conditions on coal solvent extraction

The reaction temperature and duration are factors which influence the solvent extraction process of coal to a greater extent. The behavior of the solvent-coal mixture depends on whether its temperature is below the onset of the active thermal decomposition of the coal or above it [1]. For example, for lignite coal and tetralin, previous work [12, 21] showed that below 200 °C the coal dissolution yield steadily increased with temperature but the maximum yield for each temperature was reached within 15 minutes, remaining unchanged if the operation was continued up to 30 h.

When higher temperatures (250 – 350 °C) are reached, the coal starts to decompose, generating free radicals which are stabilized by the solvent donated hydrogen. Therefore, the extraction yield in these conditions varies significantly with temperature. Reaction time in this temperature interval showed a significant influence on the tetralin extraction yield of lignite coals [12], by almost doubling the yield reached after 15 min – 3 h, when 30 h of reaction time had elapsed. This trend amplifies with increasing temperatures, but as temperatures are getting higher and higher, the rate of coal decomposition is starting to surpass the rate in which hydrogen atoms can stabilize the newly formed free radicals, leading to retrogressive reactions forming highly stable, high molecular weight compounds through the condensation and crosslinking of the free radicals. The yield will therefore decrease at these high temperatures, as the coal is becoming progressively less soluble [1].

Pressure is usually controlled in order to maintain the solvent in liquid phase (in contact with the coal particles) [22].

2.4.3 Heating approaches

Different heating approaches have been proven to influence the overall yield of the extraction process. Experiments involving subbituminous coal and tetralin undergoing temperature-programmed liquefaction have shown a conversion improvement which made this method to be thought as a "promising approach" [23]. These experiments involved the staged heating of the coal-solvent slurry, starting with a 15 min interval at 200 °C, followed by a 30 min hold at temperatures between 300 and 400 °C. This approach is based on the hypothesis that the retrogressive reactions are being minimized and the liquid yield is being increased when the low temperature extraction step is included, by balancing the hydrogenation and condensation reactions. The same idea is backed up by other research papers showing similar temperature programming techniques [24, 25].

Other experiments showed dramatic conversion shifts from 32% to 77% when specific heating scenarios were employed in the coal liquefaction with tetralin. These experiments involved adding a 10 min step at 316 °C before a 5 min step at 427 °C, but the same approach did not show any yield increase when the first step was carried out at lower temperatures (177 °C), suggesting that the temperature staging is effective only after the coal thermal decomposition limit is being exceeded by the first step [26]. This conclusion was backed up by research involving experiments which replaced the isothermal temperature steps with different heating profiles [11]. By comparing the outcome of a constant heating rate with the outcomes of heating rates with higher, respectively lower mean temperatures, the conclusion was that the more time is being spent at temperatures higher than the coal thermal decomposition threshold, the higher the conversion will be.

2.5 Product quality indicators

2.5.1 Aromatic content

The aromatic content of fuels can be correlated with their physical properties such as density and refractive index, while considering their boiling point distribution [27-29]. An example of such a correlation is given in Figure 2.5.1.1. From a refining point of view, the aromatic content is relevant when considering coal liquids as fuels.

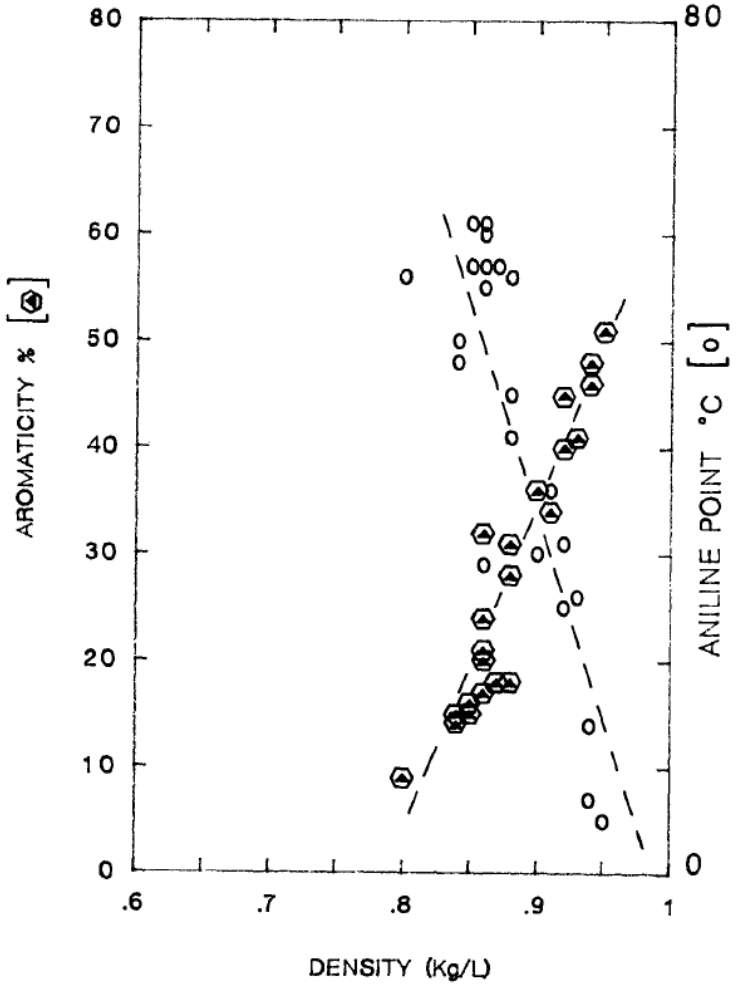

Figure 2.5.1.1. Example of correlations between fuel density and fuel aromatic data as determined by proton nuclear magnetic resonance (PNMR) and aniline point determination techniques [28]

2.5.2 Sulfur content

Sulfur is present in coal as part of its macromolecular structure as organic sulfur, but it is also present as inorganic sulfur, in form of minerals such as iron pyrite (FeS_2). Under high temperature conditions, these compounds are undergoing transformations which generate sulfur. During coal solvent extraction, this can lead to a higher sulfur content in the coal organic matrix, or to higher amounts of sulfur being dissolved into the coal liquids or released as H_2S.

Literature involving pyrolysis experiments on lignite coals showed pyrite decomposition taking place at various temperatures between 350 °C and 1000 °C, depending on the specific lignite coal [30, 31]. This can be seen in Figure 2.5.2.1 and in Figure 2.5.2.2.

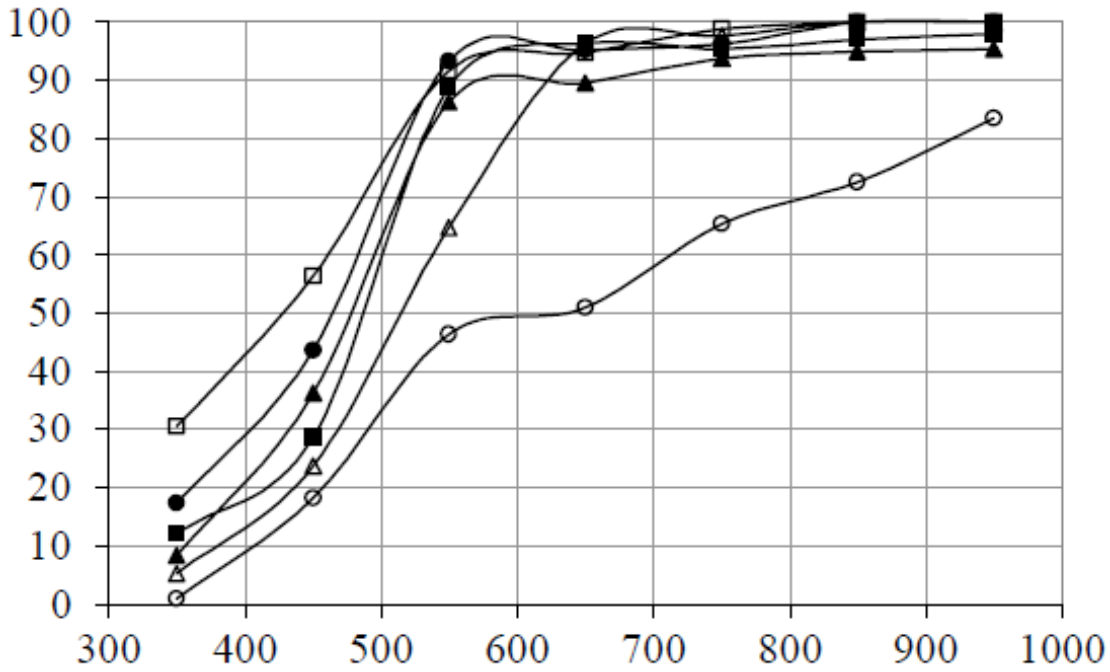

Figure 2.5.2.1. Pyritic sulfur removal from different lignite coals, during pyrolysis at different temperatures (the ordinate represents the sulfur removal % while the abscissa represents the pyrolysis temperature °C) [30]

The results shown in Figure 2.5.2.1 are based on a series of pyrolysis experiments involving untreated, HCl treated and demineralized lignite samples, which were analyzed along with their chars [30].

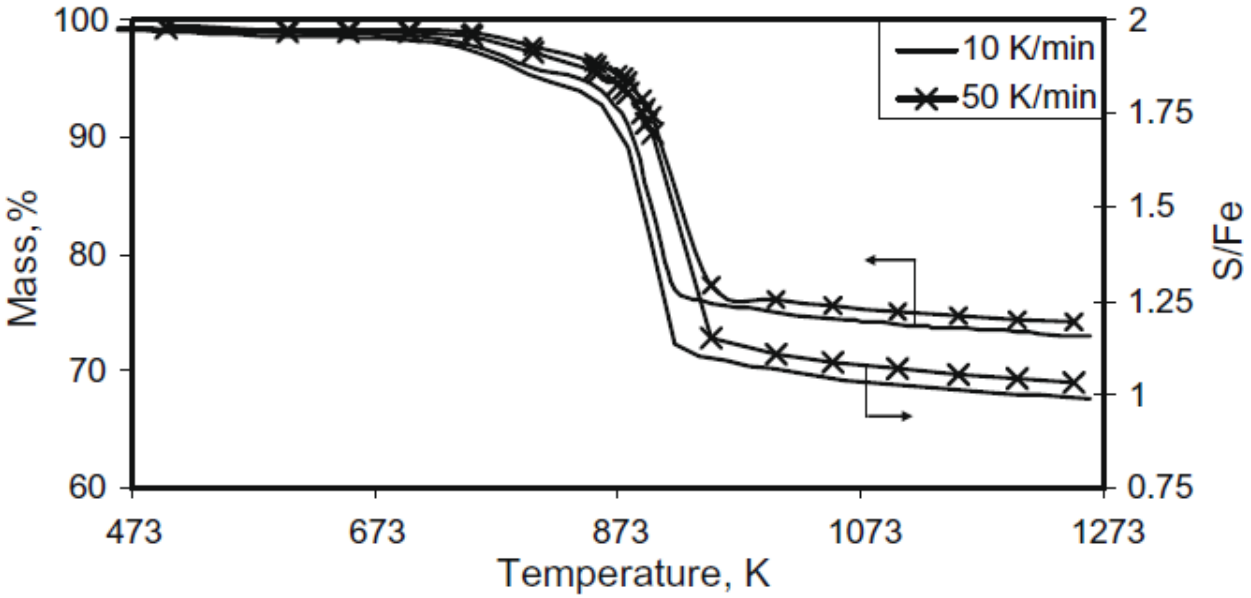

Figure 2.5.2.2. TGA mass loss and Fe/S ratio profiles of pyrite decomposition in an Australian lignite sample [31]

By comparing Figure 2.5.2.1 with Figure 2.5.2.2, it seems that in the second case there is very little pyrite decomposition taking place below 450 °C. This is because of the different heating programs used in these two cases. The experiments in Figure 2.5.2.1 [30] involved heating programs which included isothermal steps at temperature points highlighted in the figure, while the TGA experiments shown in Figure 2.5.2.2 [31] do not include isothermal conditions, the heating profile being a dynamic one. With dynamic heating, the amount of pyrite decomposed at a certain temperature is the integral of the reaction rate over time at that temperature, whereas during isothermal conditions the pyrite conversion is time dependent.

Other pyrolysis experiments highlight the uneven distribution of sulfurs, indicating sulfur transfer from the bulk of the coal to the char surface during the process [32]. These studies also showed that pyrite sulfur can be converted into organic sulfur incorporated into the bulk of the char at temperatures exceeding 500 °C.

Under coal liquefaction conditions, studies have confirmed that iron pyrite converts to iron pyrrhotite ($Fe_{1-x}S$, with $0 < x < 0.125$) at about 400 °C [33], or starting at 300 and reaching complete conversion at 400 °C [34]. The sulfur transfer into the bulk of the coal has also been confirmed at 400 °C [35, 36].

References

[1] Berkowitz, N., *An introduction to coal technology.* Academic Press: New York, 1979.

[2] Shinn, J. H. From coal to single-stage and two-stage products: A reactive model of coal structure. *Fuel* **1984***, 63*, 1187-1196.

[3] Mitchell, G. D. In *Chapter 6 - Direct Coal Liquefaction;* Suárez-Ruiz, I., Crelling, J. C., Eds.; Applied Coal Petrology; Elsevier: Burlington, 2008; pp 145-171.

[4] Davis, A.; Spackman, W.; Given, P. H. Influence of the properties of coals on their conversion into clean fuels. *Energy Sources* **1976***, 3*, 55-81.

[5] Fisher, C. H.; Sprunk, G. C.; Eishner, A.; Clarke, L.; Storch, H. H. Hydrogentation of the Banded Fusain. *Ind. Eng. Chem.* **1939***, 31*, 190-195.

[6] Neavel, R. C. Liquefaction of coal in hydrogen-donor and non-donor vehicles. *Fuel* **1976***, 55*, 237-242.

[7] Shibaoka, M. Behaviour of vitrinite macerais in some organic solvents in the autoclave. *Fuel* **1981***, 60*, 240-246.

[8] ASTM *Standard Practice for Proximate Analysis of Coal and Coke;* ASTM Standard D3172 – 07a; ASTM International: West Conshohocken, PA, 2007.

[9] ASTM *Standard Method for Ultimate Analysis Of Coal And Coke;* ASTM Standard D3176; ASTM International: West Conshohocken, PA, 2011.

[10] Rivolta, M. Solvent Extraction of Coal: Influence of solvent chemical structure on extraction yield and product composition. MSc. Thesis, University of Alberta, University of Alberta, Spring 2012.

[11] Haghighat, F. Investigation of solvent extraction of coal at low temperatures. MSc. Thesis, University of Alberta, University of Alberta, Fall 2013.

[12] Figueroa Murcia, D. C. Modelling of solvent extraction of coal. MSc. Thesis, University of Alberta, University of Alberta, Spring 2012.

[13] Franck, H.; Stadelhofer, J. W.; Biermann, D. Solubilization of bituminous coal in aromatic and hydroaromatic solvents. *Fuel* **1983***, 62*, 78-80.

[14] Tsonopoulos, C.; Ambrose, D. Vapor-Liquid Critical Properties of Elements and Compounds. 3. Aromatic Hydrocarbons. *J. Chem. Eng. Data* **1995***, 40*, 547-558.

[15] Yaws, C. L. Yaws' Critical Property Data for Chemical Engineers and Chemists. Knovel 2012.

[16] Giri, C. C.; Sharma, D. K. Mass-transfer studies of solvent extraction of coals in N-methyl-2-pyrrolidone. *Fuel* **2000***, 79*, 577-585.

[17] Laskowski, J. S. Chapter 10 Fine-coal utilization. *Developments in Mineral Processing* **2001***, 14*, 307-351.

[18] Mishra, S. K.; Klimpel, R. R. *Fine coal processing;* Noyes Publications: NJ, 1987.

[19] Kuznetsov, P. N.; Kuznetsova, L. I.; Borisevich, A. N.; Pavlenko, N. I. Effect of Mechanochemical Treatment on Supramolecular Structure of Brown Coal. *Chemistry for Sustainable Development* **2003***, 11*, 715-721.

[20] Makgato, M. H.; Moitsheki, L. J.; Shoko, L.; Kgobane, B. L.; Morgan, D. L.; Focke, W. W. Alkali-assisted coal extraction with polar aprotic solvents. *Fuel Process Technol.* **2009***, 90*, 591-598.

[21] Haghighat, F.; De Klerk, A. Direct coal liquefaction: Low temperature dissolution process. *Energy Fuels* **2014**, *28*, 1012-1019.

[22] Robinson, K.,K. Reaction Engineering of Direct Coal Liquefaction. *Energies* **2009***, 2*, 976-1006.

[23] Song, C.; Schobert, H. H.; Hatcher, P. G. In *Temperature-programmed liquefaction of low rank coal. Evaluation of coal depolymerization reactions by CPMAS ^{13}C NMR and Pyrolysis-GC-MS;* Ltd, International Energy Agency Coal Research, Ed.; 1991 International Conference on Coal Science Proceedings; Butterworth-Heinemann: 1991; pp 664-667.

[24] Derbyshire, F.; Davis, A.; Epstein, M.; Stansberry, P. Temperature-staged catalytic coal liquefaction. *Fuel* **1986***, 65*, 1233-1239.

[25] Stenberg, V. I.; Gutenkunst, V.; Nowok, J.; Sweeny, P. G. Low severity lignite liquefaction: temperature programming to 350 °C in an inorganic solvent system. *Fuel* **1989***, 68*, 133-135.

[26] Wham, R. M. Effect of slurry heating rate on short-contact-time coal liquefaction. *Fuel* **1987***, 66*, 283-284.

[27] Sachanen, A. N. *The chemical constituents of petroleum*; Reinhold: New York, 1945, p. 102-107.

[28] Lee, S. W., Preto, F., & Hayden, A. C. Determination of fuel aromatic content and its effect on residential oil combustion. *Preprints Papers Am. Chem. Soc., Div. Fuel Chem* **1986**, *31*, 275-293.

[29] Abdul-Halim Abdul-Karim, M.; Hadi, G.A. The Relationships between the Physical and Chemical Properties of Narrow Fractions Distilled From Mixed Kirkuk and Sharki-Baghdad Crude Oils. *Iraqi Journal of Chemical and Petroleum Engineering* **2008**, *9*, 1-8.

[30] Uzun, D.; Özdoğan, S. Sulfur removal from original and acid treated lignites by pyrolysis. *Fuel* **2006***, 85*, 315-322.

[31] Yani, S.; Zhang, D. An experimental study into pyrite transformation during pyrolysis of Australian lignite samples. *Fuel* **2010***, 89*, 1700-1708.

[32] Liu, F.; Li, W.; Chen, H.; Li, B. Uneven distribution of sulfurs and their transformation during coal pyrolysis. *Fuel* **2007***, 86*, 360-366.

[33] Bommannavar, A. S.; Montano, P. A. Mössbauer study of the thermal decomposition of FeS_2 in coal. *Fuel* **1982**, *61*, 523-528.

[34] Montano, P. A.; Bommannavar, A. S.; Shah, V. Mössbauer. Study of transformation of pyrite under conditions of coal liquefaction. *Fuel* **1981**, *60*, 703-711.

[35] Cleyle, P. J.; Caley, W. F.; Stewart, I.; Whiteway, S. G. Decomposition of pyrite and trapping of sulphur in a coal matrix during pyrolysis of coal. *Fuel* **1984**, *63*, 1579-1582.

[36] Rivolta Hernández, M.; Figueroa Murcia, C.; Gupta, R.; De Klerk, A. Solvent-coal-mineral interaction during solvent extraction of coal. *Energy Fuels* **2012**, *26*, 6834-6842.

CHAPTER 3 – COAL LIQUEFACTION LIQUID QUALITY: IMPACT OF TEMPERATURE AND IRON PYRITE

Abstract

Direct coal liquefaction studies are focused mainly on the liquid yield. This study evaluated the impact of the reaction temperature and of the coal contained iron pyrite on the quality of the coal liquids that can be obtained by solvent extraction in the temperature range from 340 to 415 ^{0}C, nitrogen atmosphere, autogenous pressure and 1 hour liquefaction time. The experiments were performed with a Canadian lignite coal from Boundary Dam and tetralin as prototypical hydrogen donor solvent in a 1:3 coal to solvent ratio. It was found that as the liquefaction temperature was increased from 343 to 368 ^{0}C, the density of the coal liquids increased by ~50 kg/m^3, while their boiling points predominantly decreased, indicating an increase in the aromatic content. This trend continued with increasing temperatures, but at a much slower rate, the coal liquid density beyond reaction at 368 ^{0}C remaining constant. Iron pyrite was increasingly converted as temperature was increased. The sulfur was transferred out of the residue, implying that with increasing temperature more transferrable hydrogen was sacrificed to reduce iron pyrite. However, this was not conclusively demonstrated, because of the heterogeneous character of the coal, which increased sample to sample variation. With increasing temperature, a decrease in residue moisture could also be observed.

Keywords: coal, liquefaction, temperature, yield, quality, sulfur

3.1 Introduction

Direct coal liquefaction studies are often focused on the liquid yield that can be obtained from the coal, with the quality of the coal liquids being of secondary importance. A reason for this tendency might be the fact that a coal liquid quality improvement can also be achieved through the adjustment of product properties by downstream hydroprocessing. It is recognized that the degree of heteroatom removal and the concomitant quality increase depend on hydroprocessing severity [1]. There are, however, desirable properties of the coal liquids which can be deteriorated once the hydroprocessing severity is increased, such as the octane number of the naphtha fraction [2]. Furthermore, this involves higher amounts of hydrogen being used, which is economically unfavorable. It is consequently beneficial to produce coal liquids that require less intensive downstream refining.

During the direct coal liquefaction process, there are certain possible sulfur transfer routes which might influence more or less the resulting quality of the coal liquids. Literature indicates that conversion of iron pyrite (FeS_2) to iron pyrrhotite ($Fe_{1-x}S$, with $0 < x < 0.125$) was found at 400 °C, although detectable only after 30 min of reaction time [3]. It was also shown that in the presence of a solvent, iron pyrite was transformed into iron pyrrhotite at temperatures above 300 °C and complete conversion could be achieved at 400 °C [4]. This implies sulfur transfer from the mineral matter either towards the coal molecular structure, or towards the coal liquids, being subsequently converted to H_2S. Indeed, it was shown that sulfur was transferred from the iron pyrite to the organic coal matrix on a distance of ~1 μm, after exposure to 400 °C for 20 h [5], even though the study did not evaluate transfer to liquids. Previous work confirmed the pyritic sulfur transfer to the organic coal portion at 400 °C and 1 h reaction time [6]. Consequently, the question to be answered is whether the coal liquid quality can be improved by manipulating sulfur transfer via different temperature control approaches.

This chapter is based on the hypothesis that by applying lower initial temperatures, the quality of the coal liquids produced by direct coal liquefaction can be improved. More moderate conditions would lower the rate of dissolution, leading to a smaller risk of creating zones with insufficient hydrogen transfer. The objective of this chapter was to evaluate the potential role of reaction temperature and iron pyrite on the quality of coal liquids and on the ultimate yield of

coal liquids that can be obtained by the solvent extraction of coal in the temperature range 340-415 °C.

3.2 Experimental procedure

3.2.1 Materials

A Canadian lignite coal, Boundary Dam, was employed for the liquefaction experiments as one of the feed materials. Preparation involved grinding the coal in a Retsch PM100 ball mill at 330 rpm for 5 minutes and collecting the 106-425 μm particle size range by sieving. The coal was dried at 80 °C and -45 kPa gauge for 8 hours in a Yamato DP43 vacuum drying oven before characterization and use.

The instruments used for the coal characterization were a Carlo Erba EA1108 Elemental Analyzer for the elemental analysis and a LECO TGA 701 for the proximate analysis. The method for analyzing the moisture, volatiles and ash content was a standard ASTM method for proximate analysis of coal and coke [7]. Coal characterization is shown in Table 3.2.1.1.

Table 3.2.1.1. Characterization of Boundary Dam Lignite Coal

Proximate Analysis (wt %)	
Moisture	12.8 ± 0.1
Ash	11.9 ± 0.1
Volatile Matter	35.6 ± 0.6
Fixed Carbon	39.7 ± 0.6
Ultimate Analysis (wt %, ash free)	
Carbon	53.2 ± 0.5
Hydrogen	4.2 ± 0.1
Nitrogen	0.94 ± 0.01
Sulfur	0.30 ± 0.03
Oxygen (by difference)	41.4

Sigma-Aldrich ReagentPlus 1,2,3,4-tetrahydronaphthalene (tetralin) of 99% purity was used as a hydrogen donor solvent.

3.2.2 Equipment and procedure

The coal liquefaction experiments were conducted in micro-batch reactors constructed from Swagelok 316 stainless steel tubing and fittings. For each reaction set, four reactors of 15 ml volume were fastened on a holder, one of them being equipped with an OMEGA® K-type thermocouple and a pressure gauge on its inlet pipe, as shown in Figure 3.2.2.1.

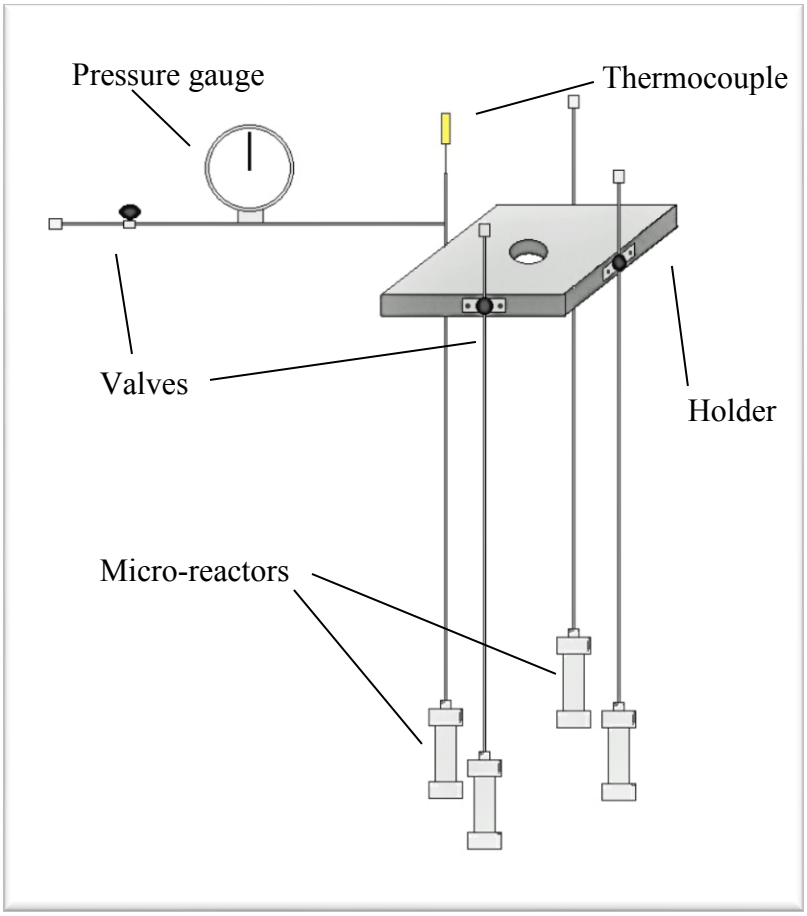

Figure 3.2.2.1. Reaction setup for coal liquefaction representing one set (four individual experiments used for calculating the average and standard deviation of the reaction set).

In a typical experiment each reactor was loaded with 2.5 g of coal and 7.5 g of tetralin. The caps of the reactors were lubricated with Swagelok® Silver Goop® oil-based thread lubricant, and then the reactors were purged with N_2 while being checked for leaks with Swagelok® Snoop® liquid leak detector. Finally, they were placed in a Techne SBS-4 fluidized sand bath heater to be heated to the required reaction temperature in the range 340-415 °C. For a total of 7 reaction sets, the sand bath was preheated to 360, 375, 395, 410, 425 and 430 °C respectively. The internal temperatures corresponding to these sand bath set point temperatures were: 343.3, 367.9, 392.6, 396.9, 408, 411 and 415.2 °C. The total reaction time was 60 minutes, which included ~6 min heat-up time. A typical heating profile can be seen in Figure 3.2.2.2. At the end of the experiment the reactors were cooled down to room temperature with air. Each reactor was weighed at certain points during the preparation process and after the reaction, as shown in Section 3.2.4 (Calculations).

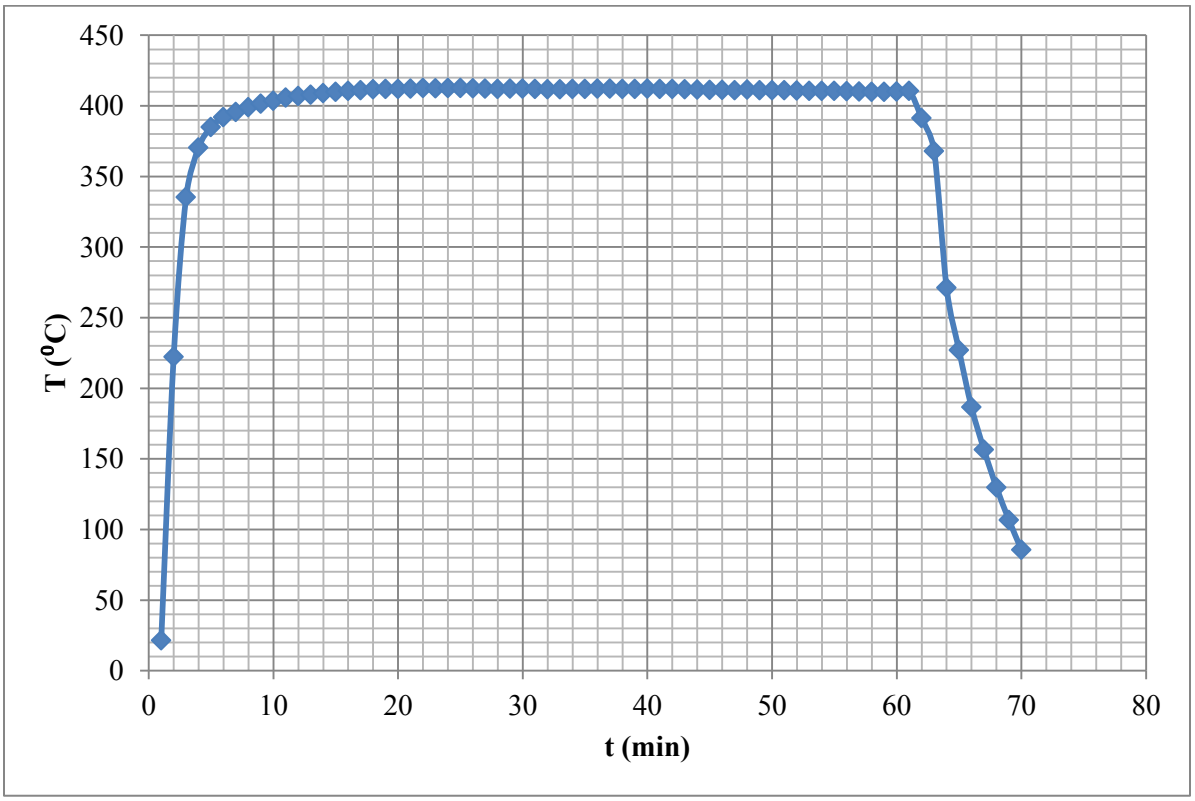

Figure 3.2.2.2. Example of a typical heating and cooling profile for the coal liquefaction experiment at 411 °C. The temperature was recorded in time intervals of 1 minute.

The products were kept in the reactors overnight, and then vacuum filtered using Millipore™ Durapore™ PVDF membrane filters of 0.22 µm pore size and 47 mm diameter. The filter membranes were placed in aluminum pans and weighed before and after filtration. The reactors were washed with 3-5 g of tetralin, the precise amount being recorded. The liquids were then stored in Fisherbrand™ Class B clear glass threaded vials in a cool, dark place. The residues were kept in aluminum pans overnight and then vacuum dried for 8 hours at 115 °C and -54 kPa gauge in a Cole-Parmer StableTemp® vacuum oven. After weighing, the dried residues were similarly stored. The procedure is summarized in the flow diagram shown in Figure 3.2.2.3.

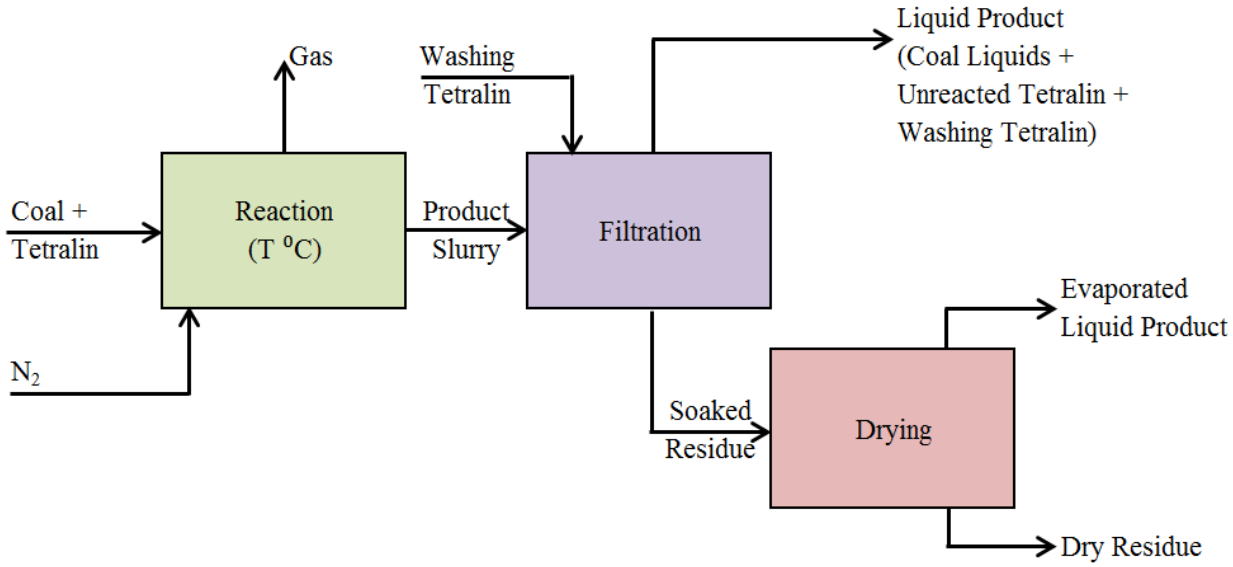

Figure 3.2.2.3. Schematic of the Experimental Procedure used for Coal Liquefaction with Tetralin at Different Temperatures.

It is important to highlight the nomenclature of the following terms, as used throughout this chapter:

Diluted liquid product refers to the mixture of coal liquids, unreacted tetralin and washing tetralin, as resulted after the filtration operation.

Liquid product refers to the mixture of coal liquids and unreacted tetralin, excluding the washing tetralin used for the filtration operation.

Coal liquids refers strictly to the coal derived products which are present in the liquid mixture, i.e. products excluding tetralin.

3.2.3 Analyses

The liquids and residues were characterized using different analytical methods:

(a) Proximate analysis of residues: LECO TGA 701. Method: ASTM D7582-12 [7]. The reaction product yield was calculated based on this analysis. The proximate analysis was performed for all of the four residues of each reaction set.

(b) Density of liquid products and coal liquids: Anton Paar DMA 4500M density meter. All density measurements were made at 25 °C.

(c) Refractive index of the diluted liquid products: Anton Paar Abbemat 200 refractometer. The refractive index was determined relative to air by using the sodium D-line (589 nm), at 20 °C.

(d) Simulated distillation (SimDis) of the diluted liquid products: ASTM D7169-11 [8]. Equipment: Varian 450-GC Gas Cromatograph operated with an Agilent Capillary Column, CP-SimDist CB High Temp, [length (m) x inner diameter (mm) x film thickness (μm) = 5 x 0.53 x 0.09]. Chromatography Software: CompassCDS, Version 3.0.0.68 (Bruker).

(e) Stereomicroscopy for the residues: Carl Zeiss SteREO Discovery V.20 stereomicroscope. Pictures were taken at 50x, 70x and 150x magnification.

(f) Scanning electron microscopy (SEM) for the residues: Zeiss EVO MA 15 equipped with a Burker Quantax 200 energy dispersive X-ray fluorescence (XRF) spectrometer. One residue sample of each reaction set was chosen for this analysis.

(g) Fourier Transform Infrared (FTIR) spectroscopy for both residues and liquid products: ABB MIRacle® FTIR Spectrometer, with the following settings: 120 transmittance scans, resolution 4 cm^{-1}, detector gain 81 and wave number range 400-4000 cm^{-1}.

(h) Proton NMR spectrometry for the liquid products: Nanalysis NMReady 60 V.0.9, 60 MHz pulsed Fourier transform NMR spectrometer, with the following settings: 14 ppm spectral width, 4K points, 20 s scan delay, 32 scans. The reference solvent used was

Chloroform-d, "100%", 99.96 atom % D from Sigma Aldrich. The NMR samples were prepared by mixing the liquefaction liquid product with chloroform-d in a volumetric ratio of 1:1, to form a total of 760 µl solution.

3.2.4 Calculations

The *mass balance*, $M_b(\%)$, for each reaction was calculated the following way:

$$M_b(\%) = 100 \cdot \frac{S_f + G_f}{S_i + G_i} \tag{3.2.4.1}$$

Where S_f = mass of suspension after reaction (g);
G_f = mass of gases after reaction (g);
S_i = mass of suspension before reaction (g);
G_i = mass of gases before reaction (g).

$$S_f = (m_6 - m_1) + (m_3 - m_2) \tag{3.2.4.2}$$

$$G_f = m_5 - m_6 \tag{3.2.4.3}$$

$$S_i = m_2 - m_1 \tag{3.2.4.4}$$

$$G_i = m_4 - m_3 \tag{3.2.4.5}$$

Where m_1 = mass of empty reactor and tubing (g);
m_2 = mass of reactor and tubing after addition of coal and tetralin (g);
m_3 = mass of reactor and tubing after thread lubrication (g);
m_4 = mass of reactor and tubing after N_2 purging (g);
m_5 = mass of reactor and tubing after reaction (g);
m_6 = mass of reactor and tubing after release of reaction gases (g).

The reason for including the second bracket in equation (3.2.4.2) was the fact that during the reaction time, most of the lubricant was lost. Without considering this fact, the mass loss

would be attributed to inexistent leaks instead of the lubricant loss, resulting in a false mass balance. Due to traces of lubricant still present on the reactor threads at the end of the reaction time, the resulting mass balance for some of the reactions slightly exceeded 100%.

The *liquid yield*, $Y(\%)$, for the liquefaction reactions was calculated the following way:

$$Y(\%) = 100 \cdot \frac{M_{coal} \cdot \left(1 - \frac{Moist_{coal} + Ash_{coal}}{100}\right) - M_{res} \cdot \left(1 - \frac{Moist_{res} + Ash_{res}}{100}\right)}{M_{coal} \cdot \left(1 - \frac{Moist_{coal} + Ash_{coal}}{100}\right)} \quad (3.2.4.6)$$

Where M_{coal} = initial mass of coal (g);

$Moist_{coal}$ = moisture percentage of coal (%);

Ash_{coal} = ash percentage of coal (%);

M_{res} = mass of residue after separation and drying (g);

$Moist_{res}$ = moisture percentage of residue (%);

Ash_{res} = ash percentage of residue (%).

Liquid product density, $\rho_{lp}\left(\frac{kg}{m^3}\right)$, was calculated based on the density measurement of the diluted product resulted after washing the reactors with tetralin, the following way:

$$\rho_{lp}\left(\frac{kg}{m^3}\right) = \frac{x_{lp/dp}}{\frac{1}{\rho_{dp}} - \frac{x_{wt/dp}}{\rho_t}} \quad (3.2.4.7)$$

Where $x_{lp/dp}$ = mass fraction of liquid product in the diluted product $\left(\frac{g\ of\ liquid\ product}{g\ of\ diluted\ product}\right)$;

$x_{wt/dp}$ = mass fraction of washing tetralin, in the diluted product $\left(\frac{g\ of\ washing\ tetralin}{g\ of\ diluted\ product}\right)$;

ρ_{dp} = density of diluted product $\left(\frac{kg}{m^3}\right)$;

ρ_t = density of tetralin: 0.973 $\frac{kg}{m^3}$.

Coal liquid density, $\rho_{cl}\left(\frac{kg}{m^3}\right)$, was calculated based on the liquid product density, using the same principle of dilution while considering the composition of the liquid product itself:

$$\rho_{cl}\left(\frac{kg}{m^3}\right) = \frac{x_{cl/lp}}{\frac{1}{\rho_{lp}} - \frac{x_{t/lp}}{\rho_t}} \tag{3.2.4.8}$$

Where $x_{cl/lp}$ = mass fraction of coal liquids in the liquid product $\left(\frac{g\ of\ coal\ liquids}{g\ of\ liquid\ product}\right)$;

$x_{t/lp}$ = mass fraction of tetralin, in liquid product $\left(\frac{g\ of\ tetralin}{g\ of\ liquid\ product}\right)$.

Liquid product composition is represented by the mass fraction of coal liquids, $x_{cl/lp}$, and the mass fraction of unreacted tetralin, $x_{t/lp}$, in the liquid product. These were calculated based on the coal liquid yield, using the following equations:

$$x_{cl/lp} = \frac{Y(\%)}{100} \cdot \frac{m_{total\ product}}{m_{lp}} \tag{3.2.4.9}$$

$$m_{total\ product} = m_6 - m_1 \tag{3.2.4.10}$$

$$m_{lp} = m_{total\ product} - m_{residue} \tag{3.2.4.11}$$

$$x_{t/lp} = 1 - x_{cl/lp} \tag{3.2.4.12}$$

Where $m_{residue}$ = mass of the residue after drying (g);

Diluted product composition is represented by the mass fraction of coal liquids, $x_{cl/dp}$, and the mass fraction of tetralin, $x_{t/dp}$, in the diluted product. These were calculated based on the coal liquid yield, using the following equations:

$$x_{cl/dp} = \frac{Y(\%)}{100} \cdot \frac{m_{total\ product}}{m_{lp} + m_{wt}} \tag{3.2.4.13}$$

Where m_{wt} = mass of tetralin used for washing (g).

$$x_{t/dp} = 1 - x_{cl/dp} \tag{3.2.4.14}$$

The *Aromatic to aliphatic proton ratio,* $R_{aro:ali}$, in the coal liquids, was calculated from the proton NMR analysis data, while considering that the values of the NMR peak integrals are proportional to the substituted aromatic respectively aliphatic protons in the diluted product.

$$R_{aro:ali} = \frac{x_{aro/cl}}{x_{ali/cl}} \tag{3.2.4.15}$$

$$x_{ali/cl} = \frac{x_{ali/dp} - x_{t/dp} \cdot x_{ali/t}}{x_{cl/dp}} \tag{3.2.4.16}$$

$$x_{aro/cl} = \frac{x_{aro/dp} - x_{t/dp} \cdot x_{aro/t}}{x_{cl/dp}} \tag{3.2.4.17}$$

$$x_{ali/dp} = \frac{I_{ali/dp}}{I_{ali/dp} + I_{aro/dp}} \tag{3.2.4.18}$$

$$x_{aro/dp} = \frac{I_{aro/dp}}{I_{ali/dp} + I_{aro/dp}} \tag{3.2.4.19}$$

Where $x_{ali/cl}$ = fraction of aliphatic protons in the coal liquids;

$x_{aro/cl}$ = fraction of aromatic protons in the coal liquids;

$x_{ali/t}$ = fraction of aliphatic protons in tetralin;

$x_{aro/t}$ = fraction of aromatic protons in tetralin;

$I_{ali/dp}$ = integral value corresponding to the aliphatic NMR peaks of the diluted product;

$I_{aro/dp}$ = integral value corresponding to the aromatic NMR peaks of the diluted product.

3.3 Results

3.3.1 Product Yield

The product yield was determined based on the residue proximate analysis mentioned in Section 3.2.3, performed in quadruplicate*, and the coal liquid yield was calculated using Equation 3.2.4.6. The results are shown in Table 3.3.1.1 and in Figure 3.4.1.1.

Table 3.3.1.1. Overall Product Yield from Boundary Dam Lignite Liquefaction with Tetralin under N_2 Atmosphere and 1 h at Different Liquefaction Temperatures

Liquefaction Temperature (°C)	Liquid Yield (wt%)	Proximate analysis of residue (wt %)			
		Volatile matter	Fixed carbon	Ash	Moisture
343	19.62 ± 3.21	29.67 ± 1.36	38.56 ± 1.15	10.29 ± 1.83	1.85 ± 0.58
368	26.19 ± 1.59	25.64 ± 0.88	35.16 ± 0.42	11.77 ± 1.09	1.25 ± 0.52
393*	37.58 ± 5.78	19.50 ± 2.68	30.03 ± 0.71	12.03 ± 2.62	0.86 ± 0.65
397	39.23 ± 3.96	18.81 ± 3.26	29.69 ± 0.57	10.77 ± 3.73	1.50 ± 1.97
411	46.15 ± 2.58	14.21 ± 2.02	26.76 ± 0.44	12.40 ± 2.23	0.49 ± 0.28
415	48.87 ± 3.58	13.32 ± 1.85	25.35 ± 0.47	12.04 ± 1.58	0.42 ± 0.17

*All the analyses were performed in quadruplicate, with the exception of the 393 °C set, for which the analysis was performed in triplicate.

3.3.2 Refractive Index and Density of the Liquid Product and Coal Liquids

The results for the density and refractive index analyses are shown in Table 3.3.2.1. Densities were measured for the samples diluted with washing tetralin. The liquid product density represents the undiluted liquid, as calculated with Equation 3.2.4.7. The coal liquid density corresponds to the coal liquids void of any unreacted tetralin, as calculated with Equation 3.2.4.8. Refractive index measurements, on the other hand, represent the tetralin diluted samples.

Table 3.3.2.1. Refractive Index and density of the Liquid Products and Coal Liquids Obtained by Liquefaction at Different Temperatures

Liquefaction Temperature (°C)	Diluted Product Refractive Index at 20 °C	Liquid Product Density at 25 °C (kg/m^3)	Coal Liquid Density at 25 °C (kg/m^3)
343	1.5448 ± 0.0004	963.8 ± 0.6	933.9 ± 8.8
368	1.5482 ± 0.0006	977.5 ± 1.2	987.5 ± 3.9
393	1.5526 ± 0.0011	981.4 ± 0.9	992.2 ± 4.4
397	1.5544 ± 0.0011	983.5 ± 1.4	996.8 ± 6.0
411	1.5564 ± 0.0008	982.2 ± 0.7	990.7 ± 2.5
415	1.5557 ± 0.0013	983.0 ± 1.1	991.6 ± 3.6

3.3.3 Simulated Distillation

The results from the SimDis analysis reveal the highly diluted nature of the liquid samples with tetralin. This can be observed in Figure 3.3.3.1, where the true boiling point (TBP) curves include a very wide, low-sloped portion at around 200 °C.

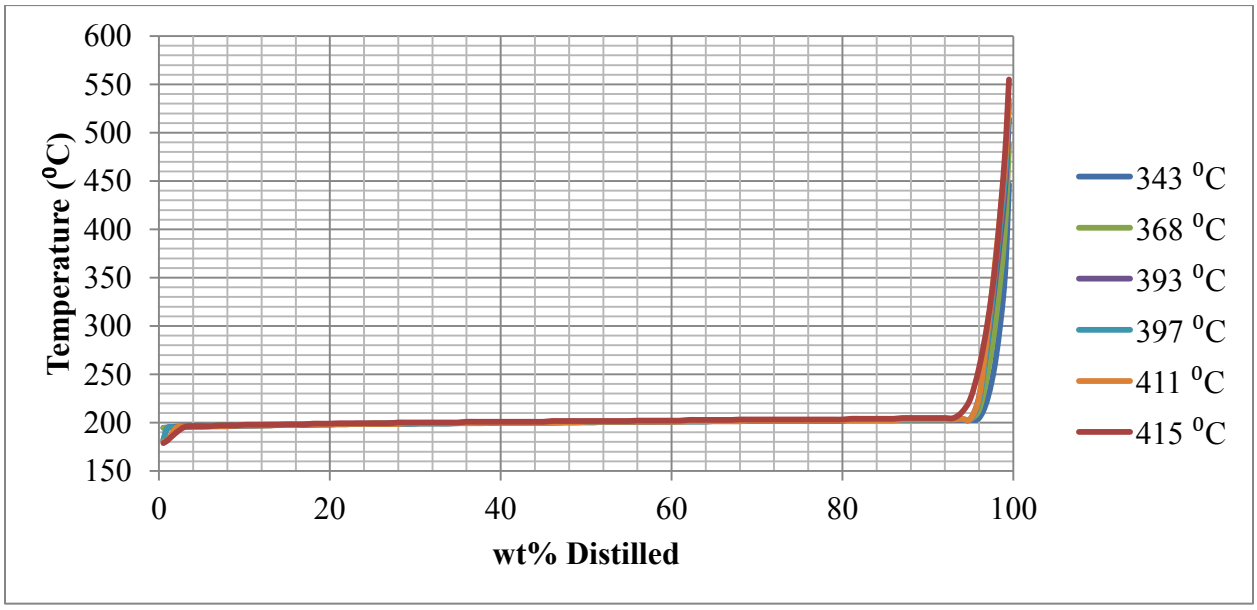

Figure 3.3.3.1. TBP Curves of the Diluted Liquid Products, as resulted from the SimDis Analysis

The same dilution can be observed in Figure 3.3.3.2, in form of a very large peak in the SimDis chromatogram. These dilution effects were corrected by processing the SimDis data after subtracting the known amount of tetralin. These results are discussed in Section 3.4.2.

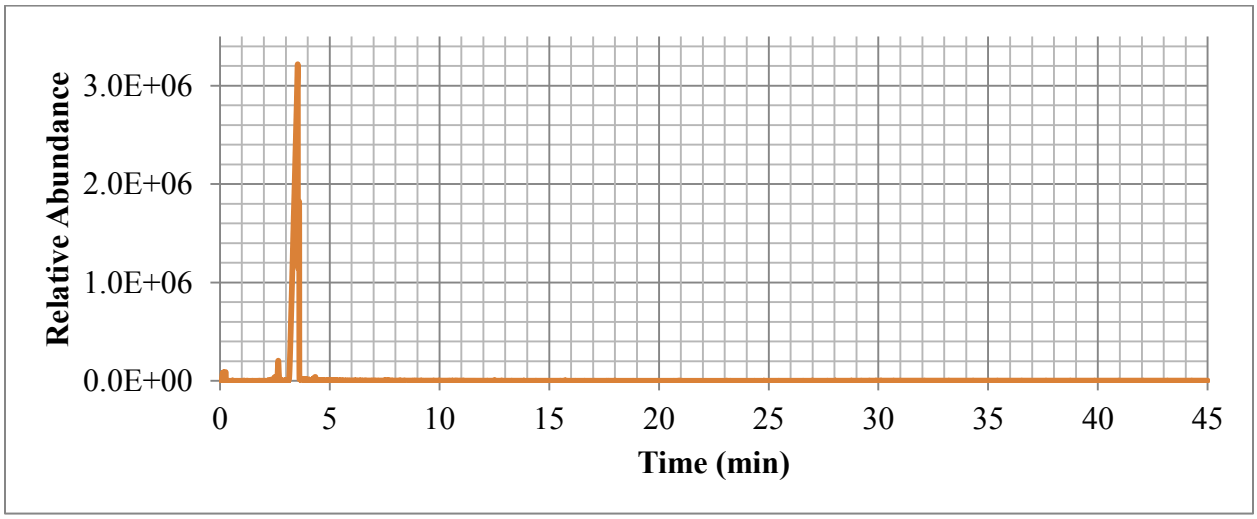

Figure 3.3.3.2. SimDis Chromatogram showing a high tetralin amount in the liquid samples

3.3.4 Residue Stereomicroscopy

Pictures of the liquefaction residues were taken at three different scales (50x, 70x, 150x) for each quadruplicate of each reaction set. Two examples are shown in Figure 3.3.4.1. The rest of the pictures are being discussed in Section 3.4.3.

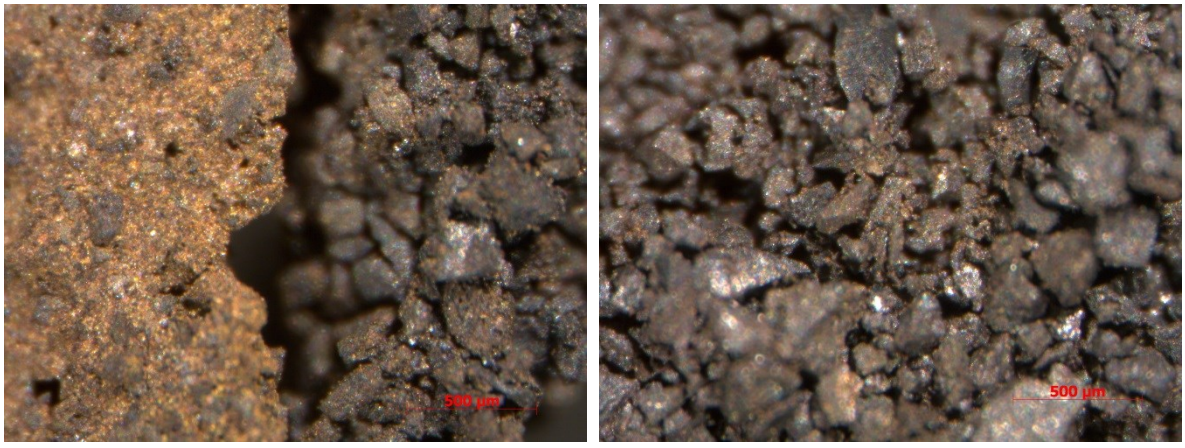

Figure 3.3.4.1. Examples of stereomicroscopy pictures of residues from coal liquefaction at 368 °C (left) and 393 °C (right)

3.3.5 Scanning Electron Microscopy and XRF Spectrometry

The coal liquefaction residues were analyzed by SEM and the compositions of different regions were determined by XRF spectrometry. The regions chosen for XRF analysis were areas representative for larger portions of the coal matrix, but also small mineral particles as shown in the example below. The aim of this analysis was to see whether there is a particular trend in sulfur transfer for different liquefaction temperatures, as discussed in Section 3.4.4. An example of the SEM-XRF analysis is shown in Figure 3.3.5.1 (SEM picture), and in Figures 3.3.5.2 and 3.3.5.3 (XRF spectra for the points marked on the SEM image).

Figure 3.3.5.1. Example of SEM analysis of residue from coal liquefaction at 368 °C, with XRF analysis for the area 1, and point 2 as noted in the picture (XRF spectra shown in Figures 3.3.5.2 and 3.3.5.3).

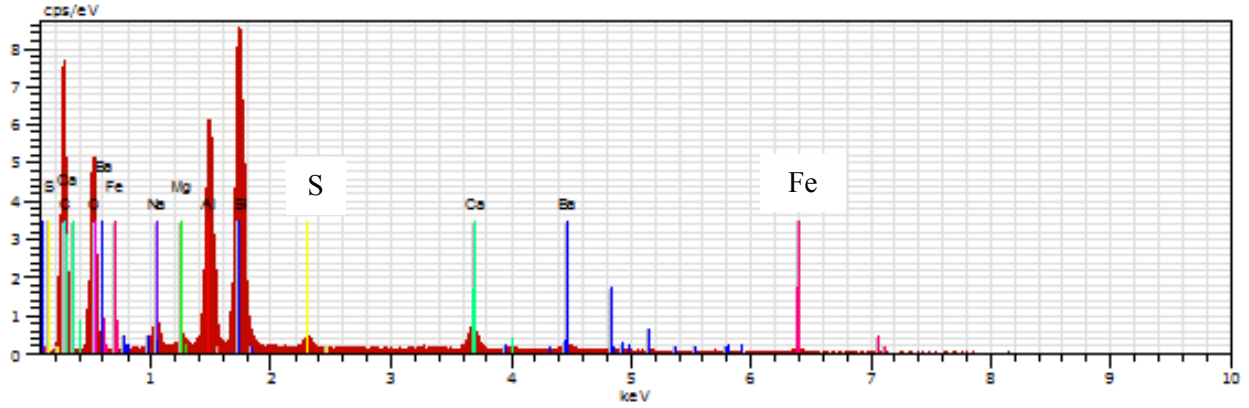

Figure 3.3.5.2. XRF spectrum of residue from coal liquefaction at 368 ºC, for the area marked "1" in Figure 3.3.5.1.

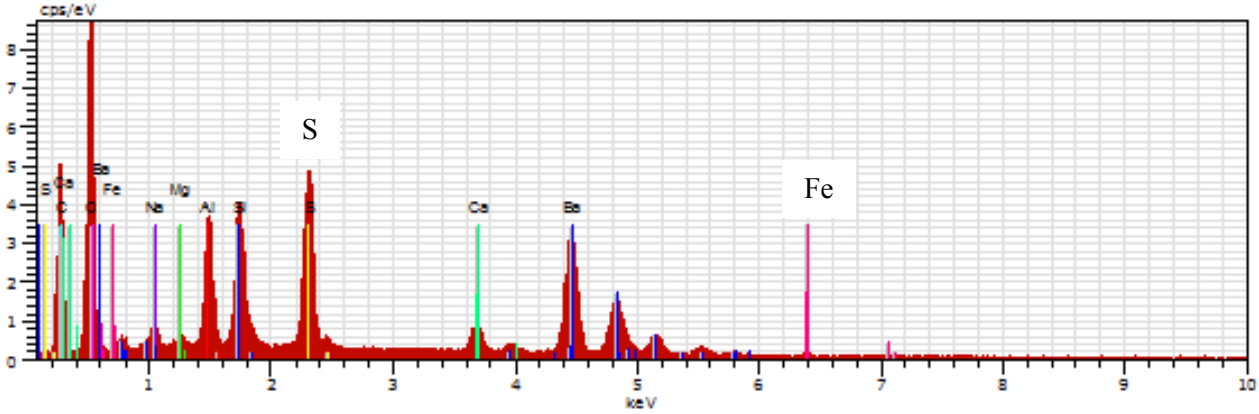

Figure 3.3.5.3. XRF spectrum of residue from coal liquefaction at 368 ºC, for the point marked "2" in Figure 3.3.5.1.

3.3.6 Fourier Transform Infrared Spectra

Both liquefaction residues and diluted liquid products were analyzed by FTIR spectroscopy. Due to the tetralin dilution, not much difference could be seen between the FTIR spectra of the liquid products of different liquefaction temperatures. On the other hand, the residues did present a few changes in terms of new transmittance peaks and also in terms of peak intensity. The results are shown and discussed in Section 3.4.5.

3.3.7 Proton NMR spectra

A typical NMR spectrum of a diluted liquid sample is shown in Figure 3.3.7.1. The comparison with the spectrum of tetralin (Figure 3.3.7.2) reveals the difficulty of an accurate calculation of the ratio between aromatic and aliphatic protons in the undiluted coal liquids.

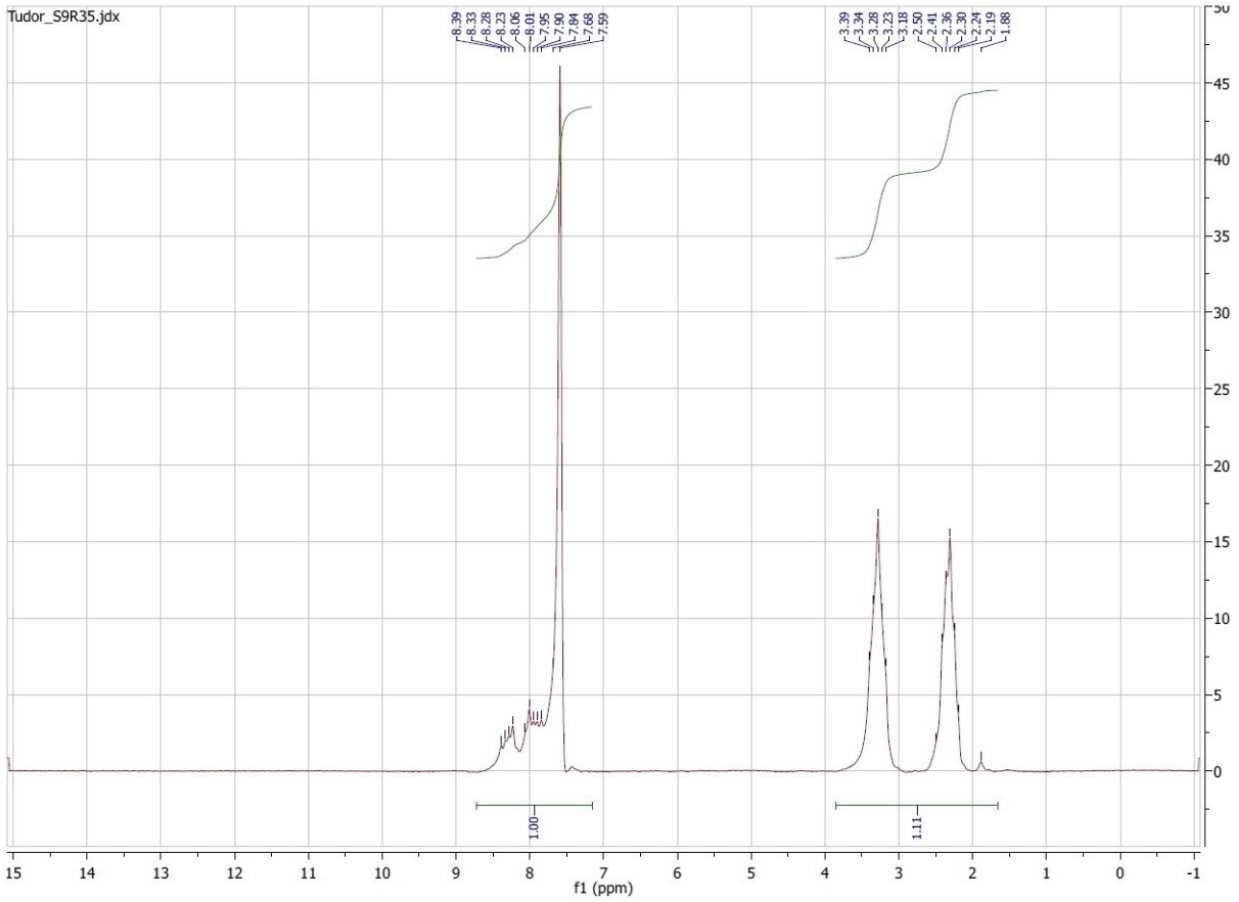

Figure 3.3.7.1. Example of a proton NMR spectrum for one of the diluted liquid products of coal liquefaction at 397 °C

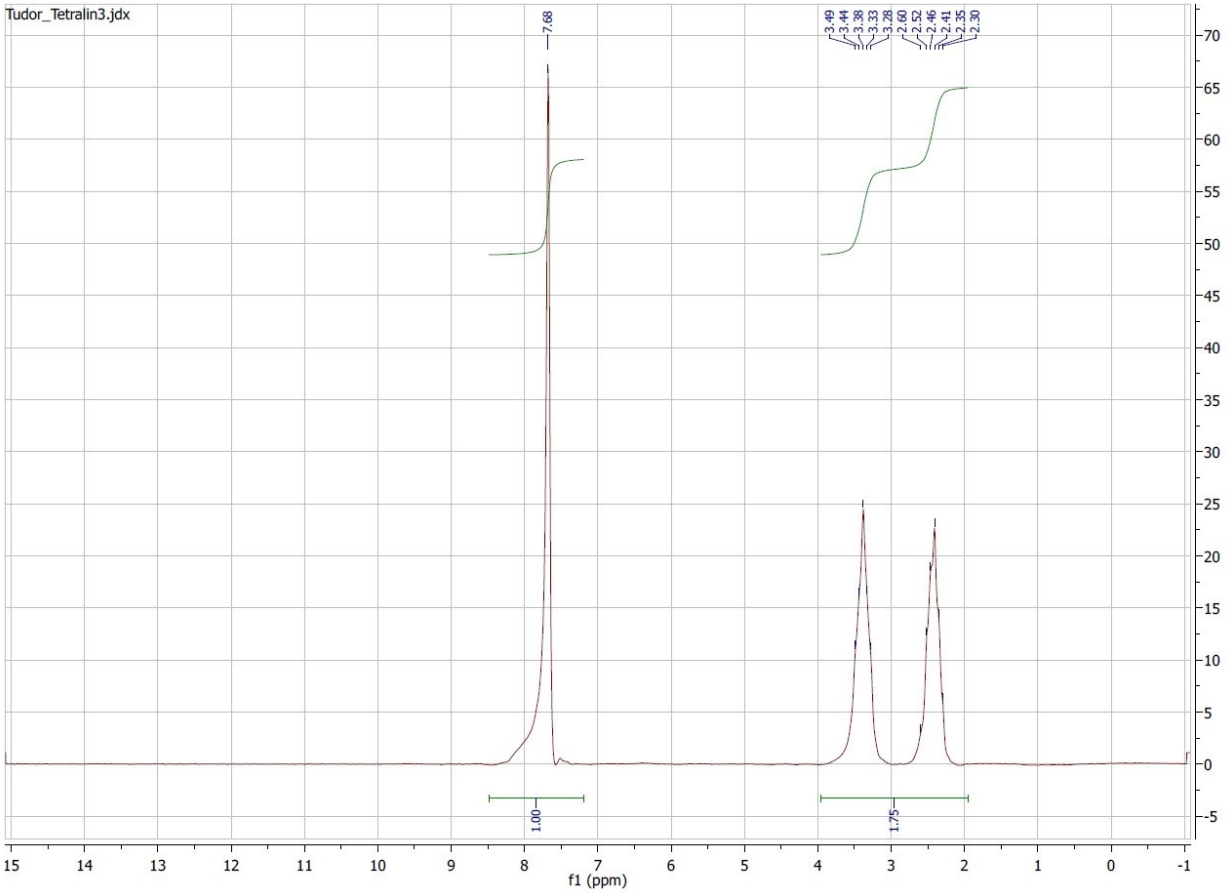

Figure 3.3.7.2. Proton NMR spectrum for tetralin.

Despite this dilution generated difficulty, the ratio was calculated by using Equation 3.2.4.15, and the results are shown in Table 3.3.7.1, while being discussed in Section 3.4.6.

Table 3.3.7.1. Effect of Liquefaction Temperature on the Aromatic to Aliphatic Proton Ratio of the Coal Liquids. Unreliable data points at low temperatures due to the high tetralin dilution.

Liquefaction Temperature (^{0}C)	Aromatic : Aliphatic Protons Ratio
343	26.112 ± 35.461
368	4.268 ± 2.258
393	2.875 ± 0.759
397	1.87 ± 0.295
411	1.709 ± 0.404
415	1.532 ± 0.613

3.4 Discussion

3.4.1 Temperature Influence on Product Yield

The results shown in Table 3.3.1.1 can be seen in bar graph form in Figure 3.4.1.1:

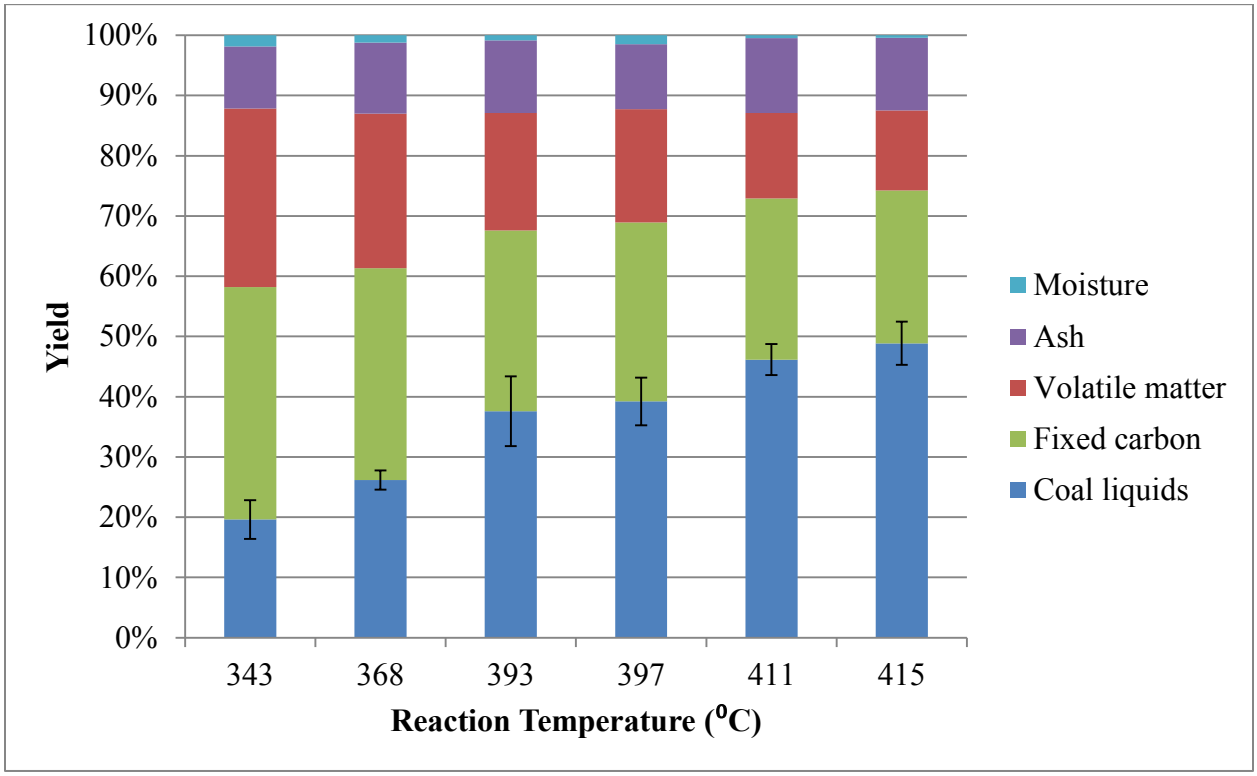

Figure 3.4.1.1. Product Yield for Coal Liquefaction at Different Temperatures

The liquid yield predictably increased with liquefaction temperature. For the first three temperature points, 343, 368 and 393 °C, there is a clear increase. However, between 393 and 397 °C the increase is not statistically significant. The same can be said about the 411 and 415 °C yield values, but the fact that there is a significant increase between 397 and 411 °C indicates that the reason for these close yield values is the small temperature difference between these points: 4 °C. This can be better observed in Figure 3.4.1.2:

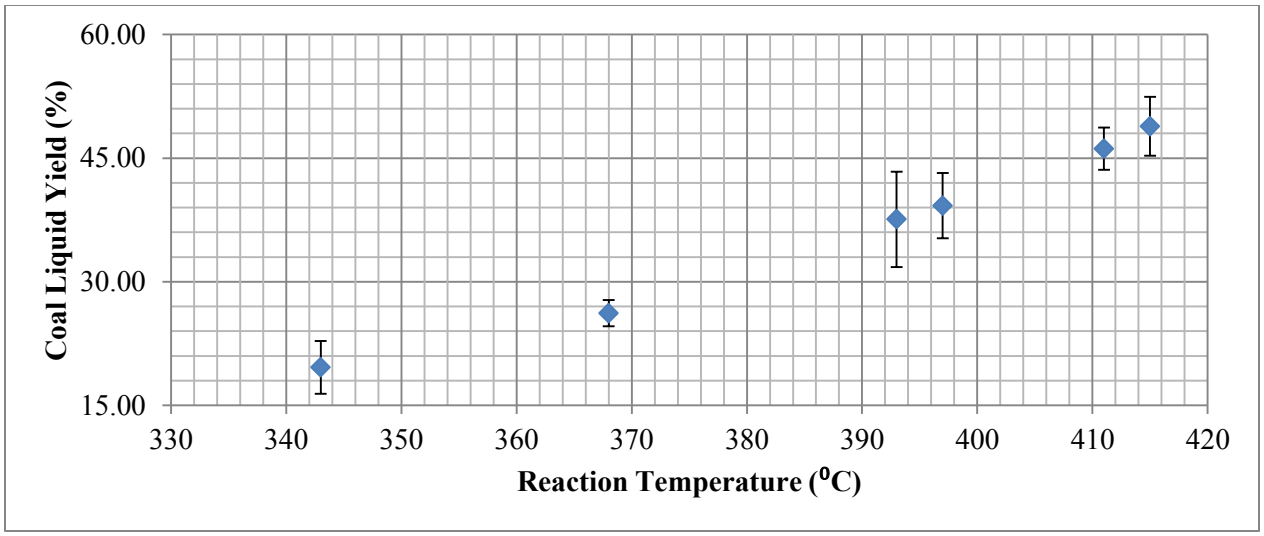

Figure 3.4.1.2. Coal Liquid Yield for Coal Liquefaction at Different Temperatures

3.4.2 Temperature Influence on Liquid Quality: Density, Refractive Index and Boiling Ranges

The results from Table 3.3.2.1 have been rearranged in form of charts, and can be seen in Figure 3.4.2.1 and in Figure 3.4.2.2:

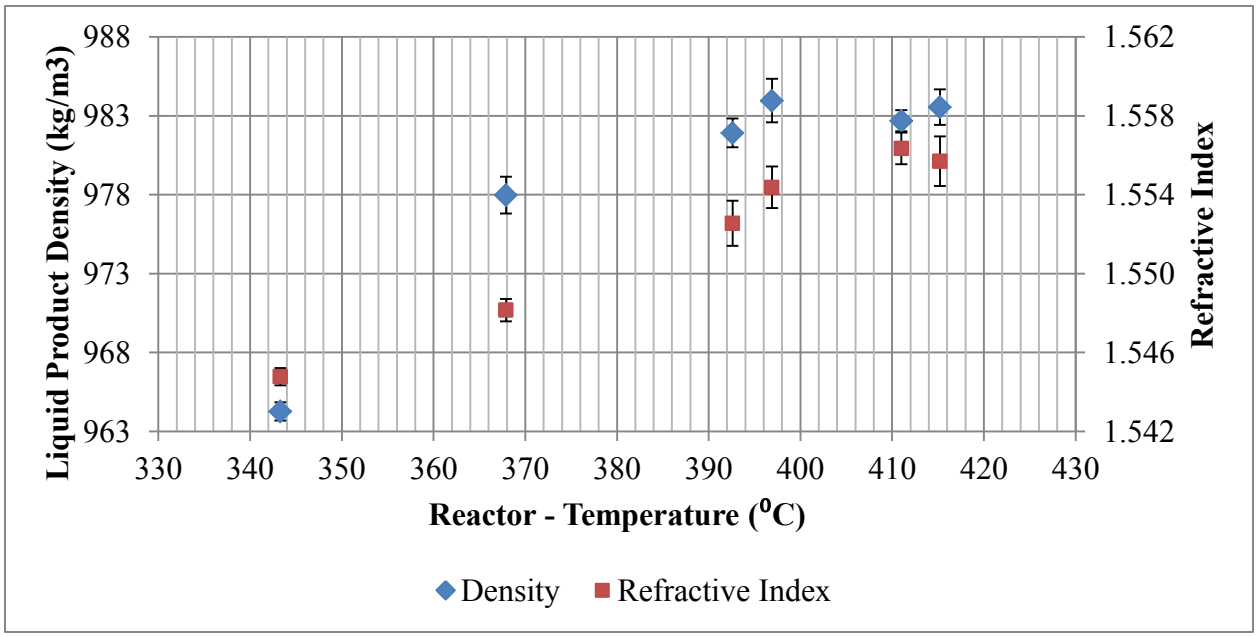

Figure 3.4.2.1. Density and Refractive Index of Coal Liquefaction Liquid Product for Different Reaction Temperatures

The refractive index of the diluted liquid product is increasing with liquefaction temperature for the first five points. The decrease for the last reaction temperature is most probably caused by a slightly higher dilution of the liquid samples of that temperature set with washing tetralin, but statistically the last two refractive index points are equivalent. Similarly, the liquid product density shows a clear increase for the first 3-4 points, remaining statistically unchanged for the higher temperatures. According to literature, physical properties like the density and the refractive index are indicators of the aromatic content of the coal liquids [9-11], which is a measure of coal liquid quality (see Chapter 2). But before concluding anything about the aromatic content of these samples, we have to consider the fact that each of these reaction sets has been carried out at a different temperature, leading to a higher or lower coal conversion. Based on the liquid yields (Figure 3.4.2.1), the amount of unreacted tetralin was calculated (Equation 3.2.4.14) and its effect on the resulting densities was removed (Equation 3.2.4.8). The resulting coal liquid density profile can be seen in Figure 3.4.2.2. As for the refractive index, no further calculation was made, its increase being susceptible to the yield difference, as well as to the washing tetralin dilution.

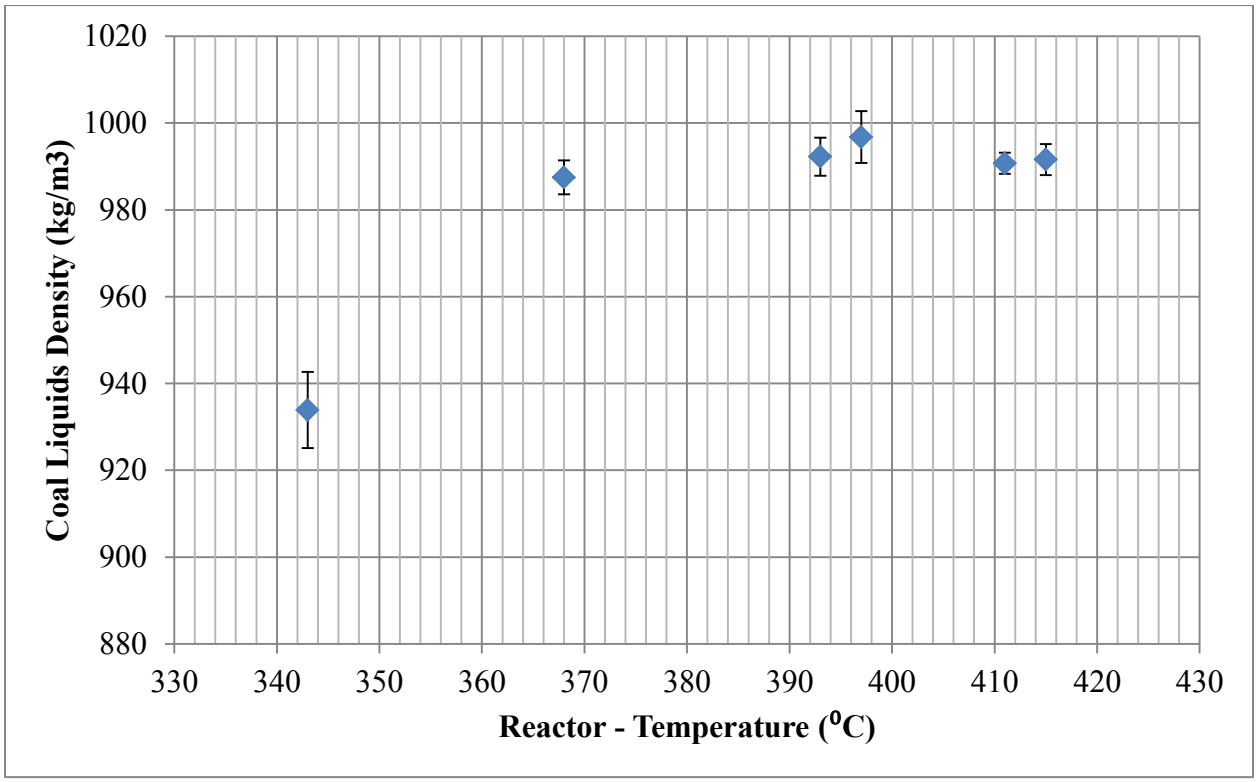

Figure 3.4.2.2. Density of Coal Liquids for Liquefaction at Different Temperatures

These densities (Figure 3.4.2.2) are now representative of the coal liquids devoid of any unreacted tetralin, so a better judgment can be made in terms of the aromatic content of the coal liquids. One thing that needs to be considered, however, is that the aromatic content is not the only factor influencing density. Density also changes with boiling point. The TBP curves shown in Section 3.3.3 were recalculated in order to exclusively represent the coal liquids present in the samples. This was done for each temperature set, by subtracting the wt% representing the known quantity of tetralin from its TBP curve, more specifically from the wide, low-sloped region around the 200 °C boiling point. That region was hence reduced to a percentage representative of the coal liquids boiling in the same temperature range as tetralin (each set had a different amount of coal liquids boiling in that range). After the adjustment of the slope of this segment, the whole curve was normalized to its original limits (0.5 – 99.5 %). The resulting curves are shown in Figure 3.4.2.3.

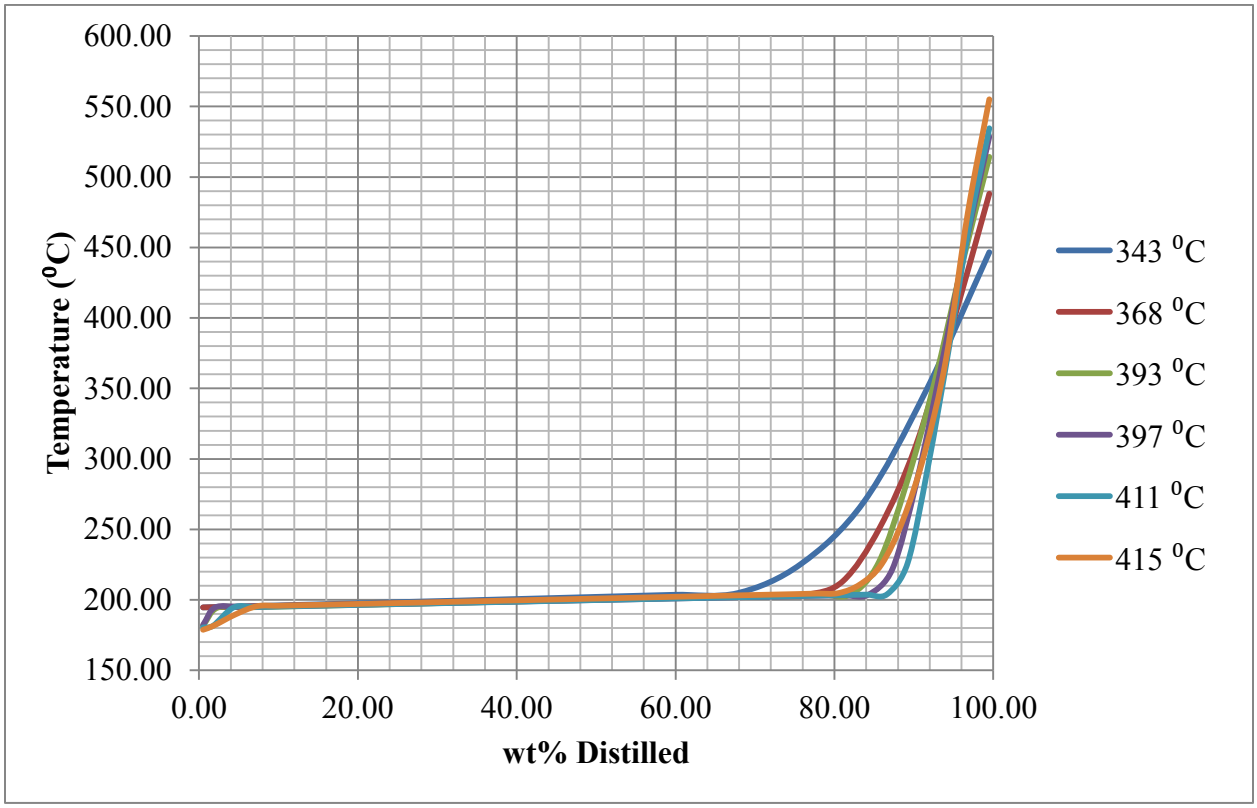

Figure 3.4.2.3. TBP Curves of the Coal Liquids, after Tetralin Subtraction and Normalization of the SimDis Curves

Comparing Figure 3.4.2.3 with Figure 3.4.2.2, there are conclusions which can be made for each temperature interval between the reaction sets. The only significant density increase (53.6 kg/m^3) appears when extraction temperature is moved from 343 °C to 368 °C. By comparing the TBP curves of these two sets (Figure 3.4.2.4), it can be seen how 67% of their boiling point distribution is identical, while 27% of the liquid is being distilled at higher temperatures for the 343 °C liquid than for the the 368 °C one, and 6% of the liquid is being distilled at lower temperatures for the 343 °C liquid than for the 368 °C one. Overall, the coal liquid obtained at 343 °C seems to contain larger amounts of heavier fractions than the one obtained at 368 °C, which would lead to a higher density. However, the observed density trend contradicts this. So if the increase in density is not caused by the boiling points, it means it could be due to an increase in aromatic content.

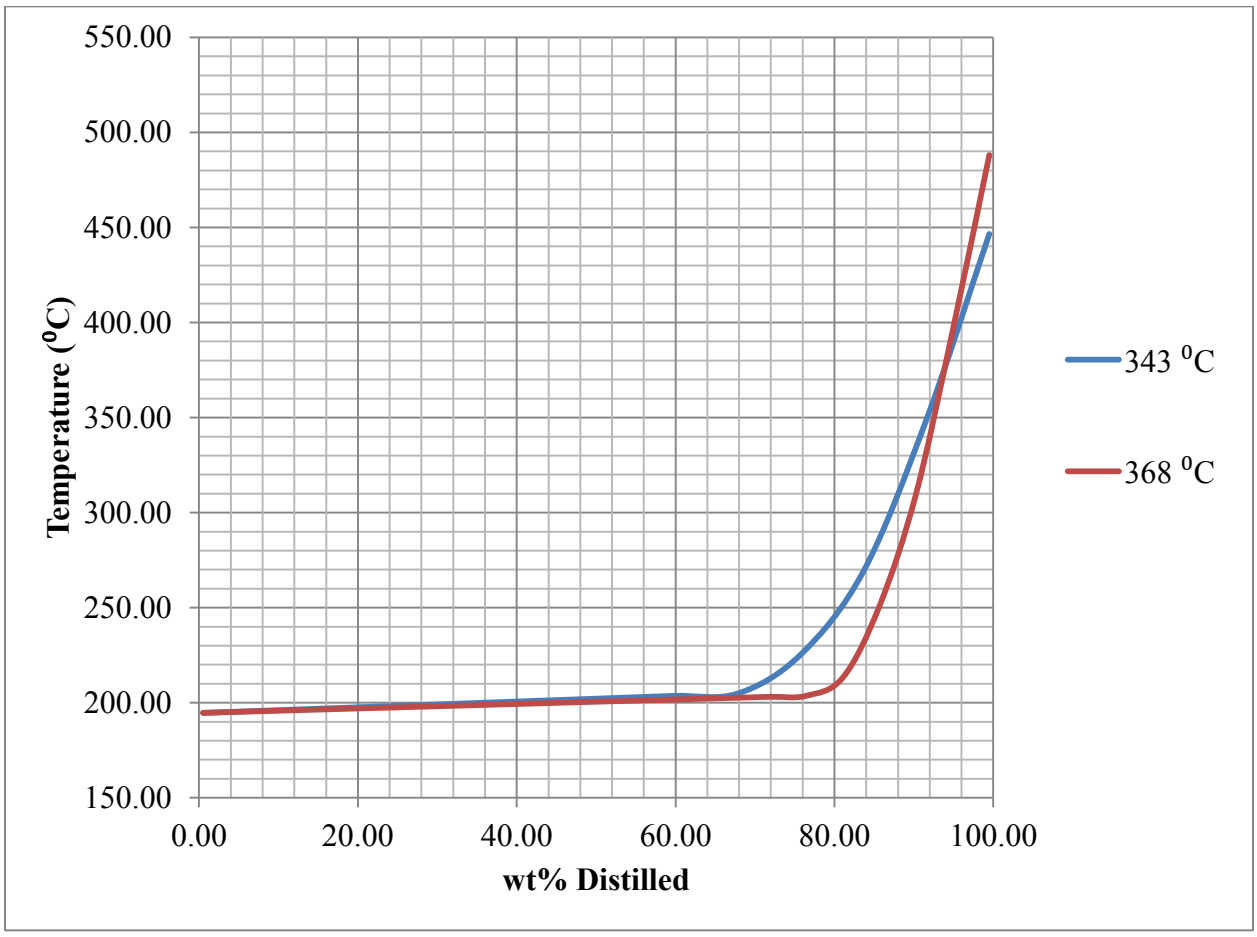

Figure 3.4.2.4. TBP Curves of the 343 °C and 368 °C Coal Liquids, after Tetralin Subtraction and Normalization of the SimDis Curves

For the coal liquids obtained at temperatures higher than 368 °C, the density is statistically unchanged, while the boiling points continue to follow the same trend (Figure 3.4.2.5), even though this time the 2 proportions surrounding the intersection point of the curves, which before were 27% and 6%, are less disproportionate. If we assume that the density is affected only by aromatic content and boiling point distribution, then the conclusion would be that the aromatic content of these samples is slowly increasing with temperature (at a decelerated rate), this way keeping the liquids at constant density, in spite of the lighter liquid fractions obtained at higher temperatures. In other words, the increase in aromatic content is balancing out the effect of the increasing amounts of low boiling liquids.

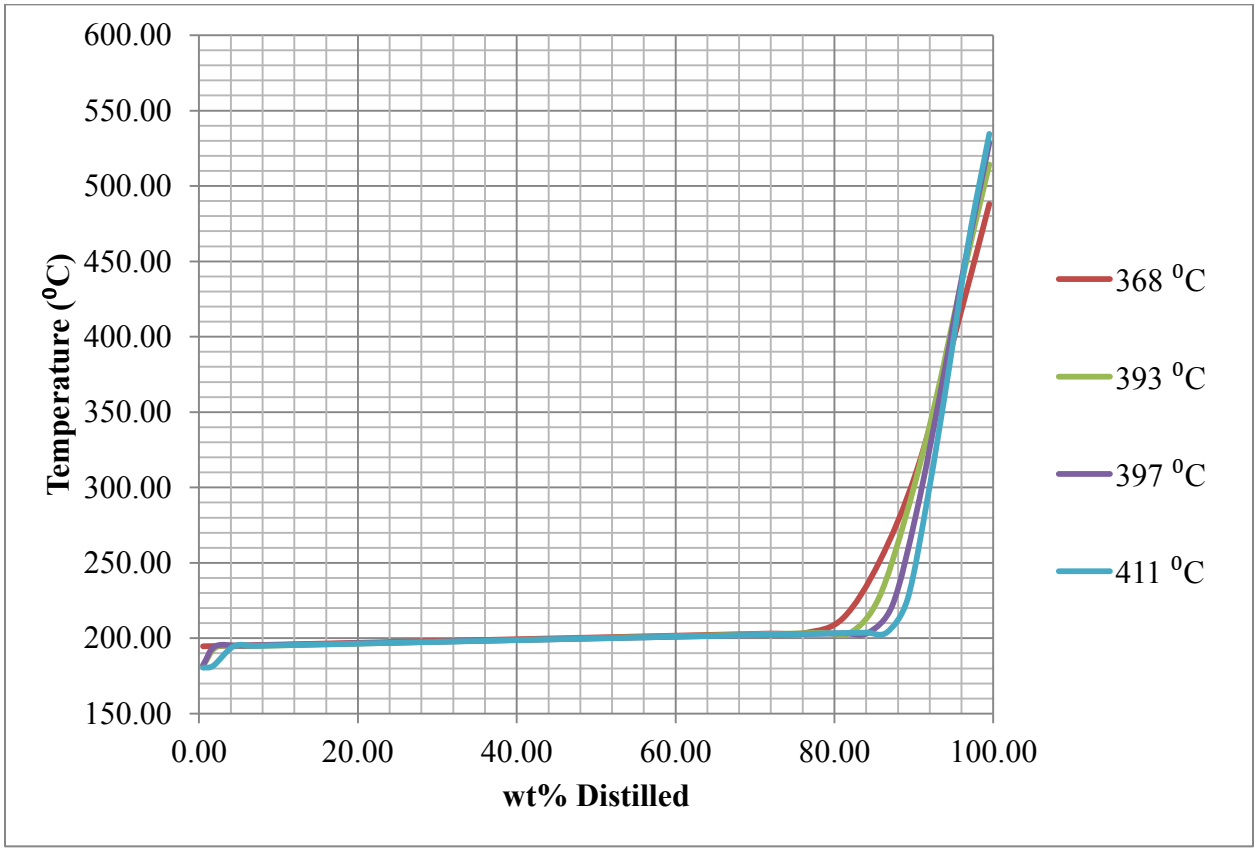

Figure 3.4.2.5. TBP Curves of the Coal Liquids (obtained at 368 °C - 411 °C), after Tetralin Subtraction and Normalization of the SimDis Curves

The trend of the TBP curves is interrupted on the last interval of liquefaction temperatures, where the 415 °C curve shows a heavier composition than the 411 °C one (Figure 3.4.2.6). This indicates an aromatic content decrease on this interval, since the densities are statistically the same.

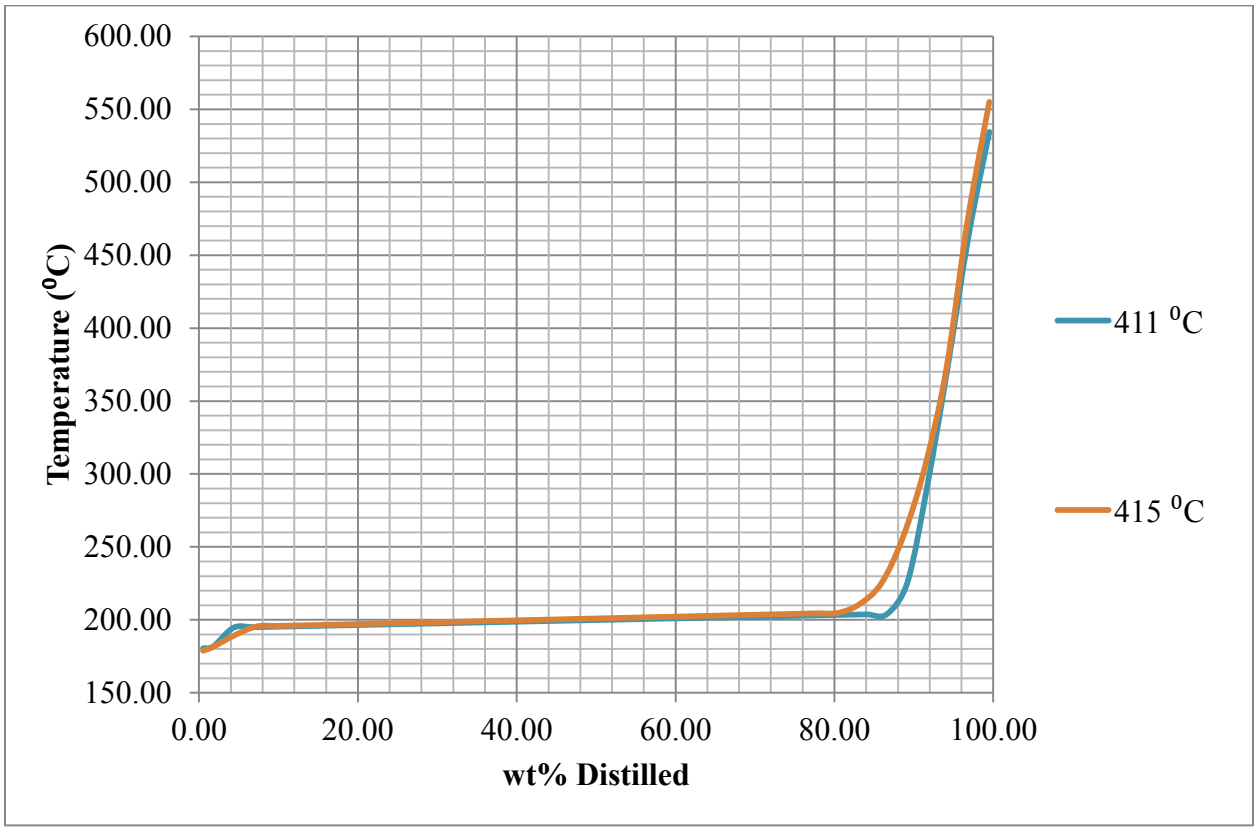

Figure 3.4.2.6. TBP Curves of the Coal Liquids (obtained at 411 °C and 415 °C), after Tetralin Subtraction and Normalization of the SimDis Curves

To put things into perspective, the average boiling points can be calculated for each temperature and overlapped with the density trend (Figure 3.4.2.7). All the above mentioned deductions about the aromatic content trend become clearer this way.

Based on the boiling point trend, it seems as if larger molecules are being liberated first, at lower temperatures, this trend continuing until ~410 – 415 °C. This is somewhat consistent with literature describing successive solvent extractions of coal [12], where the same tendency is observed (larger colloids and molecules were primarily liberated).

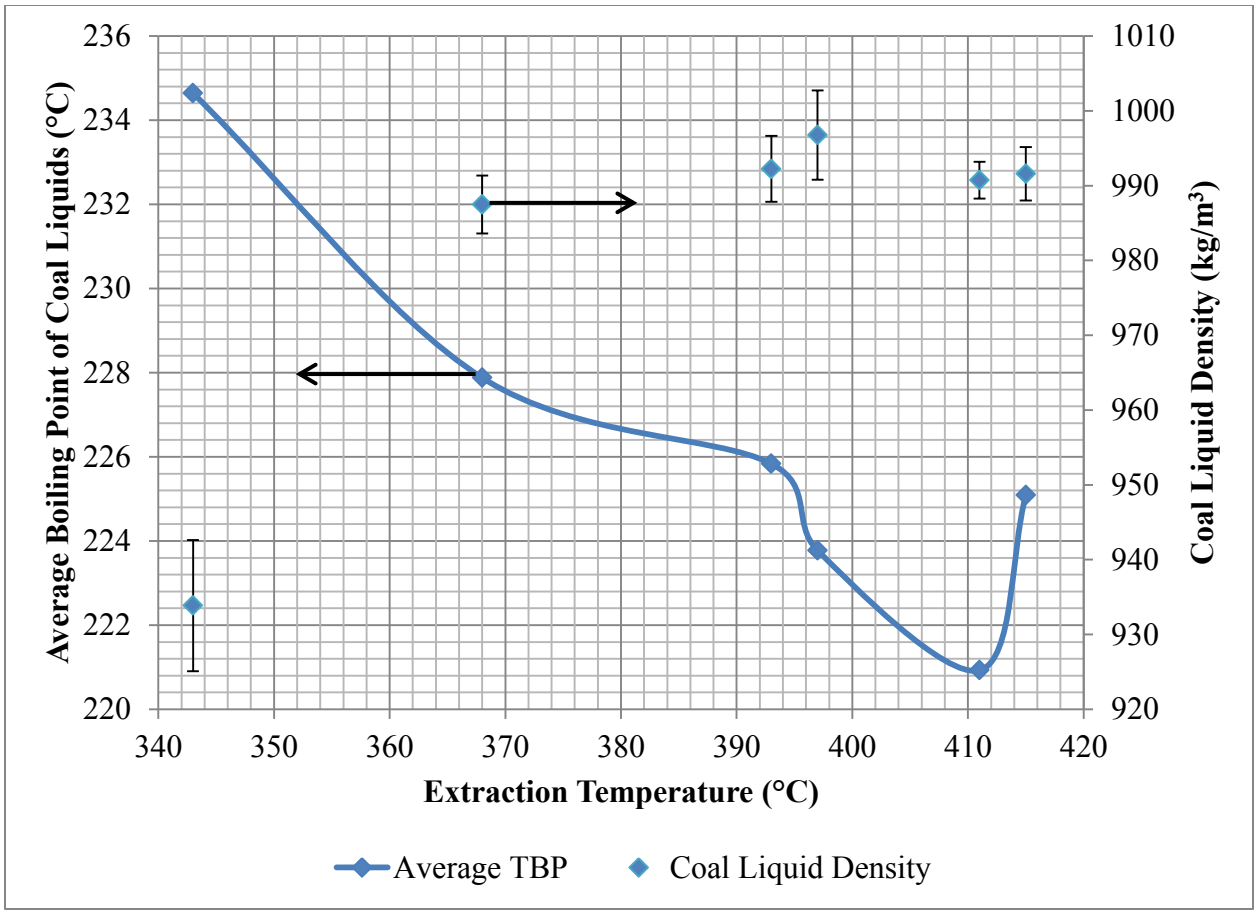

Figure 3.4.2.7. Comparison between the Density and Average TBP of the Coal Liquids obtained at Different Temperatures.

From a refining point of view, another observation can be made. With increasing liquefaction temperature, there is also an increase in the boiling points of a small fraction of the coal liquids (~6%). This can be best seen in Figure 3.4.2.3. The boiling ranges of typical crude oil fractions at atmospheric pressure indicate that the fractions boiling at temperatures higher than ~427 ^{0}C require separation by vacuum distillation, because their impact on the fuel properties derived from straight run distillate obtained by atmospheric distillation becomes too large [13]. This means that, except for the coal liquids obtained at 343 ^{0}C, the rest of the liquids contain about 4% products which have higher and higher boiling points as liquefaction temperature increases (exceeding 550 ^{0}C for the 415 ^{0}C liquefaction). Obtaining vacuum gas oil from these fractions requires vacuum distillation.

3.4.3 Temperature Influence on Iron Pyrite Conversion: Residue Stereomicroscopy

Iron pyrite (Fool's gold), has a characteristic golden sheen. The iron pyrite that was present in the residue fractions from liquefaction at lower temperatures (Figure 3.4.3.1.a,b), gradually disappeared at higher temperature (Figure 3.4.3.1.e,f).

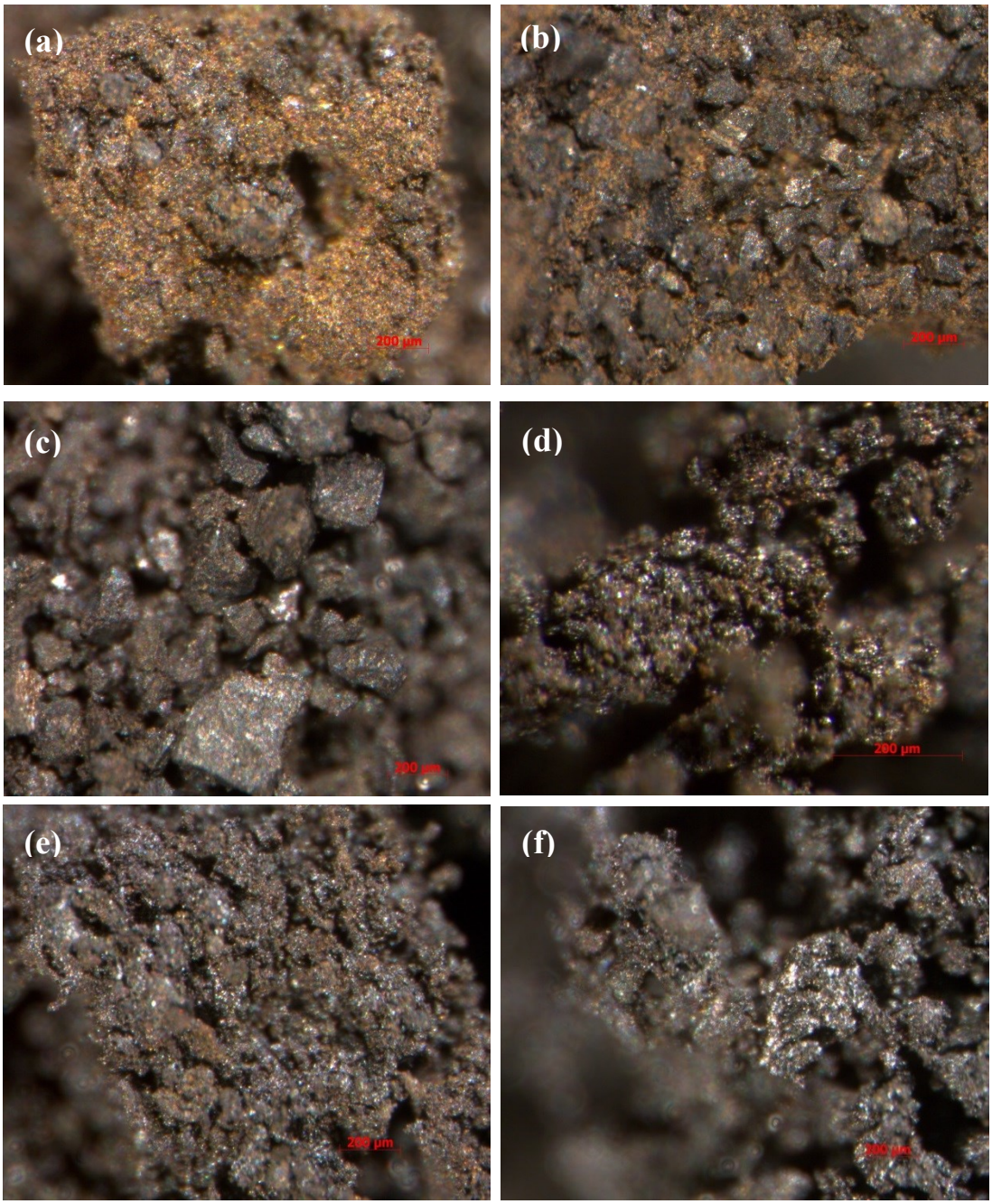

Figure 3.4.3.1. Selection of stereomicroscopy pictures of residues from coal liquefaction at: (a) 343, (b) 368, (c) 393, (d) 397, (e) 408, (f) 415 °C

As stated in the introduction of this chapter, according to literature, iron pyrite (FeS_2) is converted to iron pyrrhotite ($Fe_{1-x}S$, with $0 < x < 0.125$) at temperatures above 300 °C, complete conversion being achieved around 400 °C [3,4]. The pictures shown in Figure 3.4.3.1 indicate that iron pyrite is indeed being converted, even though they are only a small, representative, selection of all the pictures taken. Due to the heterogeneous nature of coal, some of the residue regions captured did not necessarily display this trend as clearly, especially for the smaller temperature intervals. However, an overall look at all the pictures visibly indicates that the golden sheen of iron pyrite is fading away with an increase in temperature (Figure 3.4.3.2).

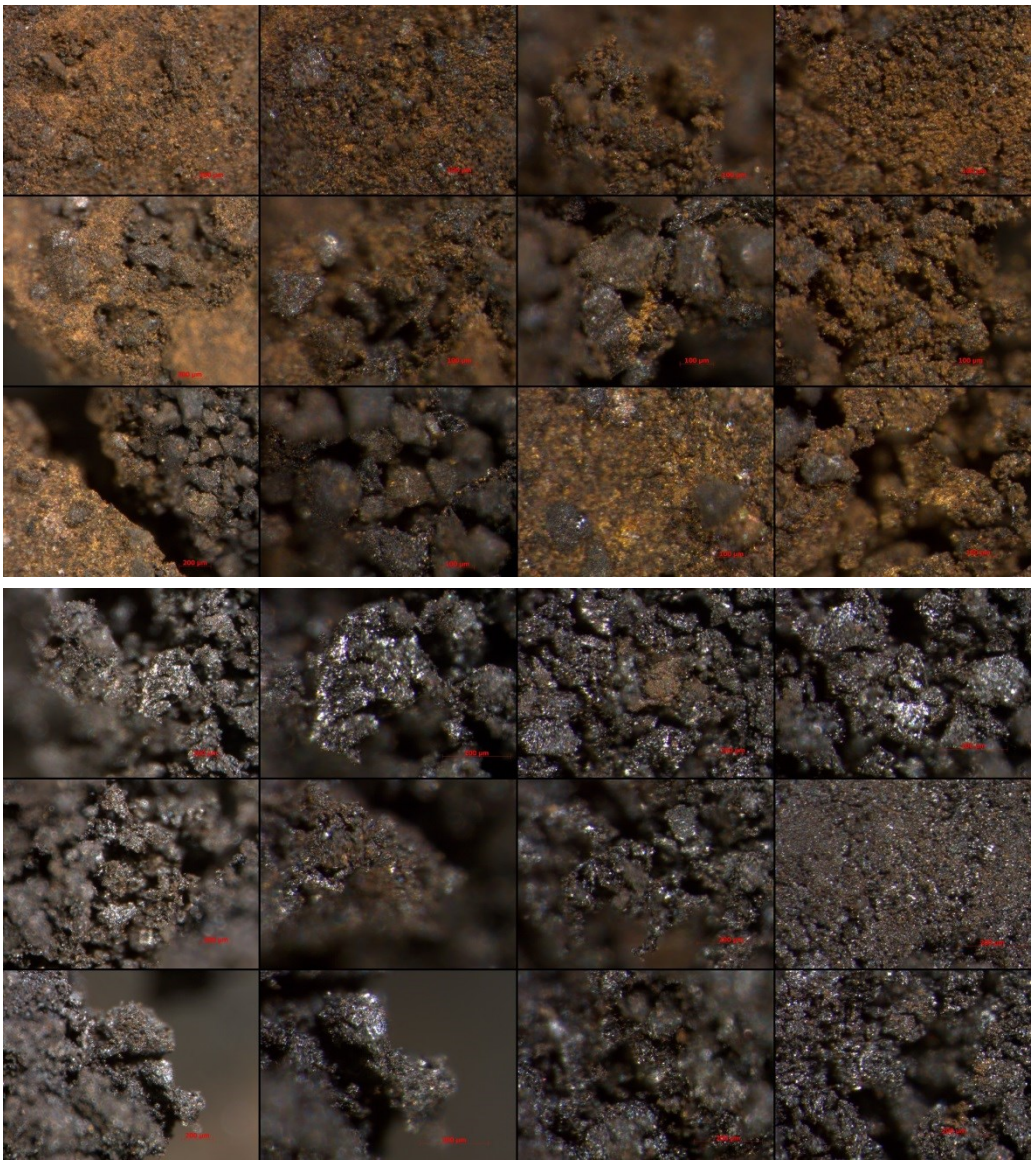

Figure 3.4.3.2. Larger selection of residue stereomicroscopy pictures from coal liquefaction at 368 °C (top) and 415 °C (bottom)

This transformation is accompanied by transfer of sulfur, either to the surrounding residue, or to the coal liquids. Sulfur transferred to the liquid product can either remain in the liquid, or form H_2S. In the presence of excess tetralin, direct reduction of FeS_2 by the tetralin to produce H_2S was anticipated. However, if the most sulfur was transferred to the residue, then it could potentially decrease the ultimate liquefaction yield by "vulcanizing" the organic matter in the residue. In such a case the sulfur of the organic matter in the residue would increase and that of the Fe_xS_y minerals would decrease. Either way, the iron pyrite reduction implies more transferrable hydrogen being sacrificed with increasing liquefaction temperature.

In order to determine which one of this transfer routes the sulfur followed, the residues were further analyzed by SEM and the compositions of different regions were determined by XRF spectrometry.

3.4.4 Sulfur Transfer Routes: Scanning Electron Microscopy and XRF Spectrometry

An indicator for the possible sulfur transfer routes is the S:Fe molar ratio which was determined by XRF spectrometry. In case of a sulfur transfer from the iron pyrite to the coal matrix, an increase in this ratio would be expected on average coal portions analyzed, while the Fe_xS_y minerals would present a decrease. Unfortunately, the analysis outcome was inconclusive due to the highly heterogeneous character of the coal residues. The presence of Ba-containing minerals, which apparently acted as sulfur scavengers, further complicated the interpretation.

Table 3.4.4.1. Impact of Liquefaction Temperature on the S:Fe Molar Ratio in the Residue

Temperature (°C)	S:Fe molar ratio	
	Average	Fe- and S-rich particles
343	1.2	0.9
367	1.3	1.0
392	1.1	- *
396	1.1	0.8
408	1.0	1.1
415	1.8	0.9

* No suitable mineral particles found in the sample that was analyzed.

3.4.5 Fourier Transform Infrared Spectra

As seen in Figure 3.4.5.1, the FTIR spectra of the diluted liquid products is not changing with temperature, remaining very similar to the FTIR spectra of their dilution solvent: tetralin. There is, however, an exception: one peak which is not present in the tetralin spectra appears in the 343 ºC liquid product spectrum and its intensity increases with liquefaction temperature. The peak corresponds to a wave number of 783 cm^{-1}. In aromatic molecules, the C-H out-of-plane bending results in strong absorption in the 900-700 cm^{-1} wave number range when there are no strongly electron withdrawing or electron donating groups. When this band is in the 810-750 cm^{-1} range, as it is this case, it is indicative of aromatics with three adjacent hydrogen atoms [14]. This means that with increasing liquefaction temperature, the concentration of such compounds increases.

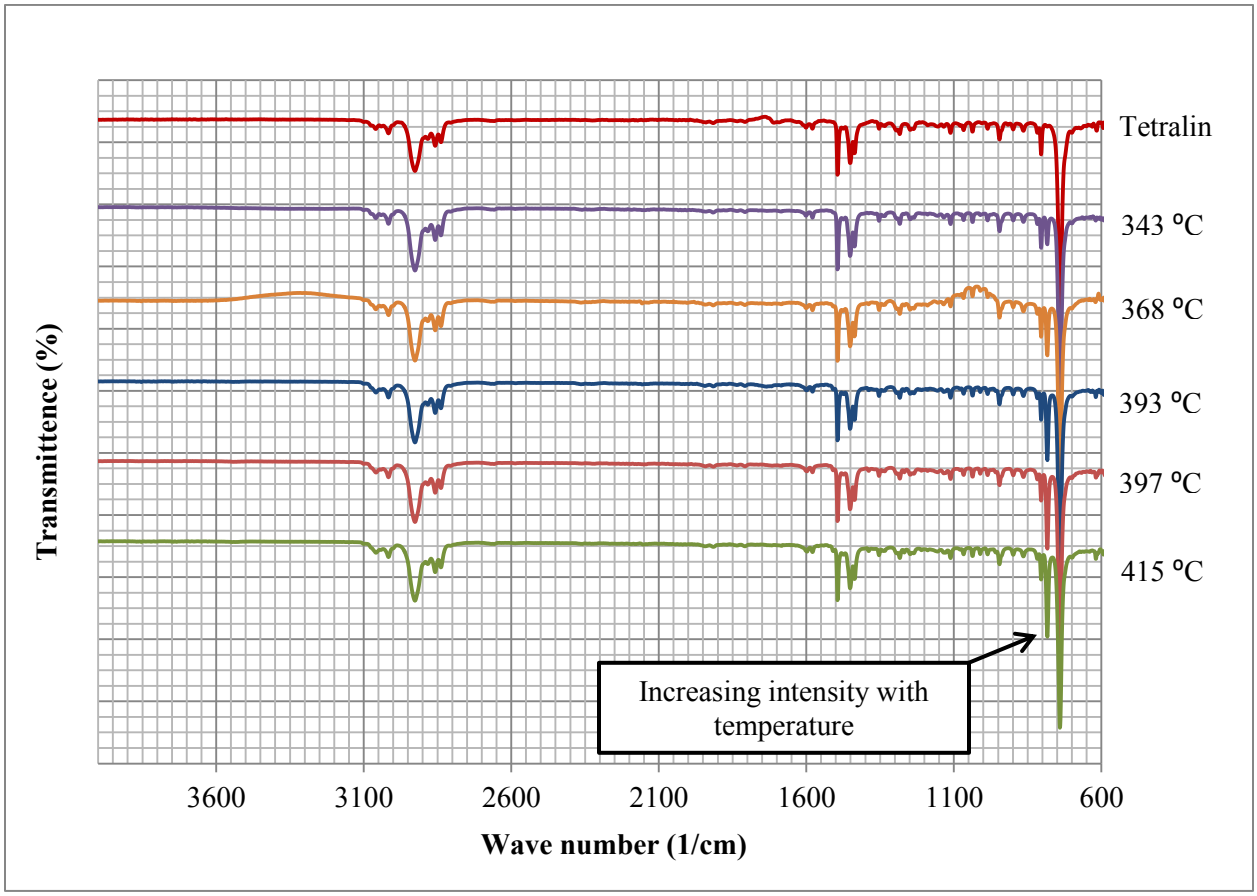

Figure 3.4.5.1. FTIR Spectra for Tetralin and for the Liquid Products of Coal Liquefaction at Different Temperatures

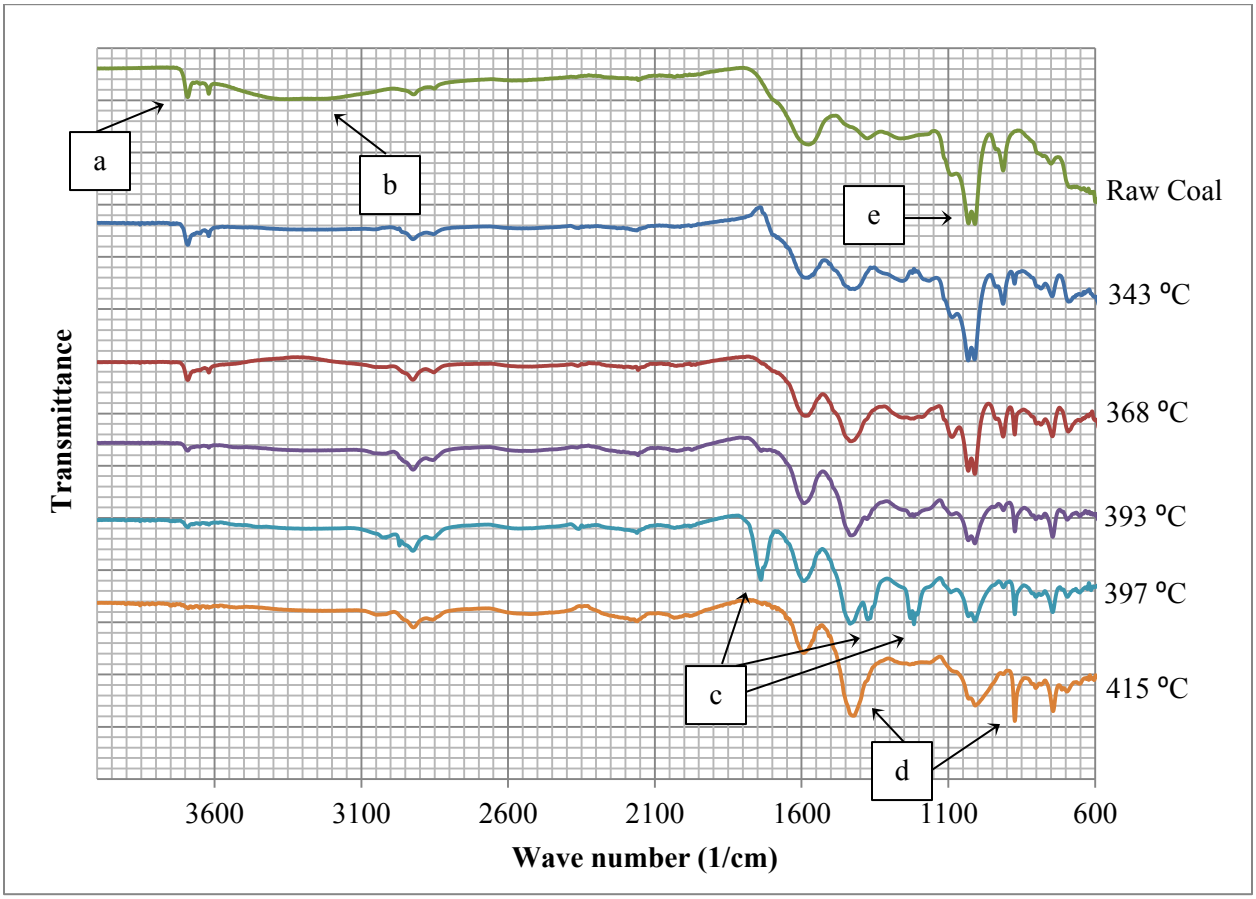

Figure 3.4.5.2. FTIR Spectra for the Raw Coal and for the Residues of Coal Liquefaction at Different Temperatures

Between the FTIR spectra of the residues (Figure 3.4.5.2), there are some qualitative and quantitative changes, but the interpretation of some of these changes proved to be difficult:

(a) The peak around 3700 cm^{-1} wave number gradually disappears with temperature. According to literature [15], this band represents free water, and it could be correlated with the loss in moisture as liquefaction temperature increases.

(b) The broad region of lower transmittance between 3600 and 3100 cm^{-1} wave number, corresponding to the raw coal sample is not present in the residues. This band represents crystallization water [15] and it seems to disappear from the coal before the liquefaction temperature reaches 343 ºC.

(c) Three strong bands appear at 397 °C, even though there is a hint of them in the slightly lower temperature of 393 °C. At 415 °C these bands do not exist anymore. Their wave numbers are 1736, 1375 and 1230 – 1205 cm^{-1}. The bands only appear in some of the quadruplicate samples and are likely to represent oxidation products.

(d) A slightly broader band (~1433 cm^{-1}) is increasing in intensity with temperature, without existing in the raw coal spectrum. The same can be said about the peak corresponding to the 872 cm^{-1} wave number.

(e) At 1035 and 1010 cm^{-1} two strong peaks present in the raw coal spectrum decrease in intensity with increasing liquefaction temperature in the residues. This observation indicates a decreasing tendency of the in-plane C-H deformation of the aromatics in the residues, supporting the above stated FTIR interpretation for the liquids, which indicated and increase in out-of-plane C-H bending for the liquids, as liquefaction temperatures were higher.

3.4.6 Proton NMR Spectra

When examining the data from Table 3.3.7.1, it seems that the calculated values of the aromatic to aliphatic protons ratio for the coal liquids obtained at lower liquefaction temperatures (343, 368 °C) are not reliable, because the standard deviations for these values are so high that they even lead to negative values, which is not physically possible. The reason for this is the high sensitivity of this ratio to the variations of the NMR data, especially for highly diluted samples. The sensitivity of the output value to small input value variations increases with the sample dilution. Thus, for the samples obtained at low temperatures, which are the most diluted, the results for the four individual runs of each temperature are varying considerably, leading to very high standard deviations (Figure 3.4.6.1).

However, when focusing on the products obtained at higher liquefaction temperatures, which are less dilute, a slight decrease in the aromatic to aliphatic protons ratio can be observed between 393 °C and 397 °C (Figure 3.4.6.2). According to the discussion from Section 3.4.2, the aromatic content on this interval is slightly increasing. The NMR results indicate that the more aromatics are obtained, the lower their aromatic to aliphatic hydrogen ratio will be.

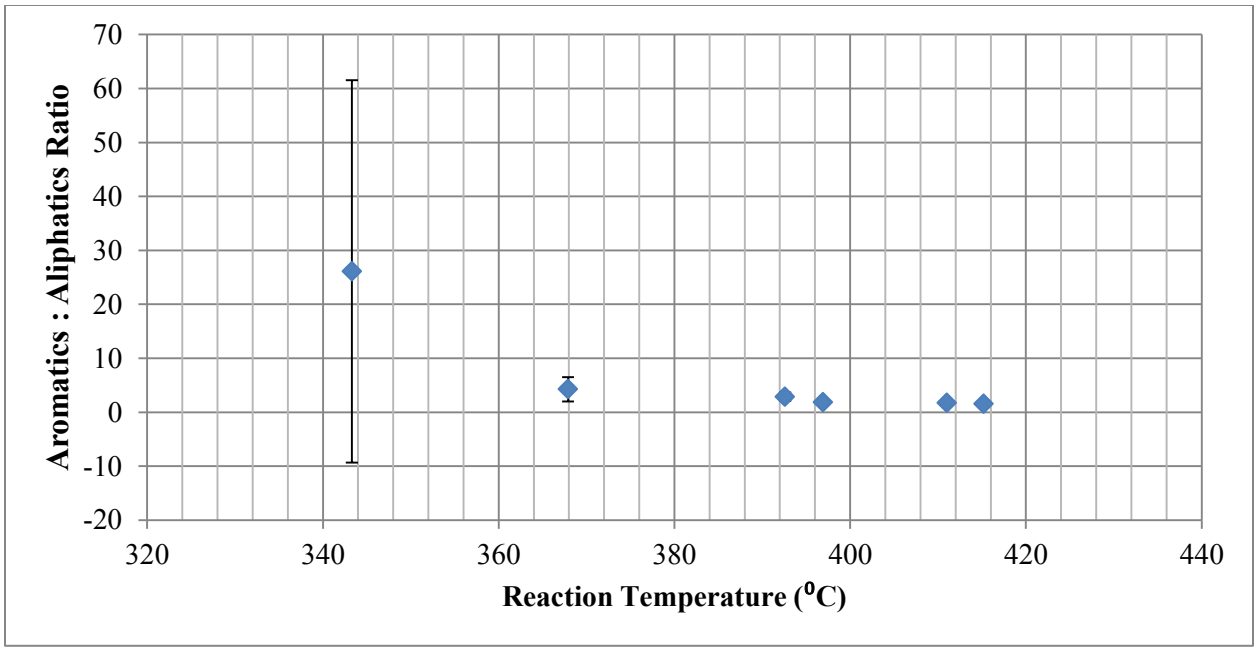

Figure 3.4.6.1. Effect of Liquefaction Temperature on the Aromatic to Aliphatic Protons Ratio of the Coal Liquids. Unreliable data points at low temperatures due to the high tetralin dilution.

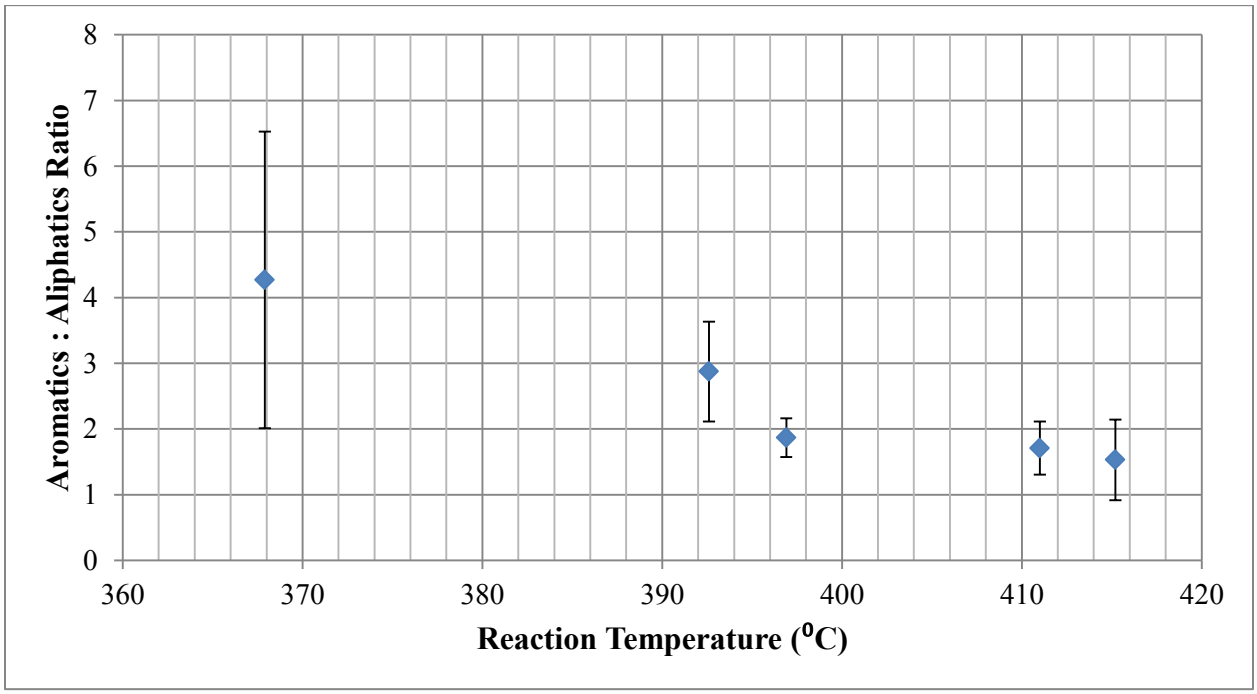

Figure 3.4.6.2. Zoom in: Effect of Liquefaction Temperature on the Aromatic to Aliphatic Protons Ratio of the Coal Liquids

3.5 Conclusions

(a) The liquid yield of coal liquefaction increased with temperature on the 340 – 415 °C interval.

(b) As temperature was increased from 343 to 368 °C, the density of the coal liquids increased with ~50 kg/m^3, while the larger portion of the coal liquids decreased its boiling points, suggesting an increase in aromatic light compounds.

(c) Beyond 368 °C the coal liquid density remained constant, while the larger portion of the coal liquids continued to decrease its boiling points at a slow, decelerating rate. This suggests that the aromatic content on this interval has a very slow increase, until 411 °C. Beyond that, by following the same assumptions, there is a small decrease in aromatic content.

(d) Proton NMR analysis indicates a slight aromatic hydrogen decrease at temperatures between 393 °C and 397 °C. This means that, on this interval, the more aromatics are obtained, the lower their aromatic to aliphatic hydrogen ratio will be.

(e) The iron pyrite conversion increases with liquefaction temperature.

(f) Although the SEM – XRF analysis was inconclusive, the sulfur from iron pyrite seems to be transferred out of the residue, implying that with increasing temperature more transferable hydrogen is sacrificed to reduce iron pyrite.

(g) The FTIR spectra for the liquids obtained at different temperatures indicate that with increasing temperature, there is an increase in aromatics containing three adjacent hydrogen atoms. The spectra for the residues showed a decrease in moisture along with other noticeable changes which support the same conclusion as the one provided by the liquid FTIR spectra.

References

[1] *Handbook of synfuels technology*; Meyers, R. E. Ed.; McGraw-Hill, New York, 1984.

[2] De Klerk, A. Transport fuel: Biomass-, coal-, gas- and waste-to-liquids processes. In *Future energy. Improved, sustainable and clean options for our planet*, 2ed; Letcher, T.M. Ed.; Elsevier: Amsterdam, 2014, p. 245-270.

[3] Bommannavar, A. S.; Montano, P. A. Mössbauer study of the thermal decomposition of FeS_2 in coal. *Fuel* **1982**, *61*, 523-528.

[4] Montano, P. A.; Bommannavar, A. S.; Shah, V. Mössbauer. Study of transformation of pyrite under conditions of coal liquefaction. *Fuel* **1981**, *60*, 703-711.

[5] Cleyle, P. J.; Caley, W. F.; Stewart, I.; Whiteway, S. G. Decomposition of pyrite and trapping of sulphur in a coal matrix during pyrolysis of coal. *Fuel* **1984**, *63*, 1579-1582.

[6] Rivolta Hernández, M.; Figueroa Murcia, C.; Gupta, R.; De Klerk, A. Solvent-coal-mineral interaction during solvent extraction of coal. *Energy Fuels* **2012**, *26*, 6834-6842.

[7] ASTM D7582-12: Standard Test Methods for Proximate Analysis of Coal and Coke by Macro Thermogravimetric Analysis; ASTM: West Conshohocken, PA 2012.

[8] ASTM D7169-11: Standard Test Methods for Boiling Point Distribution of Samples with Residues Such as Crude Oils and Atmospheric and Vacuum Residues by High Temperature Gas Chromatography; ASTM: West Conshohocken, PA 2011.

[9] Sachanen, A. N. *The chemical constituents of petroleum*; Reinhold: New York, 1945, p. 102-107.

[10] Lee, S. W., Preto, F., & Hayden, A. C. Determination of fuel aromatic content and its effect on residential oil combustion. *Preprints Papers Am. Chem. Soc., Div. Fuel Chem* **1986**, *31*, 275-293.

[11] Abdul-Halim Abdul-Karim, M.; Hadi, G.A. The Relationships between the Physical and Chemical Properties of Narrow Fractions Distilled From Mixed Kirkuk and Sharki-Baghdad Crude Oils. *Iraqi Journal of Chemical and Petroleum Engineering* **2008**, 9, 1-8.

[12] Vahrman, M. The smaller molecules derived from coal and their significance. *Fuel* **1970**, *49*, 5-16.

[13] Gary, J. H.; Kaiser, M. J.; Handwerk, G. E. *Petroleum refining: technology and economics*, 5ed; Boca Raton: Taylor & Francis, 2007.

[14] Dolphin, D.; Wick, A. *Tabulation of infrared spectral data*; Wiley: New York, 1977.

[15] Gokel, G. W. *Dean's Handbook of Organic Chemistry, 2nd ed.*; McGraw-Hill: New York, 2004, p. 6.21 – 6.53.

CHAPTER 4 – COAL LIQUEFACTION LIQUID QUALITY: INTERMEDIATE TEMPERATURE EXTRACTION STEPS

Abstract

Direct coal liquefaction by solvent extraction can be carried out in one or more intermediate temperature steps. The impact of introducing such an additional step to the single step process was investigated by applying 9 different heating scenarios involving the combination of a low temperature step (100, 150 and 200 °C) with a subsequent high temperature step (352, 397, 415 °C). The feed materials used for these experiments were a Canadian lignite coal from Boundary Dam and tetralin as a hydrogen donor solvent in a 1:3 coal to solvent ratio. The low temperature steps were carried out under atmospheric pressure and only for as long as it took for the temperature to reach the initial required value, while the high temperature steps involved nitrogen atmosphere, autogenous pressure and 1 hour liquefaction time. It was found that the liquid yields increased by up to 9% when the process included the additional low temperature step, but this was only statistically significant in one of the 9 different heating scenarios. The highest yields were obtained for a 100 °C low temperature step. Extra liquids were obtained from the low temperature step, although the yields for these products were low. The liquids obtained by the 2-step liquefaction process were found to contain carbonyl groups which were absent from the liquids obtained via the single step process. The 2-step process did not seem to have affected the density and the refractive index of the liquid products compared to the single step process, but the boiling points of the liquids were predominantly lower for the 2-step process. Proton NMR analyses showed decreased aromatic to aliphatic protons ratios for the liquids obtained in 2 heating steps, especially when the temperatures of the second step were lower. Analyses regarding the iron pyrite conversion tendencies were inconclusive.

Keywords: coal, liquefaction, intermediate, steps, yield, quality

4.1 Introduction

It was previously proposed that performing coal liquefaction in more than one heating stage might bring a benefit in terms of yield and coal liquid quality [1-5]. It was argued that by doing so, at least a part of the overall coal liquid could be obtained before high temperature liquefaction and that the coal liquid obtained at lower temperature should be of a higher quality.

The direct coal liquefaction process by solvent extraction involves mixing the coal and the hydrogen donor solvent, heating the mixture up, followed by the separation and subsequent treatment of the residues and coal liquids. Dividing the process into a staged one, with two or more heating steps, involves the repetition of the heating operation multiple times, each time using a different, higher temperature during the heating section, while separating the coal liquids obtained during each stage from the coal-solvent mixture and adding fresh solvent between the steps. Hypothetically, a series of such repetitions with an infinite number of steps would become one single continuous heating process with its heating profile dependent on the rate in which the temperature would increase from step to step. Indeed, it has been shown that performing coal liquefaction by applying differently accelerated heating profiles does have an impact on the liquid yield [6], but the solvent-coal mixture involved in this process did not have any coal liquids removed from it, nor was there any fresh solvent added.

This chapter is focusing on the impact of intermediate temperature steps on the yield and quality of the coal liquids obtained during the direct coal liquefaction process. The hypothesis is that performing coal liquefaction in two steps, a higher yield and a higher coal liquid quality could be obtained. Therefore, the previously employed experimental procedure (Figure 3.2.2.3) has been modified so that it involves two sequential heating steps. Combinations between a 100, 150 and 200 °C low temperature step respectively a 352, 397 and 415 °C high temperature step have been made in order to generate 9 different scenarios. In addition to the above suggested repetition of the heating and separation operations, the residue drying operation has also been added to the repeated group of operations (Figure 4.2.2.3). The purpose of adding this drying operation was to be able to analyze the dry intermediate residues in order to determine the yield and quality of the liquids obtained during the first heating step.

4.2 Experimental procedure

4.2.1 Materials

The materials used for this experimental section, as well as their preparation, were the same as the ones described in Section 3.2.1. The coal characterization is shown in Table 3.2.1.1.

4.2.2 Equipment and procedure

Unlike the experiments described in the previous chapter, the coal liquefaction experiments for this section included two separate extraction steps: a low temperature extraction step, followed by a high temperature extraction step.

For the low temperature extraction step, the set-up involved a 500 ml triple-neck round-bottom flask, mounted on a Heidolph MR Hei-Standard magnetic stirrer hotplate equipped with a heating block. The round-bottom flask was equipped with an OMEGA® K-type thermocouple in order to monitor the internal temperature. The tip of the thermocouple was reaching the bottom of the round flask. The flask also contained a magnetic stirring bar. Two 10 cm long water chilled Liebig condensers were mounted sequentially on one of the necks of the flask, in order to collect potential light products. The set-up for this initial extraction step is shown in figure 4.2.2.1.

The second step (the high temperature extraction step) involved the same set-up as described in Section 3.2.2 and shown in Figure 3.2.2.1, except the number of micro-batch reactors used was three instead of four. Among the three reactors, one of them was equipped with a thermocouple and pressure gauge, as shown in Figure 3.2.2.1. In addition to that, the reactors were washed with approximately 2 g of tetralin instead of 3-5 g like in the previous experiments.

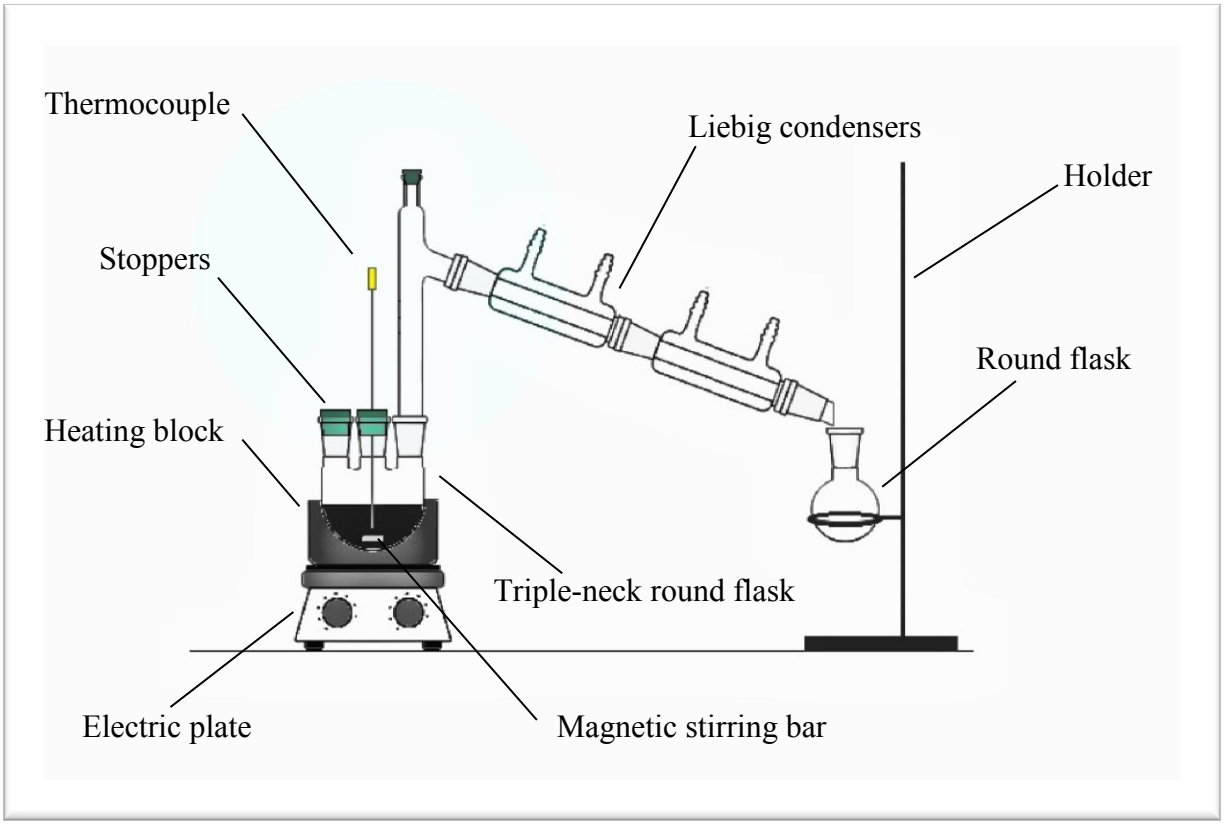

Figure 4.2.2.1. Set-up for the low temperature liquefaction step of coal

For the low temperature extraction step, the round-bottom flask was loaded with 20 g of coal and 60 g of tetralin. After weighing, the flask was placed on the heating block to be heated to the required temperature. For a total of 3 reaction sets, the heating plate was preheated to 165, 215 and 260 °C respectively, in order for the reactants to reach 100, 150 and 200 °C respectively. As soon as the temperature of the reactants reached the required value, the flask was removed from the heating block, weighed, and then the contents were vacuum filtered. The heating profiles for this step can be seen in Figure 4.2.2.2. Each reaction set was carried out in triplicate.

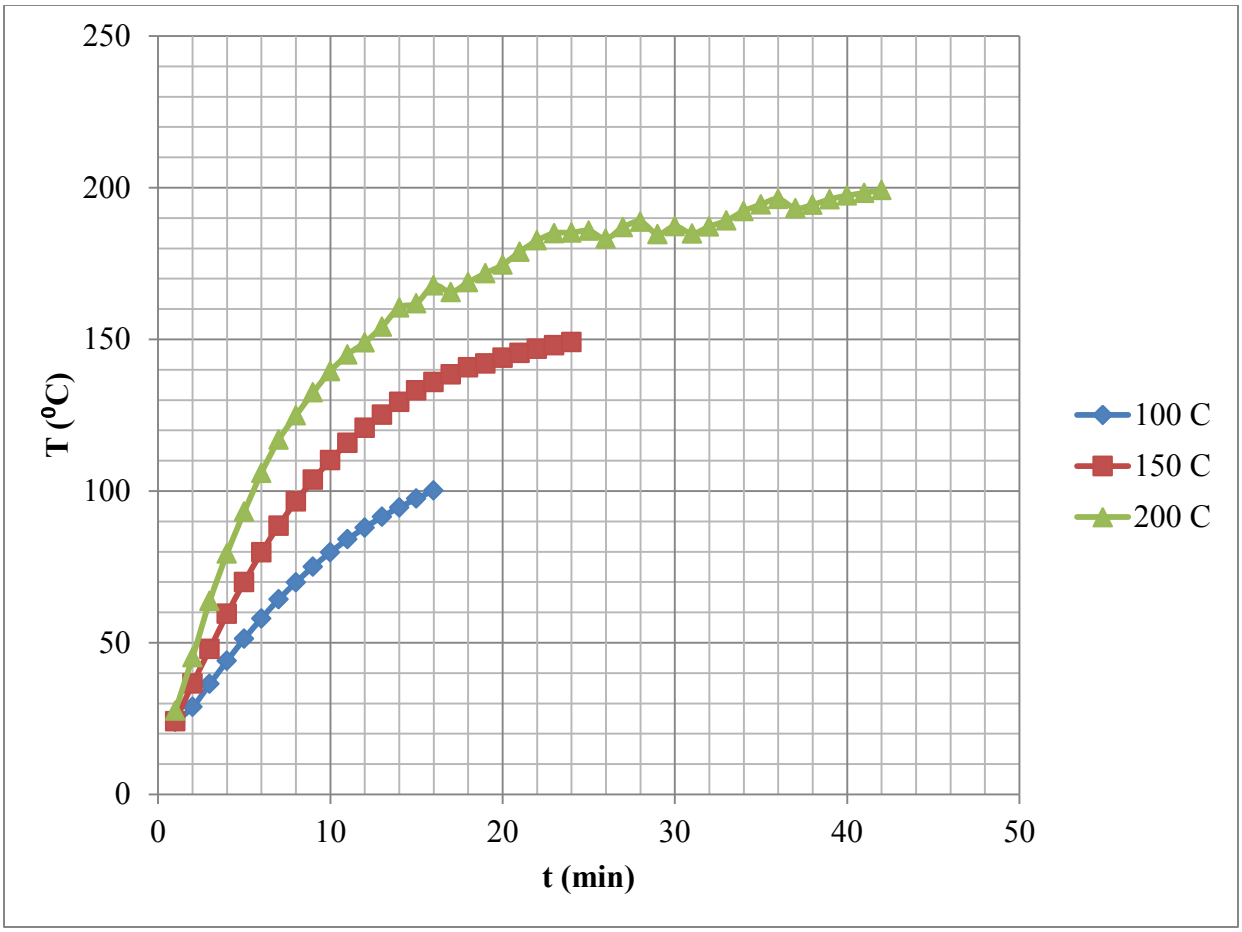

Figure 4.2.2.2. Heating profiles for the low temperature liquefaction step at 100 °C (blue), 150 °C (red) and 200 °C (green). The temperature was recorded at intervals of 1 minute.

The vacuum filtration for this step was carried out in the same way as described in Section 3.2.2, except there was no extra tetralin used for washing the round bottom flask. After the residues were dried, they were stored in Fisherbrand™ Class B clear glass threaded vials in a cool, dark place, before being used as feed materials for the second, high temperature extraction step.

Each residue from the low temperature reaction sets was divided into 4 parts: 3 parts of 2.5 g each and one part of the rest. The 2.5 g parts were used for the high temperature steps for 3 different temperatures: 352-354 °C, 397-398 °C and 415-416 °C, while the rest was used for analysis. The high temperature extraction step was carried out in the exact same way as the experiments described in Section 3.2.2. The experimental procedure is summed up in Figure 4.2.2.3.

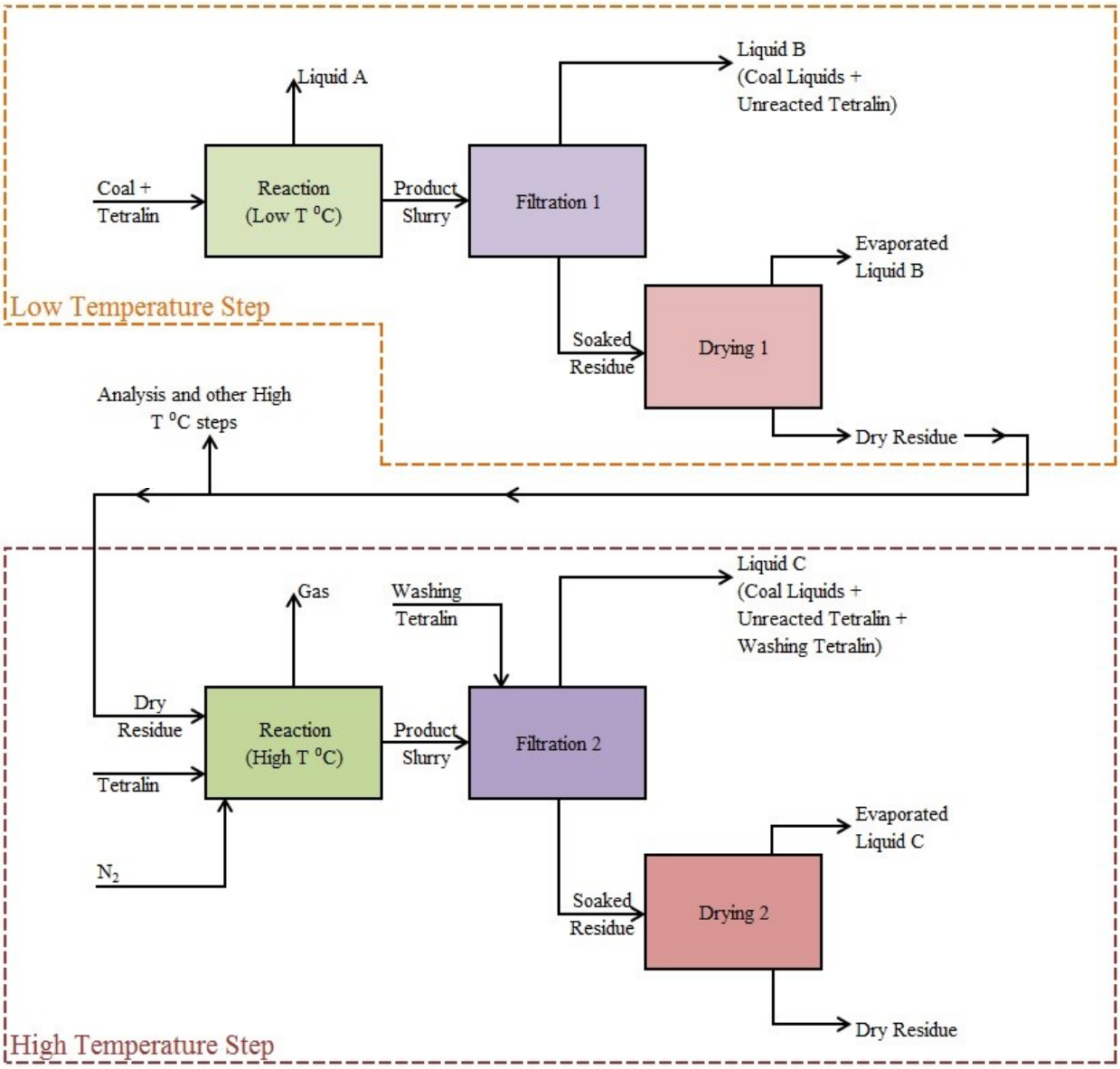

Figure 4.2.2.3. Schematic of the Experimental Procedure used for Coal Liquefaction with two temperature liquefaction steps.

It is important to highlight the nomenclature of the following terms, as used throughout this chapter:

Liquid A refers to the liquid obtained through condensation of the light gases during the low temperature step. This was only present during the 200 °C reaction set and in extremely small amounts.

Liquid B represents the liquid product obtained after the filtration of the low temperature step products.

Liquid C is the liquid product obtained at the end of the whole process, after the high temperature reaction step.

The rest of the terms follow the same nomenclature as defined in Section 3.2.2:

Diluted liquid product refers to the mixture of coal liquids, unreacted tetralin and washing tetralin, as resulted after the filtration operation of the high temperature step (Liquid C).

Liquid product refers to the mixture of coal liquids and unreacted tetralin, excluding the washing tetralin used for the filtration operation, regardless if this is Liquid B or C.

Coal liquids refers strictly to the coal derived products which are present in the liquid mixture.

4.2.3 Analyses

The liquids and residues were characterized using the same analytical methods, instruments and procedures as described in Section 3.2.3, with the exception of the SEM analysis, which proved to be inconclusive:

(a) Proximate analysis of all the residues that were obtained both during the low temperature step and the high temperature step: ASTM D7582-12 [7].

(b) Density of Liquids B and C at 25 °C.

(c) Refractive index of Liquids B and C at 20 °C.

(d) Simulated distillation (SimDist) of the Liquid C samples: ASTM D7169 [8].

(e) Stereomicroscopy for all the residues.

(f) Fourier Transform Infrared (FTIR) spectroscopy for all residues and liquid products (Liquids B and C).

(g) Proton NMR spectrometry for Liquids B and C.

4.2.4 Calculations

The *mass balance for the low temperature step*, $M_{b.low}(\%)$, for each reaction was calculated the following way:

$$M_{b.low}(\%) = 100 \cdot \frac{m_f - m_{flask} + m_{LiqA}}{m_i - m_{flask}} \qquad (4.2.4.1)$$

Where m_f = mass of full flask after reaction (g);

m_{flask} = mass of empty flask (g);

m_{LiqA} = mass of Liquid A obtained, if applicable (g);

m_i = mass of full flask before reaction (g).

The *mass balance for the high temperature step* was calculated the same way as it was calculated for the reactions in Chapter 3, by using equation (3.2.4.1).

The *liquid yield*, $Y(\%)$, for the liquefaction reactions of each temperature step was calculated the following way:

$$Y(\%) = 100 \cdot \frac{M_{in} \cdot \left(1 - \frac{Moist_{in} + Ash_{in}}{100}\right) - M_{out} \cdot \left(1 - \frac{Moist_{out} + Ash_{out}}{100}\right)}{M_{in} \cdot \left(1 - \frac{Moist_{in} + Ash_{in}}{100}\right)} \qquad (4.2.4.6)$$

Where M_{in} = initial mass of coal (for low temperature step),
or of feed residue (for high temperature step) (g);

$Moist_{in}$ = moisture percentage of coal (for low temperature step),
or of feed residue (for high temperature step) (%);

Ash_{in} = ash percentage of coal (for low temperature step),
or of feed residue (for high temperature step) (%);

M_{out} = mass of resulting residue after separation and drying (g);

Moist_{out} = moisture percentage of resulting residue (%);

Ash_{out} = ash percentage of resulting residue (%).

The densities, compositions, and the aromatic to aliphatic protons ratios of the liquids were calculated the same way as described in Section 3.2.4.

4.3 Results

4.3.1 Product Yield

Based on the residue proximate analysis mentioned in Section 4.2.3, the liquid yields of Liquid B and C were calculated using Equation 4.2.4.6. The results are shown in Table 4.3.1.1 and in Figure 4.4.1.1. There was no Liquid A obtained during the 100 and 150 °C experiments. The Liquid A amount obtained at 200 °C was very little (see Table 4.3.1.1).

Table 4.3.1.1. Overall Product Yield from Boundary Dam Lignite Liquefaction with Tetralin under N_2 Atmosphere and 1 h after Different Liquefaction Temperature Heating Steps

Step 1 Temp. (°C)	Step 2 Temp. (°C)	Yield (wt%)		Proximate analysis of residue (wt %)			
		Liquid A + B (Liquid A)	Liquid C	Volatile matter	Fixed carbon	Ash	Moisture
100	352	4.4 ± 4.0 (0)	23.3 ± 1.4	25.1 ± 0.8	34.8 ± 0.6	10.6 ± 0.5	1.8 ± 0.3
	397		43.6 ± 2.9	15.5 ± 1.9	25.3 ± 0.4	10.4 ± 1.9	0.8 ± 0.4
	415		49.4 ± 2.6	12.6 ± 1.8	22.8 ± 0.5	10.3 ± 1.3	0.5 ± 0.1
150	354	1.5 ± 0.8 (0)	26.2 ± 2.2	24.8 ± 0.9	35.2 ± 0.4	10.4 ± 1.0	1.8 ± 0.3
	398		43.9 ± 1.0	16.9 ± 0.8	26.6 ± 0.3	10.2 ± 0.9	0.8 ± 0.3
	416		51.7 ± 1.5	12.4 ±1.9	23.3 ± 0.8	10.5 ± 1.4	0.5 ± 0.1
200	352	3.6 ± 1.3 (0.7 ± 0.2)	24.9 ± 1.0	24.7 ± 0.6	34.8 ± 0.3	10.0 ± 0.5	1.9 ± 0.2
	397		41.2 ± 1.8	17.2 ± 0.6	27.0 ± 0.2	10.2 ± 0.6	0.7 ± 0.2
	415		49.0 ± 2.1	13.3 ± 1.9	23.3 ± 0.7	10.3 ± 1.4	0.6 ± 0.0

4.3.2 Refractive Index and Density of the Liquid Product and Coal Liquids

The density and refractive index analyses results are shown in Tables 4.3.2.1 and 4.3.2.2. For the liquid samples obtained after the low temperature step (Liquid B), there was no tetralin dilution by washing. Therefore, the results shown in Table 4.3.2.1 represent the values which were directly measured with the density meter. Similar to Chapter 3, the coal liquid density corresponds to the coal liquids void of any unreacted tetralin, as calculated with Equation 3.2.4.8, but based on the yield of the low temperature reactions. Unlike the previous chapter, the refractive index measurements for the Liquid B samples correspond to undiluted liquid products.

Table 4.3.2.1. Refractive Index and Density of the Liquid Products and Coal Liquids Obtained by Liquefaction after the Low Temperature Heating Step

Step 1 Temperature (°C)	Liquid B Refractive index at 20 °C	Liquid B Density at 25 °C (kg/m^3)*	Coal Liquid B Density at 25 °C (kg/m^3)
100	1.5413 ± 0.0002	964.8 ± 0.1	768.0 ± 156.9
150	1.5413 ± 0.0001	965.0 ± 0.01	659.8 ± 99.6
200	1.5414 ± 0.0001	965.0 ± 0.03	815.3 ± 42.9

*These samples contain 96 ± 3% unreacted tetralin.

For the liquid samples obtained after the high temperature step (Liquid C), the washing tetralin dilution was handled in the same way as in Chapter 3, by calculating the composition of the samples in terms of washing tetralin, unreacted tetralin and coal liquids. The equations used were 3.2.4.7, 3.2.4.8 and 3.2.4.9.

Table 4.3.2.2. Refractive Index and Density of the Liquid Products and Coal Liquids Obtained by Liquefaction after 2 Heating Steps

Step 1 Temp. (°C)	Step 2 Temp. (°C)	Tetralin Dilution (wt%)	Liquid C Refractive index at 20 °C	Liquid C Density at 25 °C (kg/m^3)	Coal Liquid C Density at 25 °C (kg/m^3)
100	352	76.3 ± 1.6	1.5463 ± 0.0007	967.7 ± 1.1	955.5 ± 4.6
	397	57.0 ± 3.1	1.5452 ± 0.0024	980.9 ± 3.2	987.7 ± 4.9
	415	51.4 ± 2.7	1.5577 ± 0.0026	980.8 ± 3.4	986.0 ± 4.8
150	354	73.7 ± 2.4	1.5472 ± 0.0004	970.2 ± 1.0	964.3 ± 3.7
	398	57.5 ± 1.1	1.5555 ± 0.0016	981.4 ± 2.5	989.2 ± 4.5
	416	52.6 ± 1.3	1.5582 ± 0.0010	984.0 ± 1.7	991.3 ± 2.2
200	352	75.2 ± 1.1	1.5465 ± 0.0004	969.4 ± 0.7	961.6 ± 2.5
	397	60.3 ± 1.7	1.5551 ± 0.0010	980.6 ± 1.5	988.3 ± 2.4
	415	54.2 ± 2.4	1.5593 ± 0.0023	985.7 ± 2.5	994.8 ± 4.8

4.3.3 Simulated Distillation

Because of the tetralin dilution of the samples, the SimDis results from this chapter needed to be adjusted the same way the ones in Chapter 3 were adjusted (by subtracting the known amount of tetralin from the low-sloped region of the TBP curves and then normalizing each series of data for 100%). The results are discussed in Section 4.4.2.

4.3.4 Residue Stereomicroscopy

Pictures of the liquefaction residues were taken at three different scales (50x, 70x, 150x) for the residues of the first temperature step, and also for the ones resulted after the second temperature step. Each triplicate of each reaction set was examined and photographed. The results are discussed in Section 4.4.3.

4.3.5 Fourier Transform Infrared Spectra

All the liquid products and residues of both liquefaction temperature steps were analyzed by FTIR spectroscopy. The results are shown and discussed in Section 4.4.4.

4.3.6 Proton NMR spectra

Concerning the NMR spectra of the liquids, the same dilution problem as in Section 3.3.7 was present, but only for the liquids obtained after the first heating step (Liquid B), due to their high tetralin dilution (the samples contain 96 ± 3% unreacted tetralin).

Table 4.3.6.1. Effect of Liquefaction Temperature on the Aromatic to Aliphatic Proton Ratio of Coal Liquids Obtained during the 2-step Extraction. Unreliable data points for Liquid B due to the high tetralin dilution.

Step 1 Temperature (^{0}C)	Step 2 Temperature (^{0}C)	Liquid C Aromatic : Aliphatic Protons Ratio	Liquid B Aromatic : Aliphatic Protons Ratio
100	352	1.191 ± 0.647	1.332 ± 0.487
	397	0.950 ± 0.021	
	415	1.272 ± 0.069	
150	354	1.202 ± 0.258	-8.131 ± 10.055*
	398	1.284 ± 0.176	
	416	1.314 ± 0.131	
200	352	0.765 ± 0.090	1.579 ± 0.789
	397	1.507 ± 0.119	
	415	1.430 ± 0.214	

*The calculation process for these numbers is very sensitive to small variations of the NMR spectra, leading to unreliable results with very high error when the samples are as diluted as the Liquid B samples, hence the negative value of the ratio.

4.4 Discussion

4.4.1 Intermediate Heating Steps Influence on Product Yield

The results shown in Table 4.3.1.1 can be seen in bar graph form in Figure 4.4.1.1:

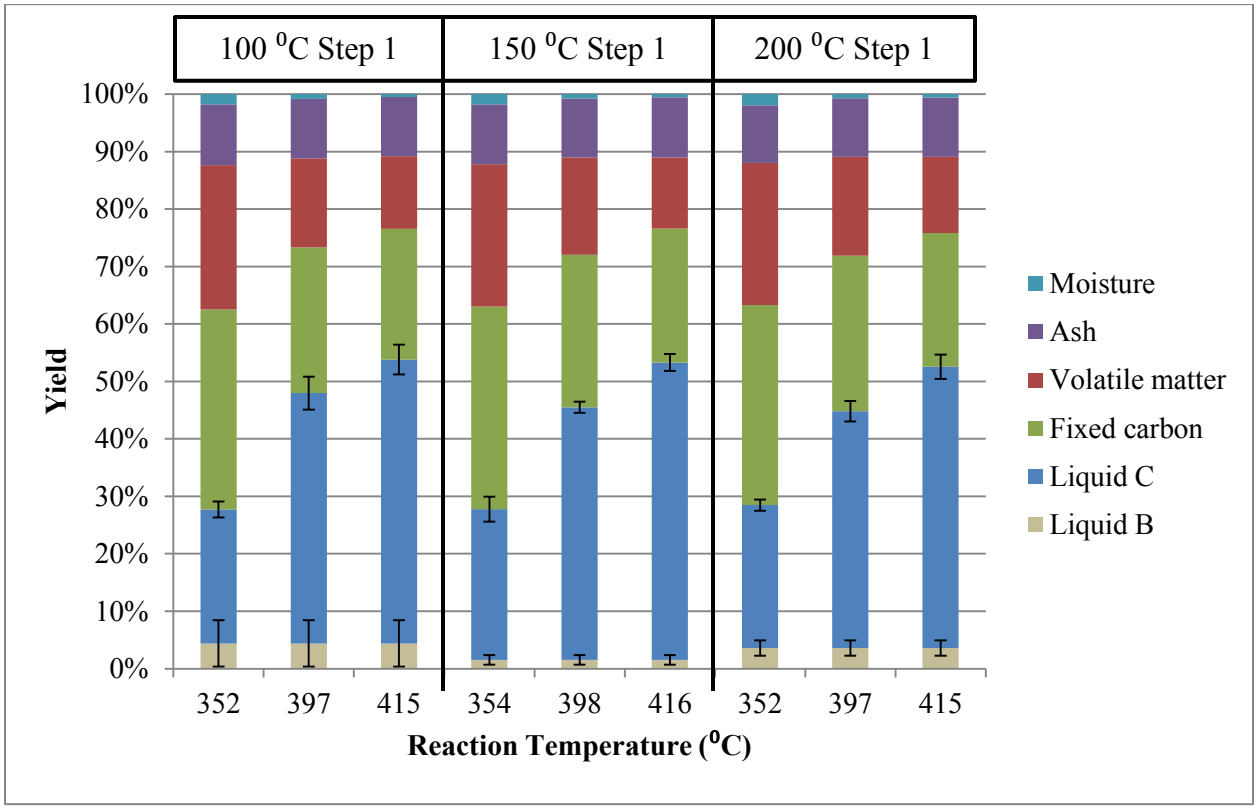

Figure 4.4.1.1. Product Yield for Coal Liquefaction in 2 Steps at Different Temperatures

The liquid yield predictably increased with liquefaction temperature for the high temperature heating step. In terms of Liquid C yields at a specific temperature, there is no significant difference between the three different temperatures used for the step 1 sets. For example, when the second step was carried out at 415 °C, the Liquid C yield for the products with the first step extraction at 100 °C was 49.4 ± 2.6, at 150 °C was 51.75 ± 1.46, and at 200 °C was 48.98 ± 2.11. The only difference which is close to a statistically meaningful one is between the scenarios involving the 397-398 °C step two, combined with the 150 °C respectively 200 °C step 1.

Overall, the liquid yields for coal liquefaction with intermediate heating steps were higher than the ones for liquefaction in a single step (Figure 4.4.1.2). Compared to the single step liquefaction process, the total yield (Liquid A, B and C) increased with 6-9% when the reaction was carried out at 397 °C and with 4-5% when it was carried out at 415 °C. However, the only statistically significant yield increase was for the scenario involving a 150 °C first step, followed by a 398 °C second step.

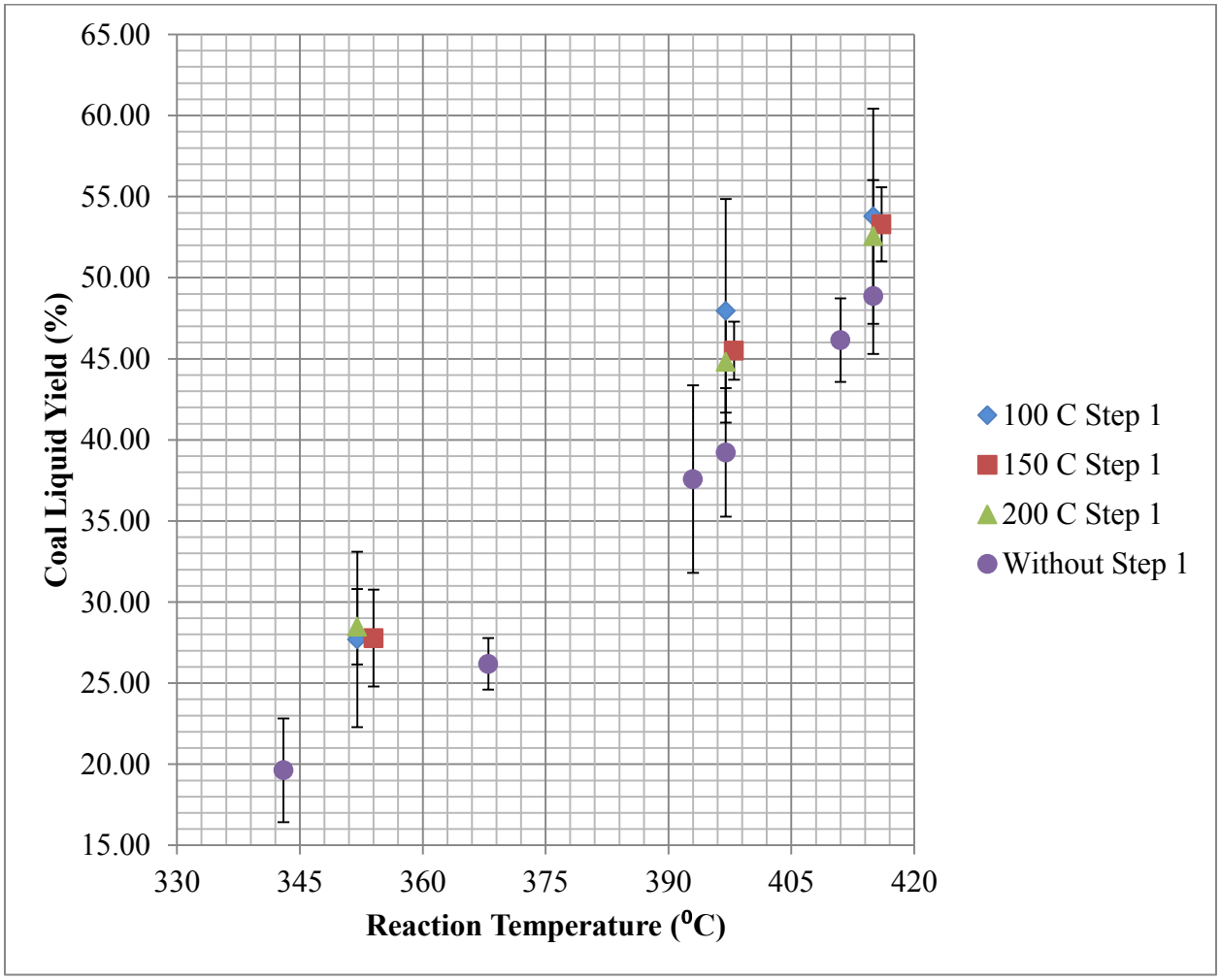

Figure 4.4.1.2. Total Coal Liquid Yield: Comparison between Different Heating Approaches

4.4.2 Intermediate Heating Steps Influence on Product Quality: Density, Refractive Index and Boiling Ranges

The same reasoning as in Section 3.4.2 has been applied in order to judge the aromatic content of the liquid products by measuring their density and refractive index, given that there is a correlation between these characteristics [9-11]. Comparisons between the results of the 2-step and the single-step heating approaches are shown in Figures 4.4.2.1, 4.4.2.2 and 4.4.2.3.

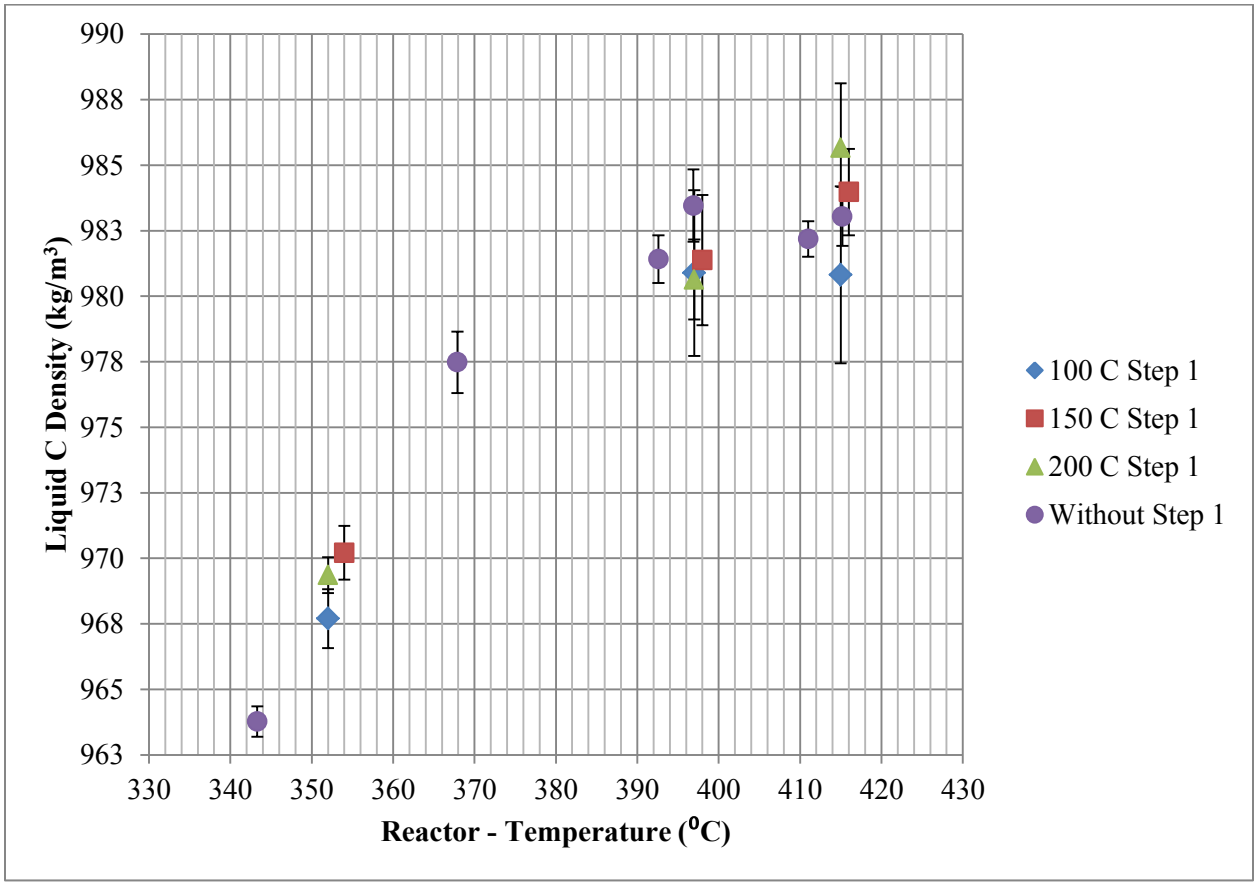

Figure 4.4.2.1. Liquid Product Density: Comparison between Different Heating Approaches

By comparing the densities of the liquids obtained after 2 heating steps with the ones obtained after a single step, the conclusion is that they follow the same pattern in both cases, with only minor changes which are not statistically meaningful. When comparing the impact of using different low temperature steps, a more meaningful difference can be observed only at

lower second-step temperatures (352-354 °C), and only between the 100 °C set and the 150 °C set, the latter one showing slightly higher liquid product densities.

By calculating the densities of the coal liquids void of unreacted tetralin (Figure 4.4.2.2), there is no additional information provided, as the density profile is almost identical to the one shown in Figure 4.4.2.1.

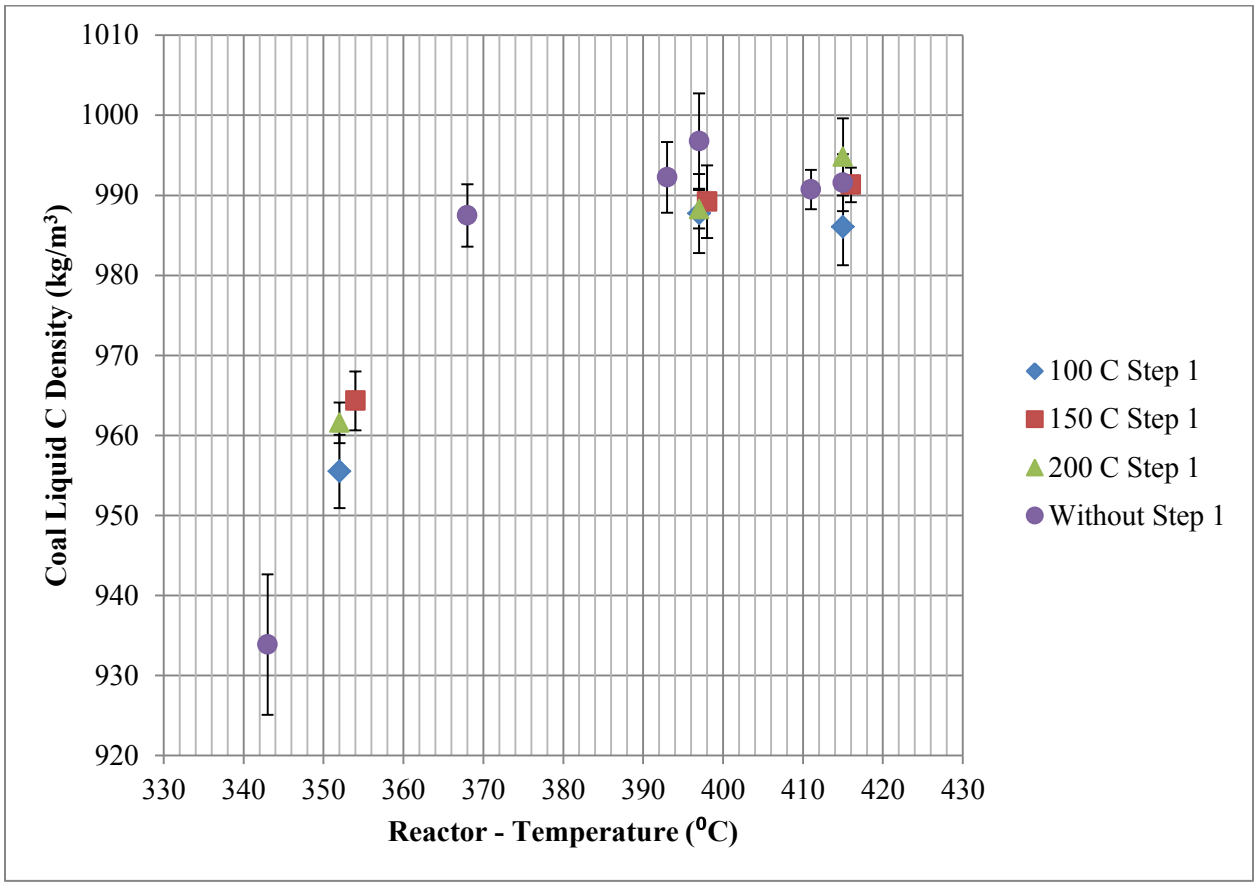

Figure 4.4.2.2. Coal Liquid Density: Comparison between Different Heating Approaches

As seen in Table 4.3.2.1, the densities of the liquid products obtained after the low temperature step (Liquid B) are identical. Due to the very high dilution of these samples, the calculated densities of the coal liquids void of unreacted tetralin are not reliable values, as suggested by the high standard deviations from Table 4.3.2.1.

The refractive index of the final liquid products does not provide any new information either, as there is no significant difference between the various heating approaches. The

exception is for the high temperatures, 415 °C, where the liquids obtained after 2 temperature steps show higher refractive index values than the ones obtained with a single heating step. As discussed in Chapter 3, the samples of the 415 °C set for the single step process was slightly more diluted with washing tetralin, and as the refractive index is the only analysis for which the results have not been adjusted based on the composition of the samples, this is suggests an apparent (yet false) difference between the two heating approaches (Figure 4.4.2.3).

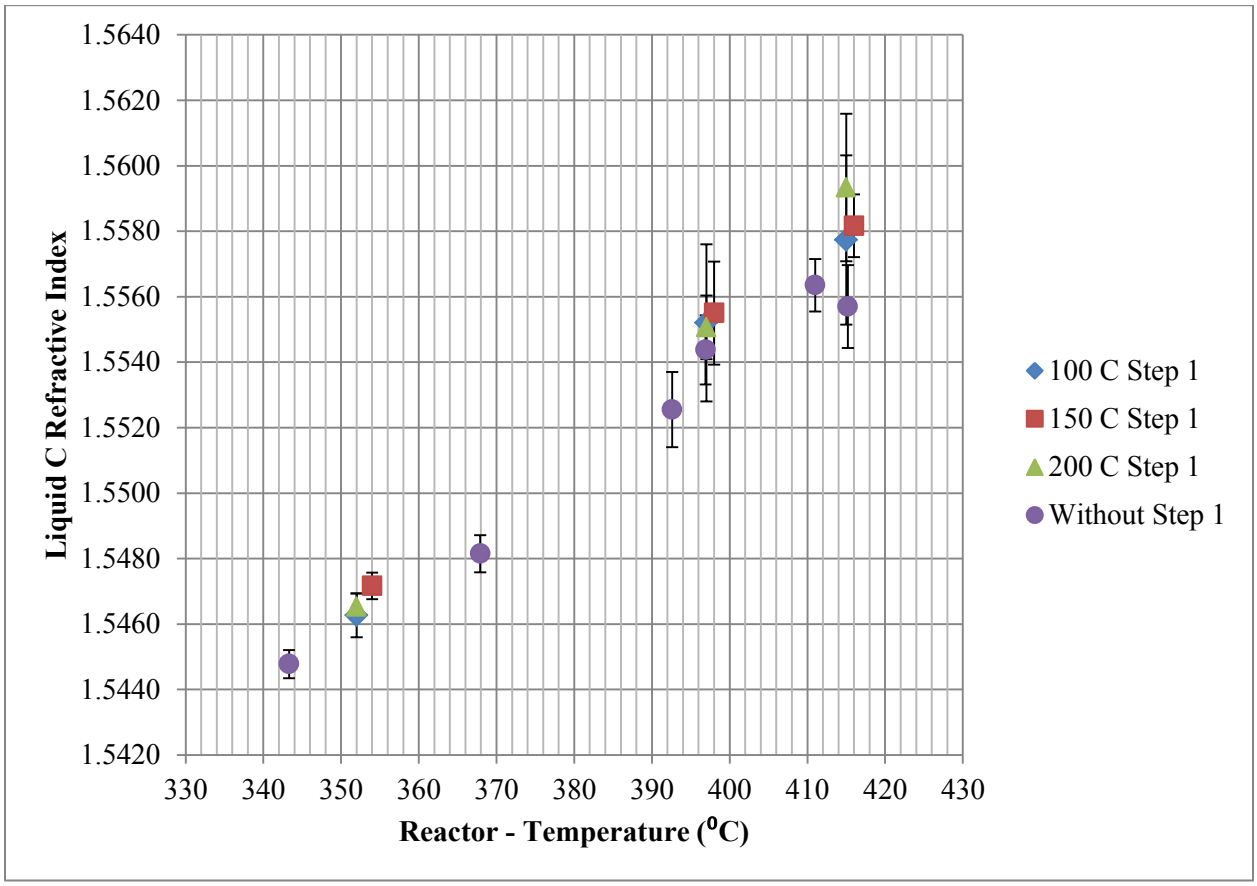

Figure 4.4.2.3. Liquid Product Refractive Index: Comparison between Different Heating Approaches

When comparing the TBP curves of the coal liquids obtained with the same step 2 temperature, but different step 1 temperatures (Figure 4.4.2.4), they do not seem to differ a lot from one another.

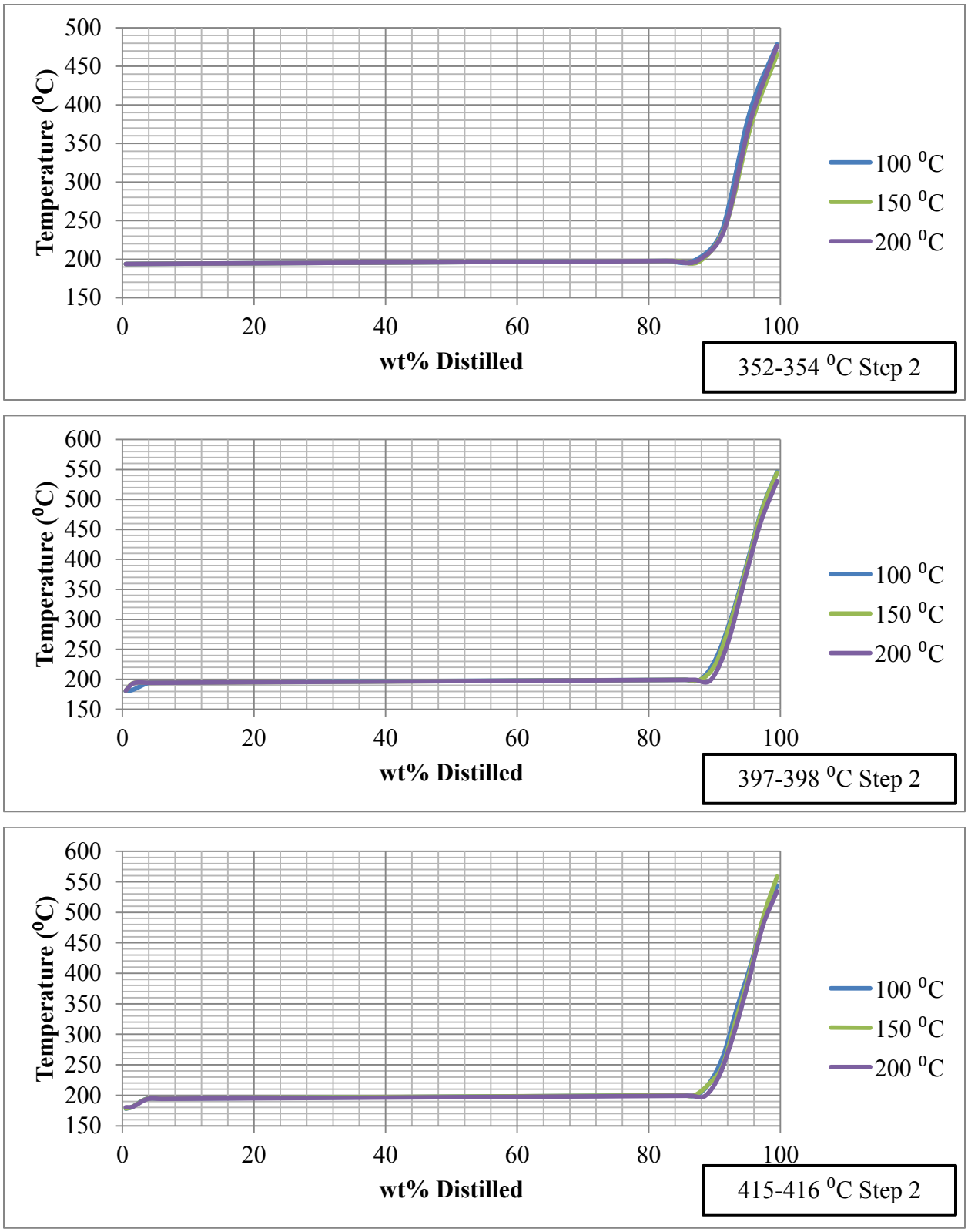

Figure 4.4.2.4. TBP Curves of Coal Liquids obtained with the same Step 2 Temperature, but Different Step 1 Temperatures

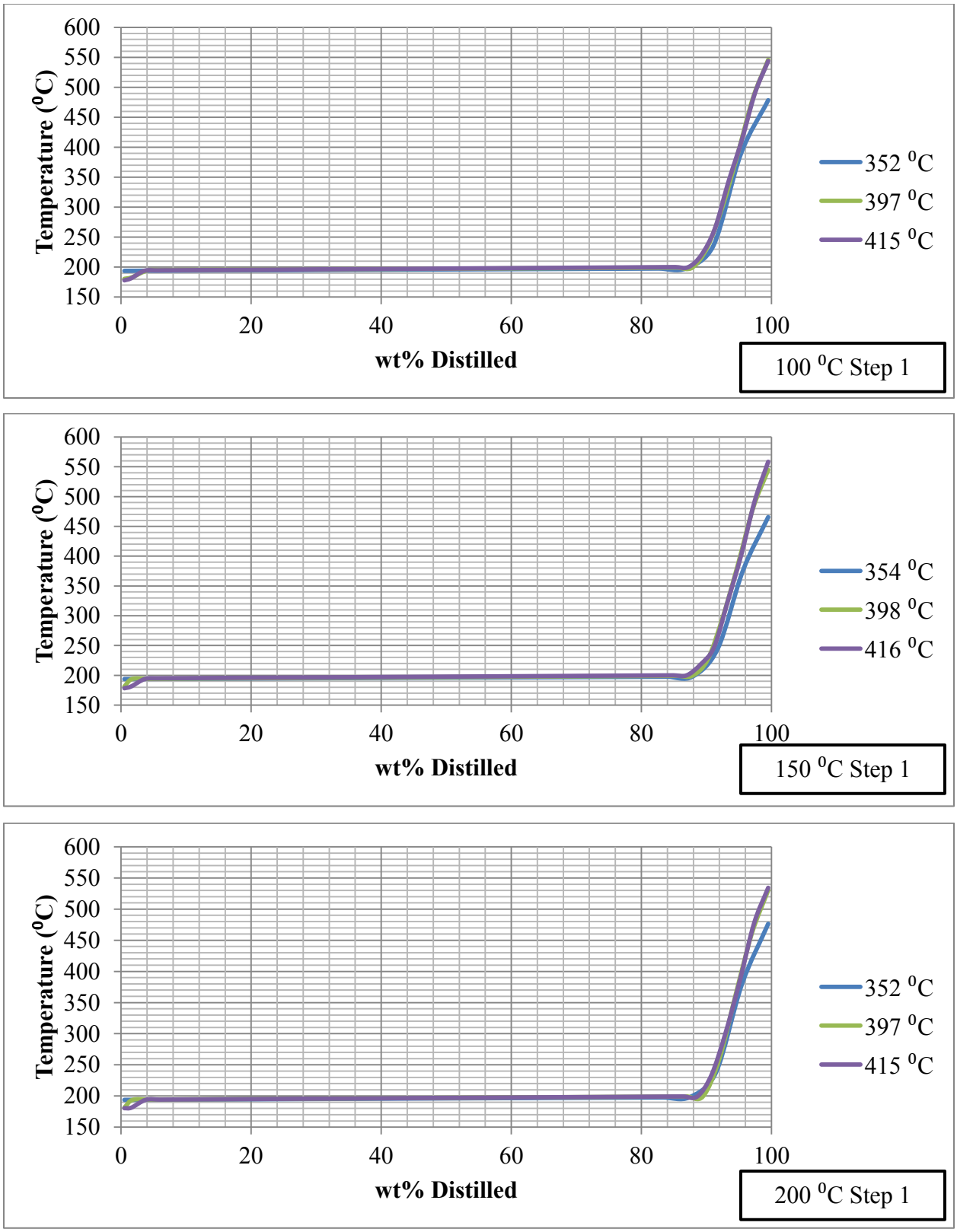

Figure 4.4.2.5. TBP Curves of Coal Liquids obtained with the same Step 1 Temperature, but Different Step 2 Temperatures

However, when comparing the TBP curves of the coal liquids obtained with the same step 1 temperature, but different step 2 temperatures (Figure 4.4.2.5), it seems that the liquids obtained at the lowest step 2 temperature (352-354 °C) contain compounds with lower boiling points. This is the opposite trend from what happened when the liquefaction was carried out in a single heating step (Chapter 3). The coal liquid densities of these samples are this time in agreement with their boiling points: the higher the boiling point, the higher the density. The density is increasing between 352 °C and 397 °C, and so do the boiling points. The density is constant between 397 °C and 415 °C, and so are the boiling points. Therefore, concerning the aromatic content of these samples, there is nothing that can be said based on this data, except maybe if the refractive index results would not have been influenced by the reaction yields (via dilution).

Interesting observations can be made when comparing the TBP curves of the single-step process with the ones of the 2-step process (Figure 4.4.2.6). The liquids obtained in a single step, at 397 °C and 415 °C have higher boiling points than all the liquids obtained in 2 steps. In case of the 343 °C single step liquids, ~27 % of them have higher boiling points than the liquids obtained in any other way, but their heaviest compounds are lighter than all the other liquids. This can better be seen in Figure 4.4.2.7.

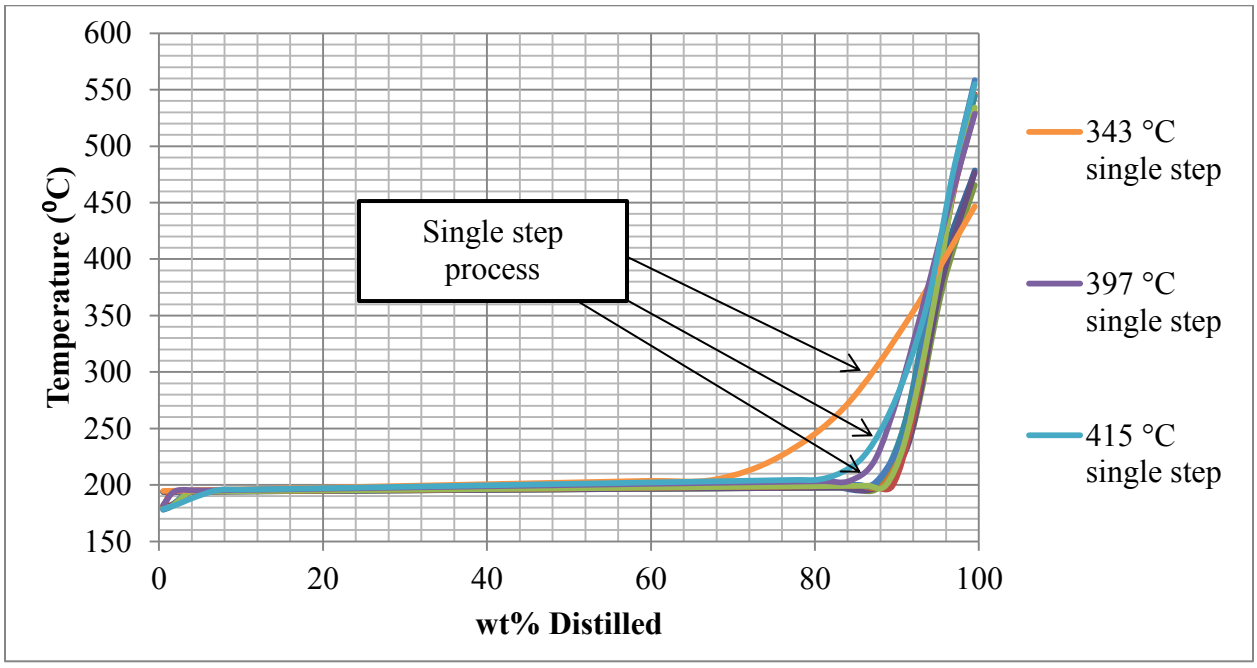

Figure 4.4.2.6. Comparison between the TBP Curves of Coal Liquids obtained in a Single-Step Process and in a 2-Step Process

Using average TBP values and overlapping them with the coal liquid densities provide a clear image of the above mentioned deductions regarding the aromatic content of the samples (Figure 4.4.2.7):

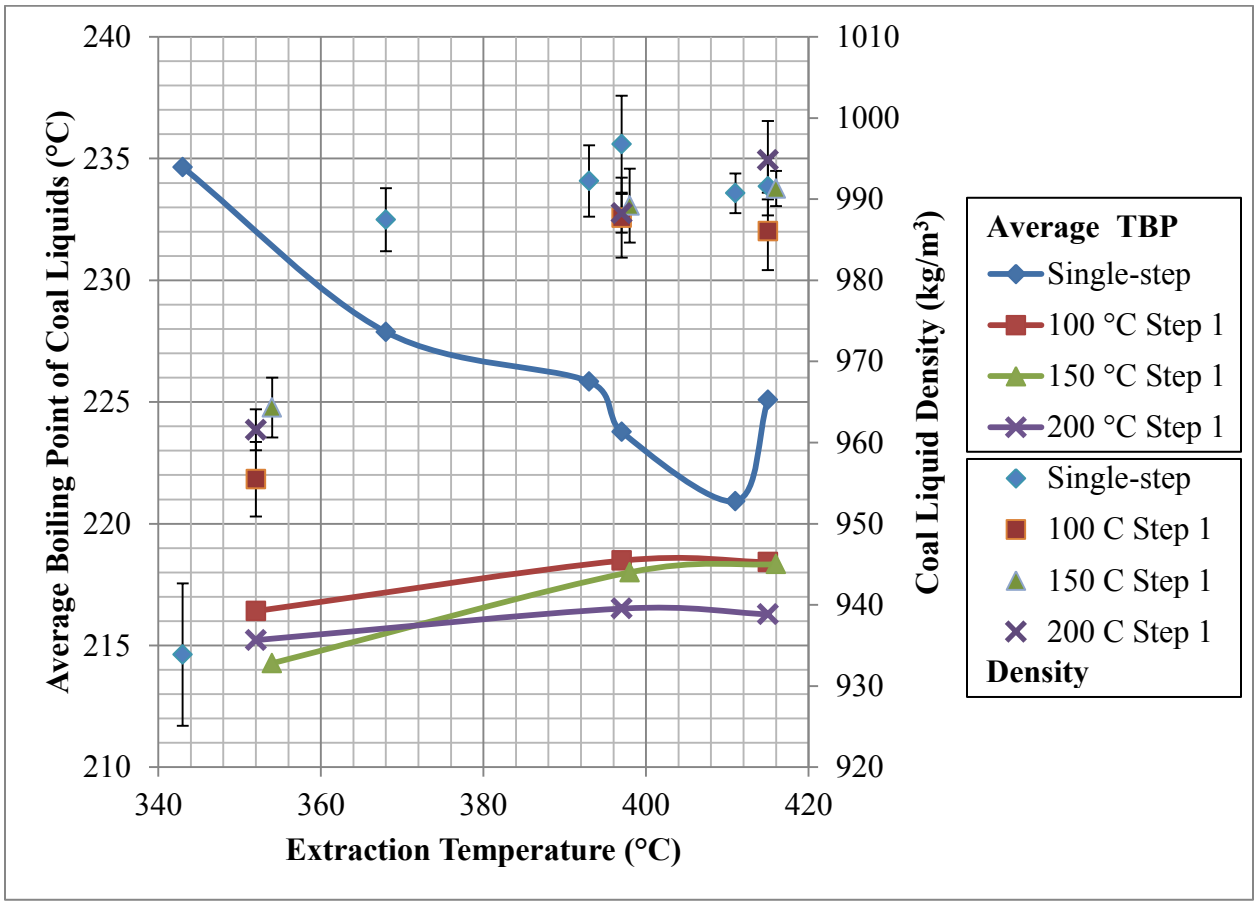

Figure 4.4.2.7. Comparison between the Density and Average TBP of Coal Liquids obtained in a Single-Step Process and in a 2-Step Process

4.4.3 Influence of Intermediate Heating Steps on Iron Pyrite Conversion: Residue Stereomicroscopy

Similarly to Section 3.4.3, a comparison between the stereomicroscopy obtained pictures of different residues was made, in order to observe the tendency of the iron pyrite conversion as influenced by different heating approaches. A selection of pictures from each reaction set is shown in Figure 4.4.3.1.

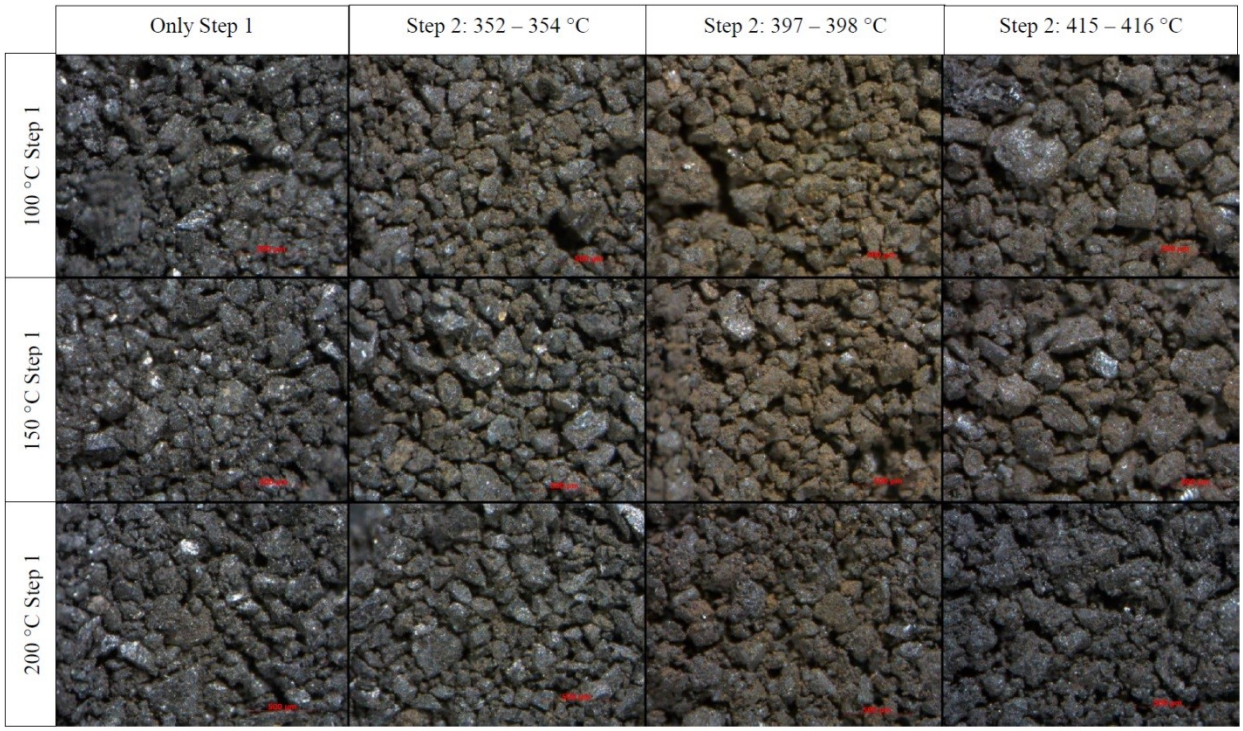

Figure 4.4.3.1. Selection of stereomicroscopy pictures of residues from coal liquefaction with different heating steps

Curiously, the pictures obtained this time were different from the ones obtained in Chapter 3 (Section 3.4.3). Not only the granular structure of the residues appeared more compact and rough while the pyritic golden sheen was absent, but their color showed an unexpected shift. If the residues obtained in a single heating step were showing a golden composition at lower temperatures which faded out with temperature increase, these residues appear to manifest a grey-to-yellow hue shift until 397 °C, after which they show the opposite trend, which is the same as in Chapter 3.

A possible explanation for this outcome is that after step 1, too little coal dissolution took place to expose the iron pyrite (as confirmed by the low Liquid B yields). After step 2, at the lower temperatures, some iron pyrite is exposed, but the amount of coal dissolved is still too little to fully expose the iron pyrite. By 397 – 398 °C the iron pyrite is exposed and probably partially converted. The maximum visible iron pyrite would probably have been observed between 350 and 400 °C. On increasing temperature to 415 °C, the iron pyrite is converted the same way as in Chapter 3.

4.4.4 Fourier Transform Infrared Spectra

Similarly to the FTIR spectra of the coal liquids obtained in a single heating step (Section 3.4.5), the coal liquids obtained after two heating steps show little to no difference from the pure tetralin spectrum. Figures 4.4.4.1, 4.4.4.2 and 4.4.4.3 show the FTIR spectra for the three different temperatures used for step 1, as well as their step 2 corresponding temperatures.

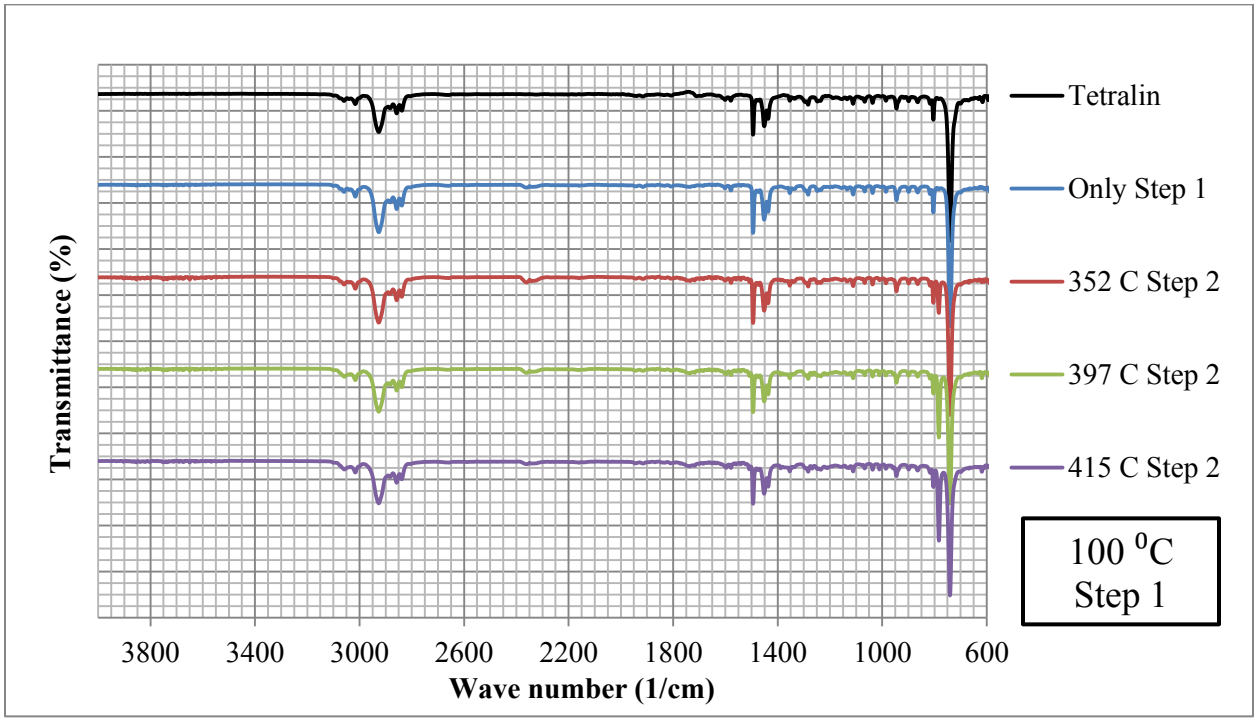

Figure 4.4.4.1. FTIR Spectra of Tetralin and of the Liquid Products of Coal Liquefaction obtained from the Residues of 100 °C low temperature step

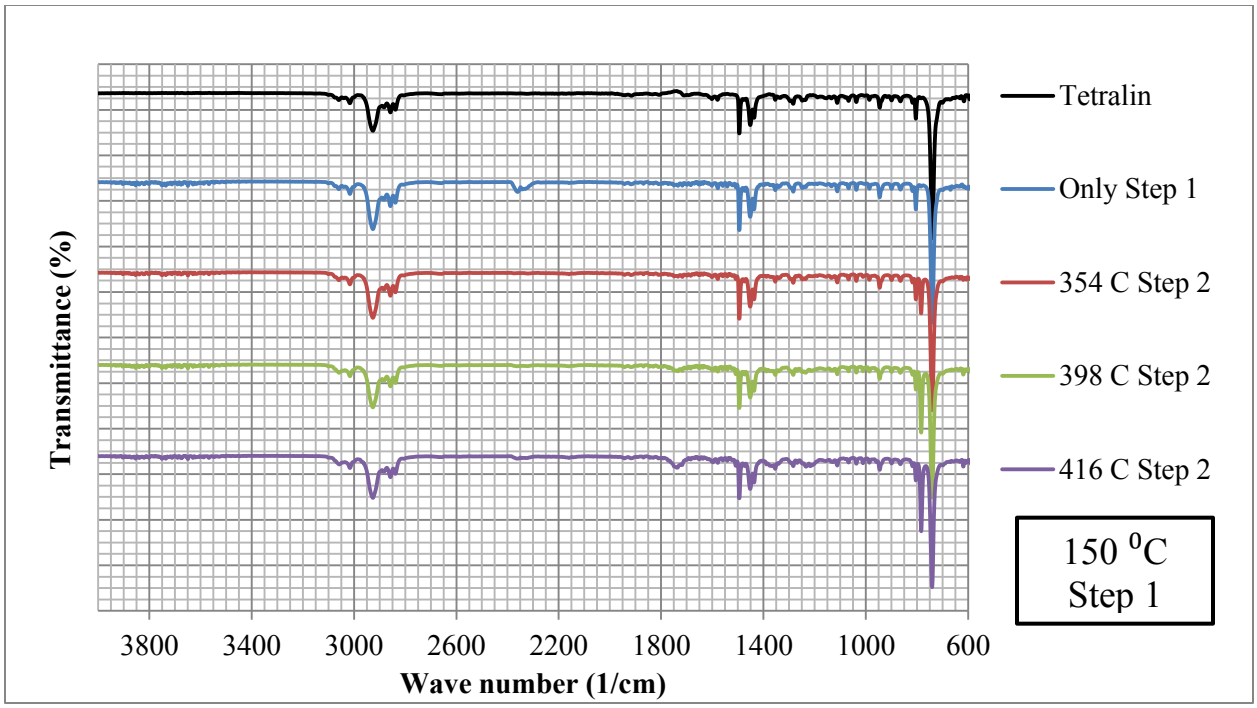

Figure 4.4.4.2. FTIR Spectra of Tetralin and of the Liquid Products of Coal Liquefaction obtained from the Residues of 150 °C low temperature step

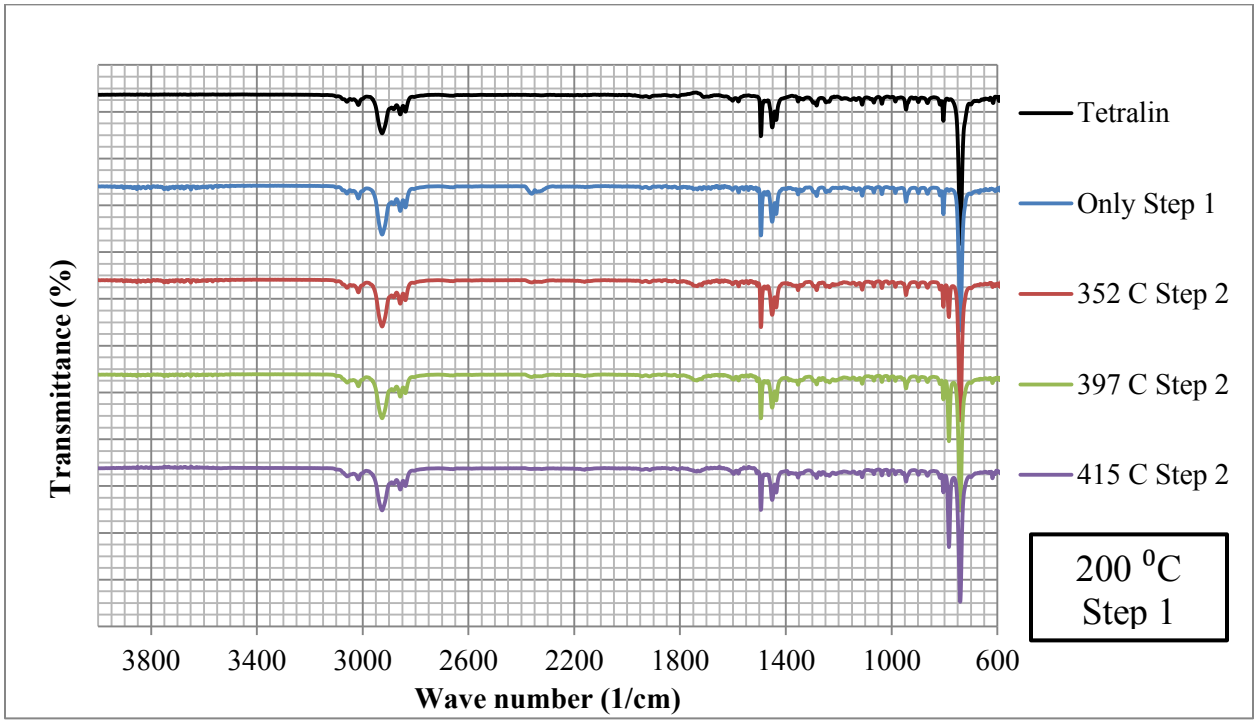

Figure 4.4.4.3. FTIR Spectra of Tetralin and of the Liquid Products of Coal Liquefaction obtained from the Residues of 200 °C Low Temperature Liquefaction Step

In addition to the 783 cm^{-1} peak mentioned in the previous chapter, which has the same behavior in this case, there are 2 new bands present, which did not exist in the spectra of the single-step obtained coal liquids. One of them is between the wave numbers of 2380 – 2315 cm^{-1} apparently (yet falsely) indicating the presence of boron compounds [12], especially in the liquids obtained right after the low temperature step, at 150 °C and 200 °C. In reality, this band is the result of a common mid-infrared spectroscopy error generated by the atmospheric intrusion of molecules in the path of the IR beam [13]. The other band, located at 1770 – 1710 cm^{-1}, indicates an increase in carbonyl groups such as esters, saturated aldehydes and ketones [12], especially in the coal liquids obtained after a 150 °C low temperature step followed by a 416 °C high temperature step.

The FTIR spectra of the residues are shown in Figures 4.4.4.4, 4.4.4.5 and 4.4.4.6. The residues seem to show similar behavior as the ones obtained after a single temperature step, described in the previous chapter.

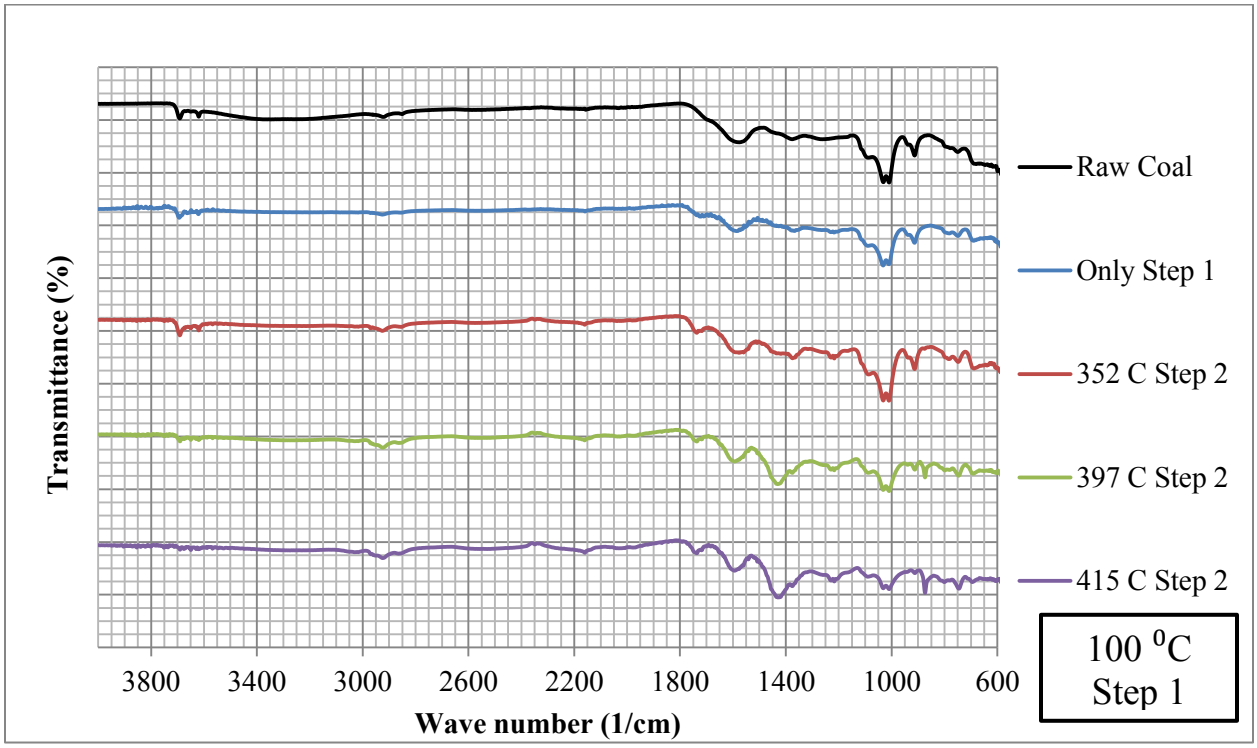

Figure 4.4.4.4. FTIR Spectra of the Raw Coal and of the Residues of Coal Liquefaction obtained at the 100 °C Low Temperature Liquefaction Step and Subsequent Heating Steps

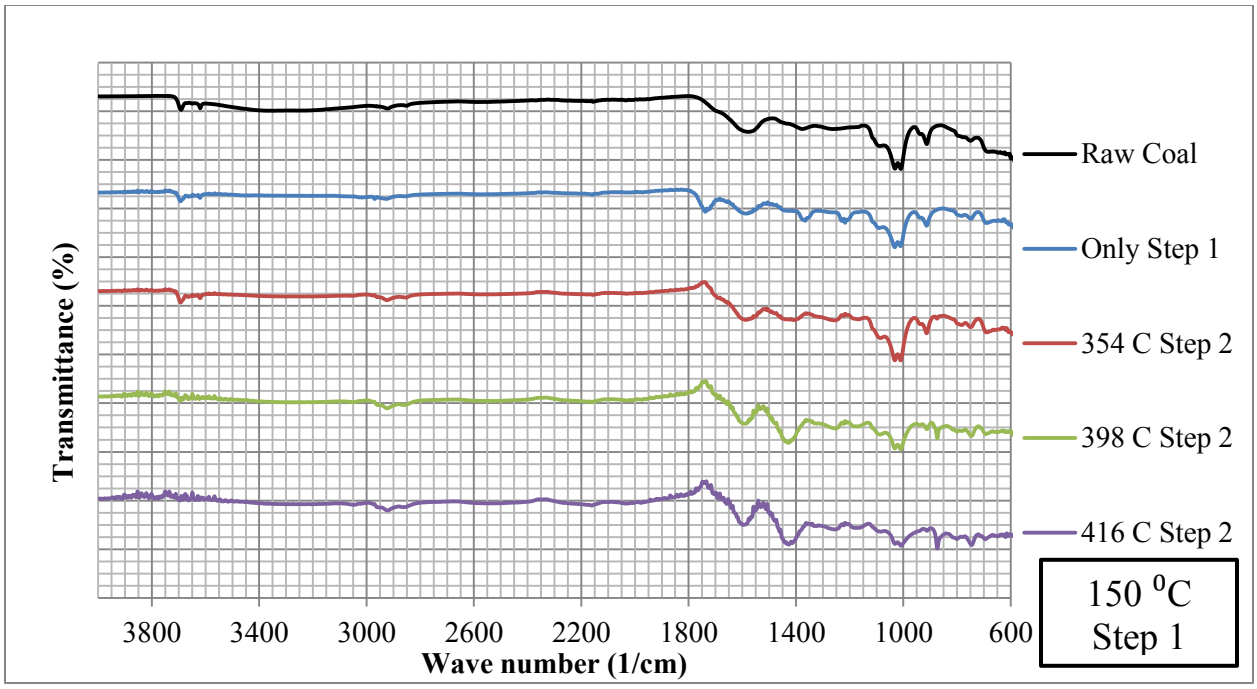

Figure 4.4.4.5. FTIR Spectra of the Raw Coal and of the Residues of Coal Liquefaction obtained at the 150 °C Low Temperature Liquefaction Step and Subsequent Heating Steps

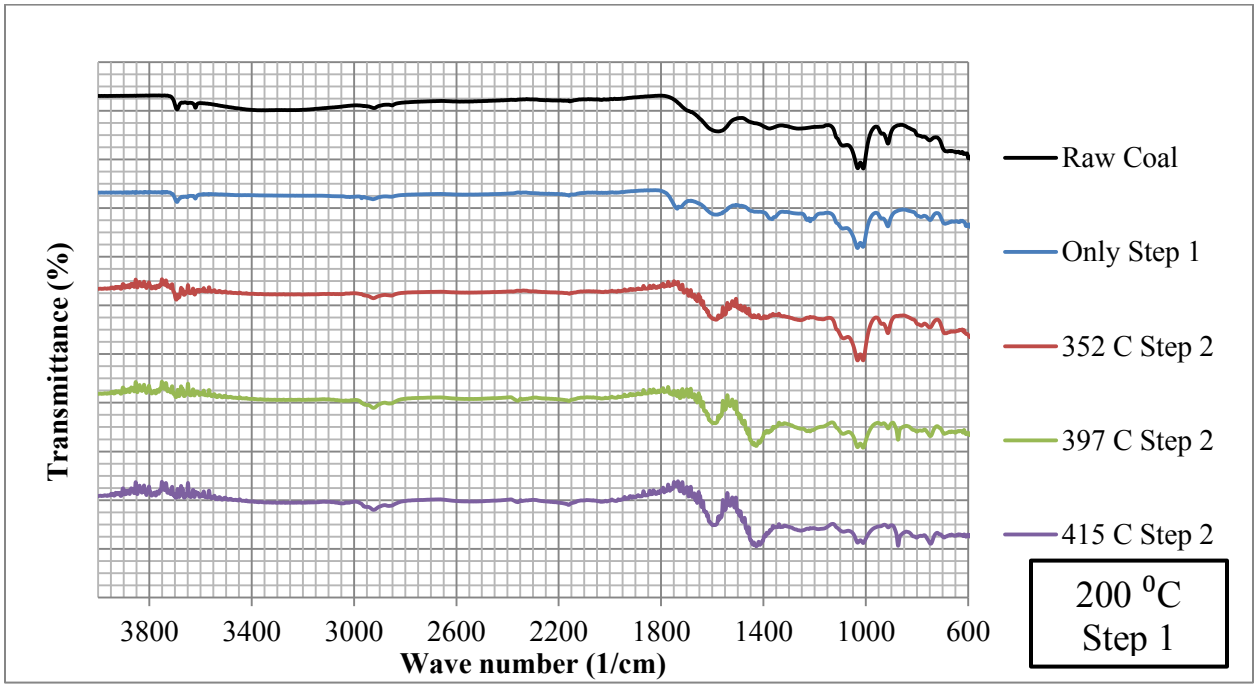

Figure 4.4.4.6. FTIR Spectra of the Raw Coal and of the Residues of Coal Liquefaction obtained at the 200 °C Low Temperature Liquefaction Step and Subsequent Heating Steps

4.4.5 Proton NMR Spectra

Unlike in the case of the liquids obtained during a single-step temperature approach, the coal liquids obtained in two consecutive heating steps did not present any problems related to their dilution as far as their aromatic to aliphatic protons ratio was concerned. This is visible in Figure 4.4.5.1, where the error bars corresponding to the experiments in two heating steps are much narrower than the ones corresponding to coal liquids obtained without a low temperature step. The reason for this is the different tetralin dilution of the samples. For the single-step temperature approach, the samples obtained at lower temperature contained up to 88% tetralin (more washing tetralin was used for these samples), whereas for the two-step approach, those samples contained an average of 75 % tetralin. On the other hand, the liquid samples obtained after the low temperature step (Liquid B) were so diluted that it was impossible to obtain reliable values, some of them even reaching negative values (Table 4.3.6.1).

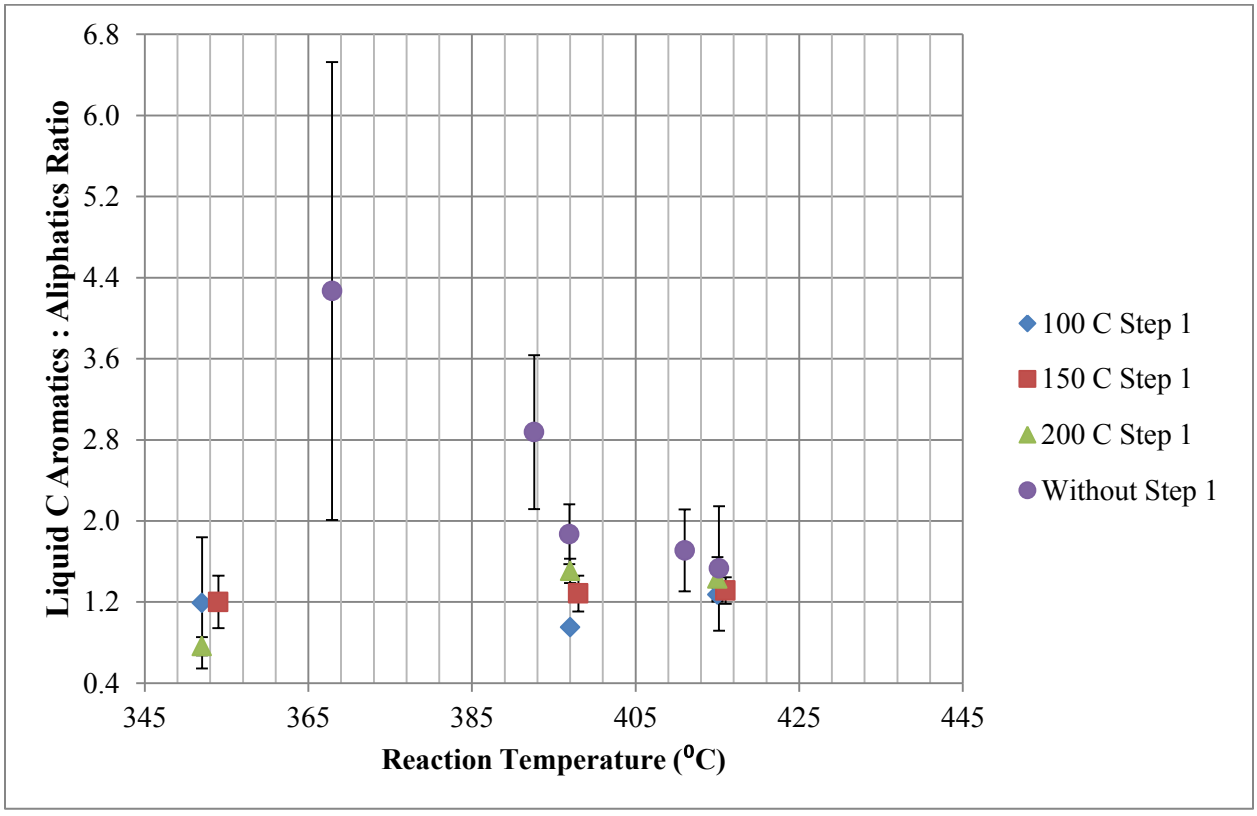

Figure 4.4.5.1. Aromatic to Aliphatic Protons Ratio in the Coal Liquids obtained during Coal Liquefaction: Comparison between Different Heating Approaches

Using two heating steps for coal liquefaction instead of a single step seems to increase the quality of the obtained liquids, in terms of aromatic to aliphatic protons ratio (from a refining point of view), especially where lower temperatures of the second step are concerned. Even at 397 °C there is still a meaningful difference between the two cases. However, when temperature is increased to 415 °C, the two cases do not show any meaningful difference.

When comparing the outcomes of the 3 different temperatures of step 1 (100 °C, 150 °C and 200 °C), the only notable difference appeared when the second temperature step reached 397 °C. For this second step, the heating scenario with the lowest initial temperature step, 100 °C, led to the lowest aromatic to aliphatic protons ratio in Liquid C.

4.5 Conclusions

(a) The liquid yield of coal liquefaction increases with temperature on the 350 – 415 °C interval, regardless if the liquefaction is carried out in one or in two heating steps.

(b) Compared to the single-step coal liquefaction process, the liquid yields of the two-step liquefaction process are higher. They increase with 6-9% when the second step is carried out at 397 °C and with 4-5% when it is carried out at 415 °C, but the only statistically significant yield increase was for the scenario involving a 150 °C first step, followed by a 398 °C second step. Moreover, in the case of the 2 step scenario, there are additional coal liquids obtained during the low temperature heating step, albeit in a much diluted form, and with statistically significant yield differences only between the 150 and 200 °C temperatures.

(c) For any fixed high temperature step, between the three different low temperature step scenarios, 100 °C, 150 °C and 200 °C, the highest Liquid C yield obtained is for 150 °C, but the only statistically meaningful difference is between the scenarios involving the 397-398 °C step two, combined with the 150 °C respectively 200 °C step 1.

(d) Final liquid product density and refractive index are not significantly affected when using two heating steps as opposed to one single step.

(e) Based on the boiling point distributions of the coal liquids, there is no conclusion regarding the aromatic content trend of the samples of the 2-step process. While the single-step process samples show an increase in aromatic content until 411°C after which there is a small decrease, the 2-step process samples do not show such a trend.

(f) The liquids obtained during the single-step process have predominantly higher boiling points than the ones obtained during the 2-step process.

(g) Proton NMR analyses show that using two heating steps rather than one single heating step leads to a lower aromatic to aliphatic protons ratio in the coal liquids, but only when the second heating step is carried out between 352 and 397 °C. Beyond that temperature there is no difference between these two approaches as far as this ratio is concerned.

(h) The stereomicroscopy images indicate that after the first temperature step (100 – 200 °C), the iron pyrite is still covered by layers of undissolved coal. After the second step, with increasing temperatures more iron pyrite is getting exposed, while also being converted, leading to a lack of iron pyrite for the 415 °C obtained residues.

(i) FTIR spectra indicate that there are carbonyl groups in the coal liquids obtained while following specific 2 step heating scenarios, whereas these compounds are absent from the coal liquids obtained during the single-step approach.

(j) The quality of the liquids obtained during the low temperature step could hardly be evaluated due to the high dilution of these samples.

References

[1] Haghighat, F.; De Klerk, A. Direct coal liquefaction: Low temperature dissolution process. *Energy Fuels* **2014**, *28*, 1012-1019.

[2] Song, C.; Schobert, H. H.; Hatcher, P. G. In Temperature-programmed liquefaction of low rank coal. Evaluation of coal depolymerization reactions by CPMAS ^{13}C NMR and Pyrolysis-GC-MS; Ltd, International Energy Agency Coal Research, Ed.; 1991 International Conference on Coal Science Proceedings; Butterworth-Heinemann: 1991; pp 664-667.

[3] Derbyshire, F.; Davis, A.; Epstein, M.; Stansberry, P. Temperature-staged catalytic coal liquefaction. *Fuel* **1986***, 65*, 1233-1239.

[4] Stenberg, V. I.; Gutenkunst, V.; Nowok, J.; Sweeny, P. G. Low severity lignite liquefaction: temperature programming to 350 °C in an inorganic solvent system. *Fuel* **1989***, 68*, 133-135.

[5] Wham, R. M. Effect of slurry heating rate on short-contact-time coal liquefaction. *Fuel* **1987***, 66*, 283-284.

[6] Haghighat, F. Investigation of solvent extraction of coal at low temperatures. MSc. Thesis, University of Alberta, University of Alberta, Fall 2013.

[7] ASTM D7582-12: Standard Test Methods for Proximate Analysis of Coal and Coke by Macro Thermogravimetric Analysis; ASTM: West Conshohocken, PA 2012.

[8] ASTM D7169-11: Standard Test Methods for Boiling Point Distribution of Samples with Residues Such as Crude Oils and Atmospheric and Vacuum Residues by High Temperature Gas Chromatography; ASTM: West Conshohocken, PA 2011.

[9] Sachanen, A. N. *The chemical constituents of petroleum*; Reinhold: New York, 1945, p. 102-107.

[10] Lee, S. W., Preto, F., & Hayden, A. C. Determination of fuel aromatic content and its effect on residential oil combustion. *Preprints Papers Am. Chem. Soc., Div. Fuel Chem* **1986**, *31*, 275-293.

[11] Abdul-Halim Abdul-Karim, M.; Hadi, G.A. The Relationships between the Physical and Chemical Properties of Narrow Fractions Distilled From Mixed Kirkuk and Sharki-Baghdad Crude Oils. *IJCPE* **2008**, 9, 1-8.

[12] Gokel, G. W. *Dean's Handbook of Organic Chemistry, 2nd ed.*; McGraw-Hill: New York, 2004, p. 6.21 – 6.53.

[13] Chalmers, J. M. In *Mid-Infrared Spectroscopy: Anomalies, Artifacts and Common Errors;* Handbook of Vibrational Spectroscopy; John Wiley & Sons, Ltd: 2006.

CHAPTER 5 – CONCLUSIONS

The conclusions are presented in 5 groups, concerning the influence of extraction temperature and heating stages on the following aspects of coal liquefaction: coal liquid yield, physical properties, aromatic content, iron pyrite conversion and other observations.

5.1 Coal liquid yield

The liquid yield increased from ~20 wt% to ~49 wt% over the 340 – 415 ^{0}C temperature interval when one single extraction step was employed.

Adding an additional low temperature heating step (in the range 100 ^{0}C – 200 ^{0}C) before the high temperature one increased the overall liquid yield with up to 9%.

5.2 Coal liquid physical properties

The liquids obtained during a single extraction step showed an increase in density from ~934 to ~988 kg/m^3 when extraction temperature was increased from 343 to 368 ^{0}C, after which the density remained statistically unchanged (until 415 ^{0}C). The average boiling points decreased from ~235 ^{0}C to ~221 ^{0}C over the 340 – 411 ^{0}C liquefaction temperature interval, and increased back to ~225 ^{0}C for the liquids obtained at 415 ^{0}C. The liquids obtained at temperatures higher than 368 ^{0}C contain about 4% products which require vacuum distillation.

When using two heating steps, the density and refractive index are not significantly affected. However, the boiling point distributions of the final liquid products are. The coal liquids obtained during the 2-step process have lower boiling points than the ones obtained during the single-step process, ranging between ~214 ^{0}C and ~218 ^{0}C.

5.3 Coal liquid aromatic content

For the single step process, there should be a relatively significant increase in aromatic content between 343 and 368 ^{0}C, since there is a big increase in density despite the boiling points getting predominantly lower. Between 368 and 411 ^{0}C the aromatic content seems to increase at a very slow, decelerating rate. Between 411 and 415 ^{0}C, the aromatic content starts to decrease. Regarding the aromatic to aliphatic proton ratio, NMR analyses showed a slight decrease between 393 and 397 ^{0}C. For these reasons, it seems as if there are more aromatics obtained as temperature is increased, while these aromatics tend to present increasing amounts of aliphatic chains.

When the 2-step extraction process is employed, the aromatic content of the coal liquids seems to be higher than in the single-step case, while the aromatics obtained are predominantly richer in aliphatic hydrogen, as the NMR analysis points out.

5.4 Iron pyrite conversion

The iron pyrite conversion is increasing with liquefaction temperature for the single-step process. This was visually confirmed by stereomicroscopy analyses performed on the liquefaction residues.

For the 2-step process, the same analyses showed that the pyrite is still covered by undissolved coal after the low-temperature step, while being progressively uncovered and converted during the high-temperature step.

5.5 Other observations

Fourier Transform Infrared (FTIR) spectra indicated that with increasing temperature, there is an increase in aromatics containing three adjacent hydrogen atoms in the coal liquids.

BIBLIOGRAPHY

1. Abdul-Halim Abdul-Karim, M.; Hadi, G.A. The Relationships between the Physical and Chemical Properties of Narrow Fractions Distilled From Mixed Kirkuk and Sharki-Baghdad Crude Oils. *Iraqi Journal of Chemical and Petroleum Engineering* **2008**, *9*, 1-8.
2. ASTM D7169-11: *Standard Test Methods for Boiling Point Distribution of Samples with Residues Such as Crude Oils and Atmospheric and Vacuum Residues by High Temperature Gas Chromatography*; ASTM: West Conshohocken, PA 2011.
3. ASTM D7582-12: *Standard Test Methods for Proximate Analysis of Coal and Coke by Macro Thermogravimetric Analysis*; ASTM: West Conshohocken, PA 2012.
4. ASTM *Standard Method for Ultimate Analysis Of Coal And Coke;* ASTM Standard D3176; ASTM International: West Conshohocken, PA, 2011.
5. ASTM *Standard Practice for Proximate Analysis of Coal and Coke;* ASTM Standard D3172 – 07a; ASTM International: West Conshohocken, PA, 2007.
6. Berkowitz, N., *An introduction to coal technology.* Academic Press: New York, 1979.
7. Bommannavar, A. S.; Montano, P. A. Mössbauer study of the thermal decomposition of FeS_2 in coal. *Fuel* **1982**, *61*, 523-528.
8. Chalmers, J. M. In *Mid-Infrared Spectroscopy: Anomalies, Artifacts and Common Errors;* Handbook of Vibrational Spectroscopy; John Wiley & Sons, Ltd: 2006.
9. Cleyle, P. J.; Caley, W. F.; Stewart, I.; Whiteway, S. G. Decomposition of pyrite and trapping of sulphur in a coal matrix during pyrolysis of coal. *Fuel* **1984**, *63*, 1579-1582.
10. Davis, A.; Spackman, W.; Given, P. H. Influence of the properties of coals on their conversion into clean fuels. *Energy Sources* **1976***, 3*, 55-81.
11. De Klerk, A. Transport fuel: Biomass-, coal-, gas- and waste-to-liquids processes. In *Future energy. Improved, sustainable and clean options for our planet*, 2ed; Letcher, T.M. Ed.; Elsevier: Amsterdam, 2014, p. 245-270.
12. Derbyshire, F.; Davis, A.; Epstein, M.; Stansberry, P. Temperature-staged catalytic coal liquefaction. *Fuel* **1986***, 65*, 1233-1239.
13. Figueroa Murcia, D. C. Modelling of solvent extraction of coal. MSc. Thesis, University of Alberta, University of Alberta, Spring 2012.

14. Fisher, C. H.; Sprunk, G. C.; Eishner, A.; Clarke, L.; Storch, H. H. Hydrogentation of the Banded Fusain. *Ind. Eng. Chem.* **1939***, 31*, 190-195.
15. Franck, H.; Stadelhofer, J. W.; Biermann, D. Solubilization of bituminous coal in aromatic and hydroaromatic solvents. *Fuel* **1983***, 62*, 78-80.
16. Gary, J. H.; Kaiser, M. J.; Handwerk, G. E. *Petroleum refining: technology and economics*, 5ed; Boca Raton: Taylor & Francis, 2007.
17. Giri, C. C.; Sharma, D. K. Mass-transfer studies of solvent extraction of coals in N-methyl-2-pyrrolidone. *Fuel* **2000***, 79*, 577-585.
18. Gokel, G. W. *Dean's Handbook of Organic Chemistry, 2nd ed.*; McGraw-Hill: New York, 2004, p. 6.21 – 6.53.
19. Haghighat, F. Investigation of solvent extraction of coal at low temperatures. MSc. Thesis, University of Alberta, University of Alberta, Fall 2013.
20. Haghighat, F.; De Klerk, A. Direct coal liquefaction: Low temperature dissolution process. *Energy Fuels* **2014**, *28*, 1012-1019.
21. *Handbook of synfuels technology*; Meyers, R. E. Ed.; McGraw-Hill, New York, 1984.
22. King, D. L.; De Klerk, A. In *Overview of Feed-to-Liquid (XTL) Conversion;* American Chemical Society: 2011; Vol. 1084, pp 1-24.
23. Kuznetsov, P. N.; Kuznetsova, L. I.; Borisevich, A. N.; Pavlenko, N. I. Effect of Mechanochemical Treatment on Supramolecular Structure of Brown Coal. *Chemistry for Sustainable Development* **2003***, 11*, 715-721.
24. Laskowski, J. S. Chapter 10 Fine-coal utilization. *Developments in Mineral Processing* **2001***, 14*, 307-351.
25. Lee, S. W., Preto, F., & Hayden, A. C. Determination of fuel aromatic content and its effect on residential oil combustion. *Preprints Papers Am. Chem. Soc., Div. Fuel Chem* **1986**, *31*, 275-293.
26. Liu, F.; Li, W.; Chen, H.; Li, B. Uneven distribution of sulfurs and their transformation during coal pyrolysis. *Fuel* **2007***, 86*, 360-366.
27. Makgato, M. H.; Moitsheki, L. J.; Shoko, L.; Kgobane, B. L.; Morgan, D. L.; Focke, W. W. Alkali-assisted coal extraction with polar aprotic solvents. *Fuel Process Technol.* **2009***, 90*, 591-598.
28. Mishra, S. K.; Klimpel, R. R. *Fine coal processing;* Noyes Publications: NJ, 1987.

29. Mitchell, G. D. In *Chapter 6 - Direct Coal Liquefaction;* Suárez-Ruiz, I., Crelling, J. C., Eds.; Applied Coal Petrology; Elsevier: Burlington, 2008; pp 145-171.
30. Montano, P. A.; Bommannavar, A. S.; Shah, V. Mössbauer. Study of transformation of pyrite under conditions of coal liquefaction. *Fuel* **1981**, *60*, 703-711.
31. Neavel, R. C. Liquefaction of coal in hydrogen-donor and non-donor vehicles. *Fuel* **1976***, 55*, 237-242.
32. Nowacki, P. *Coal liquefaction processes*; Noyes Data Corp.: Park Ridge, NJ, 1979.
33. *Reaction engineering in direct coal liquefaction*; Shah, Y. T. Ed.; Addison-Wesley: Reading, MA, 1981.
34. Rivolta, M. Solvent Extraction of Coal: Influence of solvent chemical structure on extraction yield and product composition. MSc. Thesis, University of Alberta, University of Alberta, Spring 2012.
35. Rivolta Hernández, M.; Figueroa Murcia, C.; Gupta, R.; De Klerk, A. Solvent-coal-mineral interaction during solvent extraction of coal. *Energy Fuels* **2012**, *26*, 6834-6842.
36. Robinson, K.,K. Reaction Engineering of Direct Coal Liquefaction. *Energies* **2009***, 2*, 976-1006.
37. Sachanen, A. N. *The chemical constituents of petroleum*; Reinhold: New York, 1945, p. 102-107.
38. Shibaoka, M. Behaviour of vitrinite macerais in some organic solvents in the autoclave. *Fuel* **1981***, 60*, 240-246.
39. Shinn, J. H. From coal to single-stage and two-stage products: A reactive model of coal structure. *Fuel* **1984***, 63*, 1187-1196.
40. Song, C.; Schobert, H. H.; Hatcher, P. G. In *Temperature-programmed liquefaction of low rank coal. Evaluation of coal depolymerization reactions by CPMAS ^{13}C NMR and Pyrolysis-GC-MS;* Ltd, International Energy Agency Coal Research, Ed.; 1991 International Conference on Coal Science Proceedings; Butterworth-Heinemann: 1991; pp 664-667.
41. Stenberg, V. I.; Gutenkunst, V.; Nowok, J.; Sweeny, P. G. Low severity lignite liquefaction: temperature programming to 350 °C in an inorganic solvent system. *Fuel* **1989***, 68*, 133-135.
42. Tsonopoulos, C.; Ambrose, D. Vapor-Liquid Critical Properties of Elements and Compounds. 3. Aromatic Hydrocarbons. *J. Chem. Eng. Data* **1995***, 40*, 547-558.

43. Uzun, D.; Özdoğan, S. Sulfur removal from original and acid treated lignites by pyrolysis. *Fuel* **2006***, 85*, 315-322.
44. Vahrman, M. The smaller molecules derived from coal and their significance. *Fuel* **1970***, 49*, 5-16.
45. Wham, R. M. Effect of slurry heating rate on short-contact-time coal liquefaction. *Fuel* **1987***, 66*, 283-284.
46. Yani, S.; Zhang, D. An experimental study into pyrite transformation during pyrolysis of Australian lignite samples. *Fuel* **2010***, 89*, 1700-1708.
47. Yaws, C. L. Yaws' Critical Property Data for Chemical Engineers and Chemists. Knovel 2012.